

This dissertation has been
microfilmed exactly as received 68-6957

HALBERT, Jr., William Grady, 1938-
EFFECT OF MOIST STEAM INJECTION ON
OIL RECOVERY.

The University of Oklahoma, D.Engr., 1968
Engineering, chemical

University Microfilms, Inc., Ann Arbor, Michigan

THE UNIVERSITY OF OKLAHOMA
GRADUATE COLLEGE

EFFECT OF MOIST STEAM INJECTION ON OIL RECOVERY

A DISSERTATION
SUBMITTED TO THE GRADUATE FACULTY
in partial fulfillment of the requirements for the
degree of
DOCTOR OF ENGINEERING

BY
WILLIAM GRADY HALBERT, JR.

1968

EFFECT OF MOIST STEAM INJECTION ON OIL RECOVERY

APPROVED BY

D. E. Menzies

Paul J. Root

J. M. Campbell

Ronald Steiner Wolf

John A. E. Norton

DISSERTATION COMMITTEE

ACKNOWLEDGMENT

The author wishes to express his sincere appreciation to the following:

Professor D. E. Menzie, who directed this study.

Mr. G. F. R. Kingelin, who assisted in the design and construction of laboratory apparatus and who contributed valuable constructive criticism regarding this effort.

Mr. A. E. Trimble, who assisted in the execution of experiments.

Dr. R. E. Gilchrist, who assisted in the acquisition of the crude oils used in this study and who represented the interest of his employer, Tenneco Oil Company, in this effort.

Tenneco Oil Company for providing financial support.

The dissertation committee members for their constructive criticism of this dissertation.

TABLE OF CONTENTS

	Page
LIST OF TABLES	vii
LIST OF ILLUSTRATIONS.	viii
ABSTRACT	1
INTRODUCTION	3
Historical Background	3
Experimental Developments	4
Theoretical Developments: Heat Transfer	7
Theoretical Developments: Heat and Mass Transfer	12
Summary of Contributions.	17
SOME PROPERTIES OF STEAM	19
ANALYSIS OF STEAM FRONT PROPAGATION.	25
Initial Velocity of a Steam Front	25
Frontal Velocity Including Effects of External Heat Loss.	27
Convection Constraint on Frontal Velocity	28
Computation of Critical Distance.	30
THEORETICAL BASIS.	32
OBSERVED CHARACTERISTICS OF LINEAR STEAM FLOODS.	43

	Page
EXPERIMENTAL EQUIPMENT, CORE AND OILS' PROPERTIES . . .	46
Basis for Equipment Design	46
Core Holder.	46
Equipment.	49
Preparation of Isothermal Moist Steam.	52
Porous Medium.	53
Crude Oils	55
EXPERIMENTAL PROCEDURE.	59
Preparation.	59
Execution.	60
SUPPLEMENTARY EXPERIMENTS AND OBSERVATIONS.	63
PRESENTATION AND DISCUSSION OF RESULTS.	69
Types of Data Presented.	69
Experimental Results: 27.8°API Crude Oil	69
Experimental Results: 24.3°API Crude Oil	80
Experimental Results: 15.4°API Crude Oil	86
Comparison of Experiments and Data	93
INFLUENCE OF VARIABLES WHICH WERE HELD CONSTANT	102
PREDICTION OF OIL RECOVERY.	109
Comparison Between Computed and Experimental Results.	115
27.8°API Crude Oil	115
24.3°API Crude Oil	117
15.4°API Crude Oil	119
SUMMARY AND CONCLUSIONS	121
REFERENCES.	125
APPENDIX.	133

	Page
APPENDIX.	133
Nomenclature	134
Summary of Experimental Results.	137
Example Calculation: k_{ro}/k_{rw}	140
Example Calculation: Oil Recovery By	
Steam Injection.	144
I. Water-Oil Displacement.	144
II. Steam-Oil Displacement.	151
III. Total Recovery.	154
Determination of Heat Loss Parameter:	
Core's Surroundings.	156
Computation of Critical Distance	158
Computation of External Heat Flux from Core.	159

LIST OF TABLES

Table		Page
1	Summary of Heat Transfer Models	12
2	Mineralogical Properties of Boise Sandstone .	54
3	Densities of Steamed and Unsteamed Oils . . .	96
4	Dilution Requirements To Yield Measured Oil Density Changes	97
A-1	Summary of Experimental Results: 27.8°API Oil.	137
A-2	Summary of Experimental Results: 24.3°API Oil.	138
A-3	Summary of Experimental Results: 15.4°API Oil.	139

LIST OF ILLUSTRATIONS

Figure		Page
1	Pressure-Enthalpy for Water.	21
2	Vapor-Liquid Ratio for Moist Steams.	22
3	Density of 200 Psia Moist Steam.	23
4	Viscosities of Saturated Water and Steam	24
5	Idealized Temperature Profiles at Steam Fronts	28
6	Postulated Effective Viscosity of 382°F Moist Steam.	34
7	Isothermal Moist Steam-Oil Viscosity Ratio	38
8	Dimensionless Critical Length, Cylindrical Core: 382°F Steam, Boise Sandstone	39
9	Absolute Mobilities of 200 Psia System Water in Boise Sandstone	41
10	Saturation Profile: Willman Experiments.	45
11	Temperature Profiles: Willman Experiments.	45
12	Hassler-Type Core Holder	48
13	Diagram of Experimental Equipment.	51
14	Determination of Injected Enthalpy, $H(\lambda)$	52
15	Permeability Variation with Temperature, Boise Sandstone.	54
16	Oil Viscosity, Cp., Vs. T^{-1} , $^{\circ}R^{-1}$	56
17	Oil Density Vs. Temperature.	57

Figure		Page
18	ASTM Distillation Curves.	58
19	Effluent Temperature Histories.	64
20	Temperature Profiles of Steam-Solvent Breakthrough.	66
21	Effect of Annulus Heating on Flooding Time.	68
22	Oil Recovery by Hot Fluid Injection: 27.8°API Oil.	70
23	Liquid Production Performance:27.8°API Oil.	74
24	Cumulative WOR vs. Oil Recovery: 27.8°API Oil.	75
25	Effect of Continuous Flow Quality Change On Oil Recovery	77
26	Oil Recovery by Hot Fluid Injection: 24.3°API Oil.	81
27	Liquid Production Performance:24.3°API Oil.	83
28	Cumulative WOR vs. Oil Recovery: 24.3°API Oil.	84
29	Oil Recovery by Hot Fluid Injection: 15.4°API Oil.	87
30	Liquid Production Performance:15.4°API Oil.	90
31	Cumulative WOR vs. Oil Recovery: 15.4°API Oil.	91
32	Comparison of Oil Recoveries by Steam Injection	94
33	Cumulative Water-Oil Ratio at Steam Breakthrough vs. Steam Quality.	98
34	Effect of Temperature on k_{ro}/k_{rw}	100
35	Moist Steam Mobility at Residual Oil Saturations	113
36	Computed and Experimental Recoveries: 27.8°API Oil.	116

Figure		Page
37	Computed and Experimental Recoveries: 24.3°API Oil.	118
38	Computed and Experimental Recoveries: 15.4°API Oil.	120
1-A	Waterflood Performance: 27.8°API Oil.	143
2-A	Idealized Saturation Profile.	144
3-A	Determination of Water Saturation, Liquid Side of Front	148
4-A	Steam-Oil Fractional Flow Curves.	152

EFFECT OF MOIST STEAM INJECTION ON OIL RECOVERY

ABSTRACT

This report describes a laboratory investigation of the response of an oil-saturated rock subjected to the injection of moist steam. On the premise that the apparent viscosity of saturated steam may vary significantly with isothermal quality, it was hypothesized that a spectrum of steam-to-oil mobility ratios could exist for a given system. The supposed variation in apparent viscosity of moist steam appears to be a manifestation of the density changes which accompany quality changes.

In an oil displacement process, it was surmised at the outset that the quality-dependent steam-to-oil mobility ratio would be reflected by an associated variable volumetric displacement efficiency. A theoretical analysis is presented which shows that displacement efficiency may be governed by the steam-to-oil mobility ratio for a critical time duration, the length of which is a function of steam quality and the system's thermal properties. Thereafter, displacement is seen to be governed by liquid-liquid displacement principles.

The primary objective of this work was to examine the effect of an isothermal steam's quality on the recovery of some crude oils from a linear, consolidated sandstone core. Experiments were performed at 382°F. Three crude oils were employed. For these oils and for the experimental equipment used and the conditions imposed, the results show that oil recovery increased with the quality of injected steam until 75 percent quality was achieved. There was a tendency for recovery to decrease as steam quality approached 100 percent.

An analytical procedure for predicting oil displacement which results from injecting moist steam is presented. Good agreement between computed and experimentally observed results is shown for the high gravity (27.8°API) oil. The analytical technique proved less adequate in accurately explaining the variation in oil displacement with steam quality for the intermediate (24.3°API) and low (15.4°API) gravity crudes.

INTRODUCTION

Historical Background

The feasibility of using thermal energy as a means of recovering oil from subsurface formations has been considered for over sixty years (88). Apparently, the first proposal to inject a heat-laden fluid into an oil reservoir was published by Howard (39) in 1923. He suggested that air and a combustible gas be injected into an oil bearing formation and ignited. A similar process was proposed by Lindsly (52) in 1928. Hester and Menzie show that enormous quantities of injected gases would be required for such processes (37). The possibility of injecting steam was first examined by Stovall (78) in 1934. Using crude equipment, Stovall demonstrated that displacement of oil by superheated steam was feasible, but the prevailing economic conditions rendered the idea impractical.

Interest in thermal methods of recovery waned until the early 1950's when the results of some in situ combustion projects were first published (17). Industry's attention seemed to focus on the combustion processes although some steam injection trials were in progress (43,60).

Very little technology regarding steam injection has been published to date. The proprietary nature of this process is exemplified by comparing patent records and thermal status surveys. One bibliography of thermal recovery literature lists 269 patents, only one of which is concerned with steam injection (16,40). Yet, a recent status survey of domestic thermal projects shows that steam injection currently enjoys greater popularity than do combustion processes (83).

Experimental Developments

Laboratory research relating to thermal injection processes apparently began with determinations of some heat transfer characteristics of porous media (35). Although theoretical work was initiated in 1929 (72), regular publication of experimental efforts did not appear until the early 1950's. Influenced by Schumann's theoretical analysis, laboratory tests by Greenstein and Preston (33) and Preston and Hazen (63) sought to evaluate the significance of the convective heat transfer coefficient (h_a) between a fluid and a solid matrix. Subsequent experimental analyses by Jenkins and Aronofsky (41), Hadidi et al. (34), and Green (32) indicate that heat transferred by conduction and forced convection is quantitatively more important than that transferred between fluid and solid phases by convection.

A thesis by Ramsey (66) describes an attempt to recover a viscous crude by steam injection. The author observed severe channeling by steam in his three-dimensional model, but the process was deemed superior to conventional waterflooding. A later study by Willman et al. (90) describes an analysis of steam injection into linear, consolidated cores and glass bead packs. In their valuable contribution, the authors discuss some proposed recovery mechanisms which are thought to accompany liquid displacement. They show performance comparisons between conventional waterfloods, hot waterfloods, and steam floods.

With the objective of examining steam injection as a possible wellbore stimulant, Caudle and Silberberg (11) observed that a waterflood's residual oil saturation was significantly reduced following steam injection.

Abbasov and co-workers (1) demonstrated the efficiency of superheated steam in removing high viscosity oils from an unconsolidated sand pack.

The effect of temperature on water-oil relative permeability ratios have been examined by Hossain (38) and Edmondson (20). Using an unconsolidated sand pack, Hossain's hot waterfloods of a refined oil reveal a decline in k_{rw}/k_{ro} with temperature increase. Edmondson's data corroborate those of Hossain at high water saturations. Data for crude oils do not exhibit consistent trends.

In theoretical analyses, it is generally assumed that the thermal properties of porous media are independent of temperature. This contention has not been consistently borne out by experiments. Somerton and Boozer (73) show that both thermal diffusivity and thermal conductivity of some rocks were sensitive to temperature changes. Conversely, Adivarahan et al. (2) show that thermal conductivity can be independent of temperature; their analysis indicates an inverse proportionality of thermal conductivity with porosity.

Several studies designed to quantify a rock-fluid system's effective thermal conductivity have been conducted (2,35,47,89). These efforts show that effective thermal conductivity is dependent upon the stagnant conductivity of the porous medium, the nature of the fluid which it contains, and the mass flux of the fluid. Kunii and Smith (47) and Khan and Fatt (44) observed that there is little effect of pressure on the thermal conductivity of some sandstones. Somerton et al. (74) and Waldorf (86) observed that the permeabilities of a variety of sandstones were not appreciably affected by temperature changes within the range of temperatures associated with hot fluid injection.

Theoretical Developments: Heat Transfer

The injection of a heat-laden fluid into a porous medium gives rise to both heat and mass transfer. Numerous theoretical articles describing a variety of heat transfer models are available. Basically, four approaches toward analyzing heat transfer processes have been employed:

- 1) Dimensional analysis (57);
- 2) Electrical analogs (85);
- 3) Gross heat balances;
- 4) Analytical and numerical solutions of differential heat balances.

Dimensional analysis and gross heat balances may serve as practical means-to-ends, but their contributions toward a better understanding of heat transfer processes may be limited. Conversely, some analytical solutions have provided valuable contributions. There are, however, minimal substantiative experimental data in support of analytical models.

Thermal displacement processes may be characterized by the multi-phase flow of fluids within a temperature field accompanied by possible chemical reactions and phase change effects. Mathematically, some features of miscible displacement, in situ combustion, and hot fluid injection are quite similar.

Schumann (72) is credited with the first theoretical examination of the response of a liquid saturated porous medium to the injection of a heat-laden fluid. Thermal equations for both fluid and solid phases are employed. Bailey and Larkin (5) present a very concise development of these partial differential equations. Klinkenberg (46) subsequently showed that Schumann's solution could be simplified.

An awareness that fluid and solid phases can locally experience different temperature histories prompted the early investigators to construct thermal equations for each phase. These equations are coupled through a fluid - solid convection term. Recognizing that instantaneous thermal equilibrium between fluid and solid phases may occur, Bailey and Larkin (5) show that a single differential equation is a limiting form of the two phase equations. Jenkins and Aronofsky (41) have derived a solution for such an equation. Their solution is identical with one presented by Carslaw and Jaeger (9), and it is structurally identical with that presented by Aronofsky and Heller (3) for frontal concentrations in a miscible flood.

Possible consequences of external heat losses were discussed by Nielsen and Calhoun (34), Munk (59), and Schild (71). Its effect on the flow of heat within a zone of interest was theoretically examined by Lauwerier (50) and Marx and Langenheim (56). The latter

development is a modification of Carter's analysis of the growth of a hydraulic fracture (10). Ramey (64) shows that the Marx and Langenheim analysis can be extended to cases of variable heat injection rate.

The role of heat transfer by conduction has been examined by Bailey and Larkin (6), Baker (7), Lesser, Bruce and Stone (51), Ramey (65), and Thomas (82). Heat transferred by this process is shown to be minor relative to that transported by fluid motion except at very low fluid velocities. Chu (12) and Thomas (81) show that heat which is lost to adjacent media by conduction may be partially regained by the zone of interest under specific conditions.

Zones of heat flow have been discussed by Landrum et al. (48) and Willman et al. (90). For steam injection, Landrum et al. claim that the banking of hot water ahead of a steam front is of no significance. Some experimental results submitted by Willman et al. do not support this contention. However, Stovall's observations indicate that a water-free steam drive is possible (78).

The practical utility of analytical solutions has been demonstrated by Spillette (77) and Lesser, Bruce and Stone (51). Numerical results are compared with analytical results. The latter are shown to reproduce the former with little deviation.

Since the apparent objective of most theoretical analyses has been to present an analytical solution or to illustrate the consequences of a numerical exercise, the role of some of the physical parameters in the heat transfer processes has remained rather obscure. Using a steady-state theoretical model, Sandrea and Stahl (67) have postulated that the temperature profile associated with hot fluid injection may be a consequence of the porous medium's permeability and inversely proportional to the effective thermal conductivity of the fluid - rock system. Recalling that Adivarahan observed that thermal conductivity can be inversely proportional to porosity (2), it is possible to deduce that the contribution of heat transfer by forced convection may exceed that of conduction.

The influence of formation thickness was demonstrated by Chu (12); the rate of external heat loss is shown to be inversely proportional to formation thickness. Using Marx and Langenheim's equation (56), Farouq Ali (27) shows that changes in heat capacities of the bounding strata with temperature do not appreciably alter the magnitude of computed heated area. Farouq Ali (22) also demonstrates how Marx and Langenheim's equation may be modified to accommodate thermally dissimilar bounding media.

Farouq Ali (23) proposes that a diminution in heated volume accompanies increasing connate water saturation.

This contention is supported by heat capacity arguments, but it remains to be shown whether the native water saturation is subjected to heating (4,8).

Using the Willman et al. (90) equation as a basis, Farouq Ali (23) submits that a greater volume of a reservoir may be heated at low steam pressures compared with high pressures. Implicitly, he states that low temperature steam may produce greater benefit than high temperature steam. The experimental results reported by Abbasov, Kasimov and Tairov (1) refute this argument.

In summary, a variety of heat transfer models have been proposed, few of which have been subjected to experimental testing. The distinguishing factor appears to be the various authors' suppositions regarding which of the possible modes of heat transfer are important along with their choice of assumptions designed to simplify the problem. A summary of theoretical models segregated according to heat transfer processes is presented in Table 1.

TABLE 1

SUMMARY OF HEAT TRANSFER MODELS

<u>Mode of Heat Transfer</u>	<u>References</u>
Forced Convection	(5),(7),(12),(28),(33), (41),(46),(48)-(51),(54), (56),(59),(63),(67),(69), (71),(72),(81),(85),(90)
Forward Conduction	(5),(6),(41),(51),(65), (71),(81),(82),(85)
Fluid-Solid Convection	(5),(33),(46),(63),(72)
External Heat Losses	(12),(49)-(51),(56),(65), (67),(69),(81),(82),(90)
Regain of Lost Heat	(12),(81)

Theoretical Developments: Heat and Mass Transfer

Within the scope of the theoretical heat transfer analyses, equations of fluid motion have been avoided. Except for the numerical studies, it has been necessary to employ a spatially independent velocity for the displacing fluid in quantifying convective heat flux. Steady-state fluid flow has been combined with unsteady-state heat flow.

An important initial effort regarding the hydrodynamic aspects of an underground thermal process was presented by Wilson et al. (91) in 1958. Three distinct fluid regions ahead of a burning front were assumed. Fluid movement was analyzed through material balance and relative permeability considerations.

A numerical analysis of fluid flow associated with combustion was performed by Chu (13). Conduction, convection, external heat loss, fluid vaporization and condensation, and bulk fluid flow were simultaneously considered. For his system, vaporization and condensation effects are shown to increase the linear extent of preheating ahead of the combustion front; primary preheating was produced by a bank of steam. Likewise, a similar analysis by Gottfried showed a steam plateau preceding a combustion front (31).

Using nonlinear wave theory in a theoretical analysis of hot waterflooding, Fayers (28) shows that temperature and saturation profiles at a displacement front can be coincident. Fayers also demonstrates that errors of only one to two percent are incurred by ignoring the temperature dependency of system heat capacities. Similar theoretical discussions of temperature - saturation discontinuities have been presented by Martin (54) and Scheidegger (69). Hadidi's laboratory results for linear hot waterfloods (34) suggest that temperature and saturation profiles can be identical even though a diffused temperature profile exists.

A three-region model proposed by Landrum et al. (49) wherein there is no hot water bank ahead of a steam front appears to have as part of its basis the "shock" or unit - step concept employed by Martin (12), Fayers (28), and Scheidegger (69). In these models, heat loss from a steamed zone by linear conduction and by convective flux through the front are not considered. Some experimental data submitted by Willman et al. (90) do not support the temperature-saturation "shock" concept and the attendant absence of a hot water bank.

Theoretical analyses of fluid flow associated with the movement of thermal fronts have been examined according to two similar concepts. Davidson (18), Gottfried (31), Martin (54), and Wilson et al. (91) have combined thermal equations with Darcy's law for each fluid phase. Fayers (28), Fournier (29), Farouq Ali (24), Landrum et al. (49), Malofeev and Sheinman (53), Scheidegger (69), and Willman et al. (90) have employed the Buckley-Leverett theory. In all cases, the probable temperature-dependence of relative permeability has been ignored. That relative permeability can vary with temperature has been shown by Caudle and Silberberg (11), Edmondson (20), and Hossain (38). Somerton (74) and Waldorf (86) detected only minor variations in absolute permeabilities with temperature.

Willman et al. (90) describe an approximate application of the Buckley-Leverett mechanism for flow within a

temperature field preceding a steam front. A stratified sequence of isothermal displacement layers is employed. Using a similar approach, Farouq Ali (24) claims that temperature can produce an adverse effect on the displacement efficiency of low viscosity crudes. However, if the experimental evidence that k_{rw}/k_{ro} can decrease with temperature increase were applied to Farouq Ali's fictitious example, it is possible to arrive at an opposite conclusion.

Landrum, Smith and Crawford (49) have applied the Buckley-Leverett concept to fluid flow within a steamed region. In contrast, Willman et al. (90) assumed that only steam is mobile within a steamed region.

An analysis of oil displacement by hot water was presented by Malofeev and Sheinman (53). The fractional flow approach is used in conjunction with Lauwerier's heat transfer model (50). It is shown that the use of an integrated average temperature in describing fluid properties occurring in a temperature field does not materially affect the computed values of saturations throughout the course of the flood.

Another combination of Buckley-Leverett and Lauwerier principles was performed by Fournier (29) using numerical techniques. Computed saturation profiles show that two distinct waterfloods occur sequentially. A reservoir temperature Buckley-Leverett front is shown to advance ahead of a less clearly defined hot water bank.

Claiming that the choice of injecting steam or hot water should be evaluated on the basis of equivalent rates of injection, Sarem and Hawthorne (68) have presented a theoretical discussion of fluid flow behind an advancing thermal front. Using empirical permeability models, the authors conclude that hot water can impart considerably more heat to a formation than can steam. An opposite opinion was published by Szasz and Thomas (80). Using equivalent pressure gradients, it can be shown that the volumetric rate of flow of saturated water is approximately 15 percent of that for 100 percent quality steam at 400°F. At this temperature, the heat capacity of water is about 31-times greater than that of steam. Hence, the rate of heat injection is 4.7-times greater with water than with steam. On an injection rate basis, Sarem and Hawthorne's argument is convincing. Translated to an areal basis, however, steam should produce superior effects since it, unlike water, can impart all or part of its latent heat without a loss in temperature.

Sarem and Hawthorne's presentation (68) serves to focus attention on the flow behavior of steam. An implicit assumption carried by both the Willman et al.(90) and Marx and Langenheim (56) thermal equations is that there is no viscous pressure drop associated with steam flow. Thus, these models insist upon the propagation of a constant temperature front. Having a spectrum of finite mobilities,

a viscous pressure drop is an obvious manifestation of steam flow. Thus, a time and position-dependent temperature must be associated with an incremental volume of steam flowing through a porous medium. This is clearly shown by Willman's experimental data (90).

An additional process of heat transfer becomes evident due to the temperature gradient caused by a pressure gradient within a steamed zone - that of forward conduction behind the front. Its significance may be small. Using Willman's data (90), forward conduction within a steamed region was about 3 percent of the convected heat flux for a pressure gradient of 13.3 psi/foot and an apparent net heat injection rate of 0.1 BTU/minute.

Summary of Contributions

In summary, the quantity of theoretical analyses outnumbers experimental evidence to date. Nonetheless, both efforts have contributed toward a better understanding of some of the heat and mass transfer processes which may accompany thermal processes. Modes of heat transfer have been identified and weighed in their proper perspective. The legitimacy of certain assumptions have been tested. Some physical and chemical processes which may contribute toward total oil recovery have been tentatively identified. Analytical solutions have been shown to be quite accurate.

However, a critical examination of all possible displacement and recovery mechanisms which might arise in steam injection is yet to be published. A variety of phase and temperature regimes have been assumed to exist in theoretical analyses, and each special concept has generally been experimentally observed by other researchers.

Regarding heat flow models, that of Marx and Langenheim for steam flow (56) and Lauwerier's analysis of hot water flow (50) appear to have gained the most favorable endorsement. For fluid flow within a temperature field, the present inability to anticipate relative permeability's response to temperature has prevented the development of an acceptable mass transfer model.

Only two reports dealing with steam displacement have contributed significantly toward a better understanding of this process - the Willman et al. experiments (90) with 100 percent quality steam and the Abbasov et al. investigations (1) with superheated steam. These studies show that steam displacement can be effected either with or without intermediate waterflooding. An objective of the present study is to specify the conditions at which either of these phenomena can exist.

SOME PROPERTIES OF STEAM

The quantity of heat contained by a unit mass of substance relative to some reference state is called its enthalpy, H , BTU per mass-weight. The ability with which a substance can absorb additional heat due to a rise in temperature is measured by its specific heat, C_p , in BTU's per mass-weight per degree rise in temperature. The greater is C_p , the larger quantity of heat the substance will absorb for a given temperature increase. The specific heat of liquid water varies between 1.0 and 1.1 BTU/lb_m-°F within the temperature range encountered with hot fluid injection; its specific heat is the highest of all known elements and compounds at temperatures greater than 0°F. Only liquid ammonia has a comparable heat capacity - about 1 BTU/lb_m-°F at temperatures below 0°F. Thus, water is capable of transporting more heat per unit mass above 0°F than any other substance (21).

While steam may possess a high enthalpy, its specific heat is rather low - about 0.68 BTU/lb_m-°F at 380°F. By increasing the temperature of saturated steam, its heat content increases only slightly. For example, superheating steam by 100°F increases its enthalpy by only 5.7 percent.

The term "steam quality" refers to the percent by weight of vapor contained by a two-phase steam. Likewise, quality represents the degree to which total heat of vaporization has been achieved. In the present study, the symbol λ is used to designate quality.

$$\lambda = \frac{M_v}{M_l + M_v} = \frac{H(\lambda) - H_{sw}}{\Delta H_v} \quad (1)$$

where:

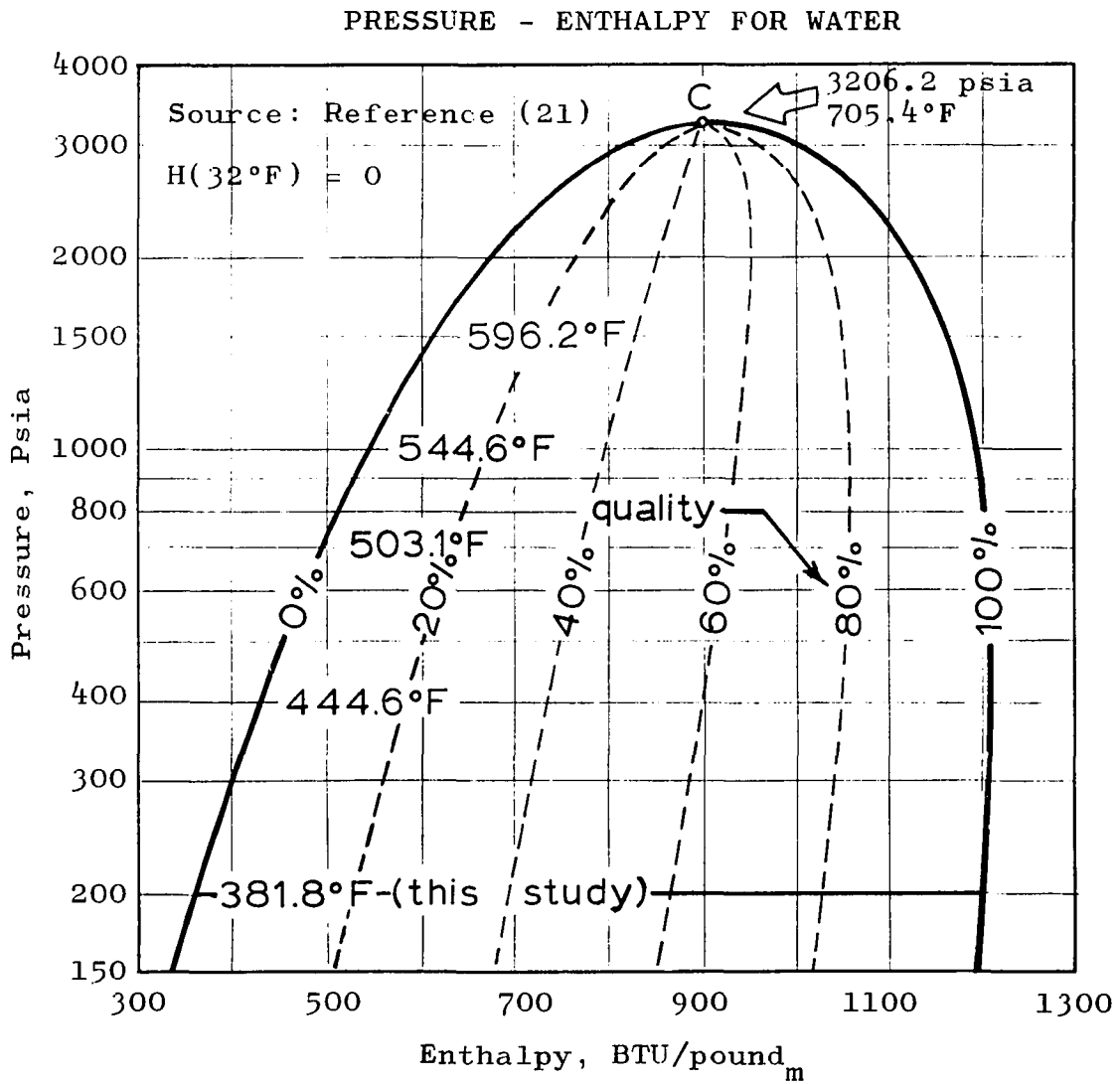
- M_v = mass of vapor in a two-phase mixture
- M_l = mass of liquid in a two-phase mixture
- $H(\lambda)$ = enthalpy of λ percent quality steam
- H_{sw} = enthalpy of saturated water (0 quality steam)
- ΔH_v = latent heat of vaporization

The terms "saturated water", "0% quality steam", and "bubble-point water" are synonymous at a given temperature. Likewise, "100% quality steam" and "dew-point steam" are identical in meaning at some temperature. Although the term "saturated steam" probably should designate 100 percent quality steam, its use has been inconsistent, and it serves as a point of confusion.

Between the triple and critical points, the Phase Rule states that the system water possesses one degree of freedom for two phases in equilibrium. The equilibrium state of a pure water system is specified by stating either its temperature or its pressure. It is redundant

to specify both the temperature and pressure of an equilibrium mixture of liquid and vapor water. As indicated by Equation (1), an additional variable - enthalpy - is necessary for characterizing the phase distribution of such an equilibrium mixture. Figure (1) shows the two - phase pressure-enthalpy envelope for steam.

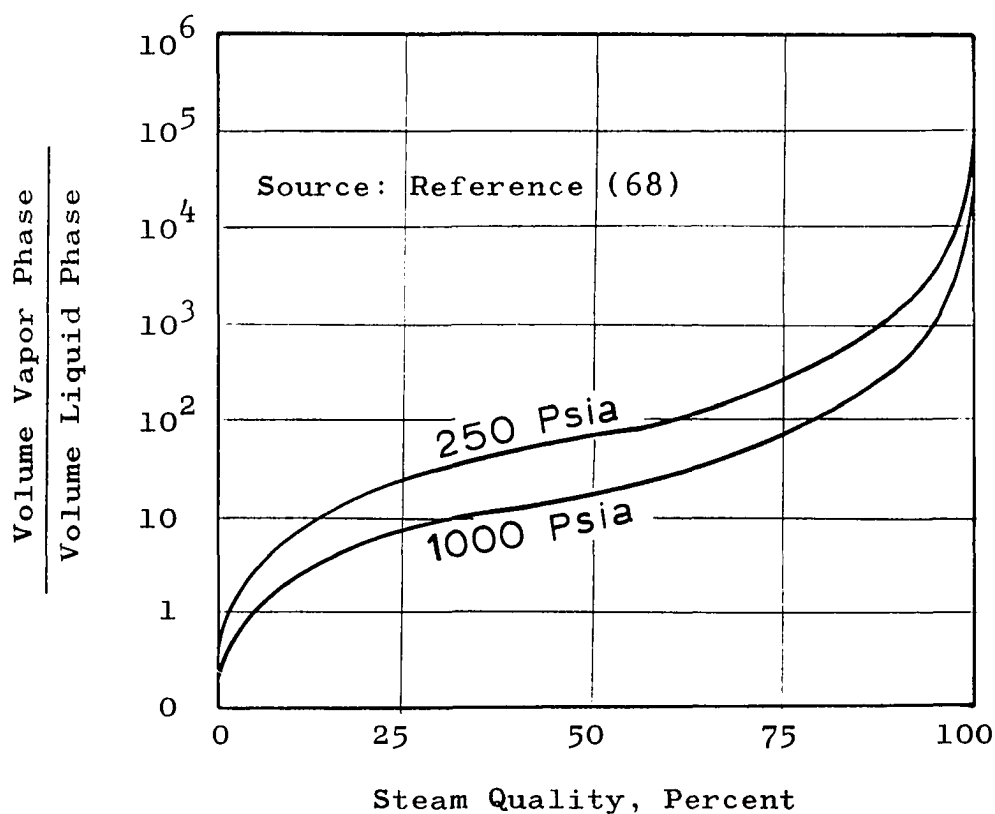
FIGURE 1



While the enthalpy - quality relationship for isothermal steam is linear, the vapor - liquid volume ratio relationship with quality is quite nonlinear as shown by Figure 2.

FIGURE 2

VAPOR - LIQUID RATIO FOR MOIST STEAMS

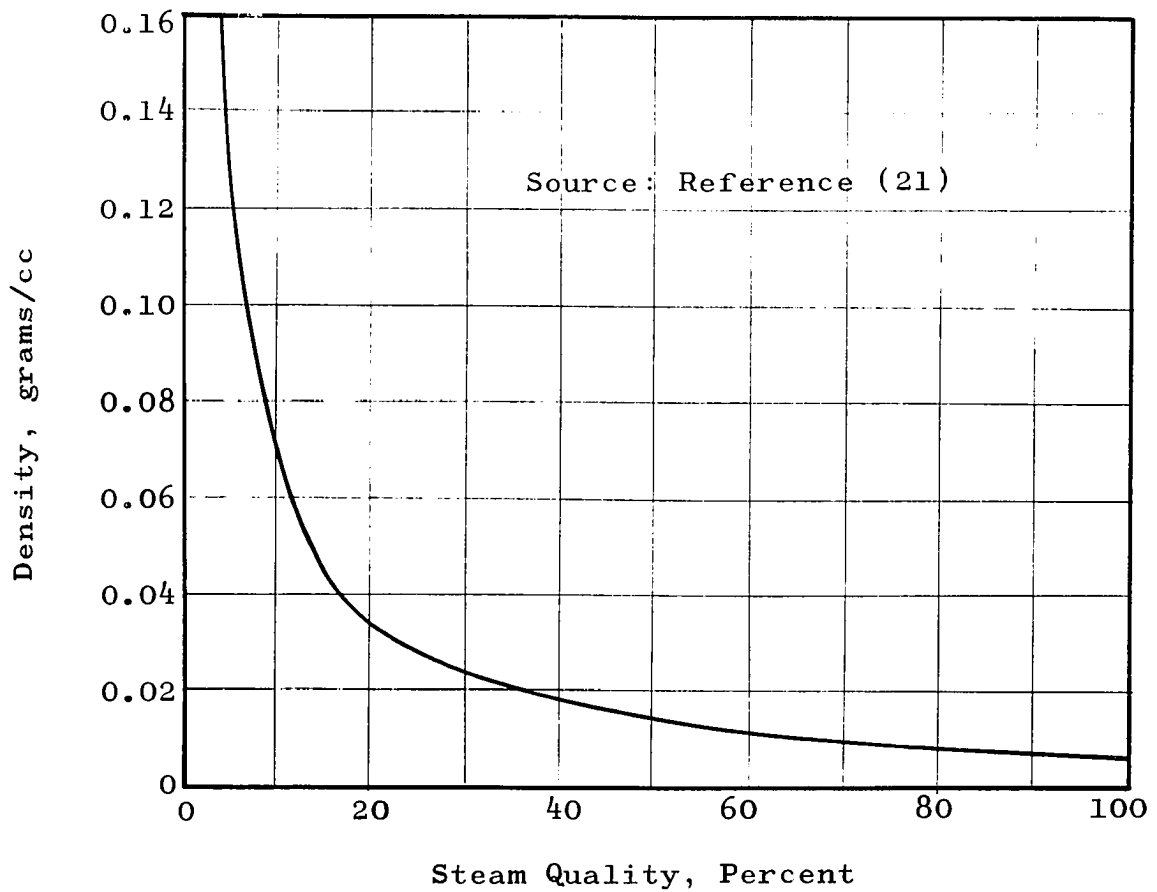


Using Figure 2 as a basis, one would anticipate that the most severe changes in a moist steam's intensive

properties would occur in the very low quality range where the volume of the liquid phase is significant relative to that of the vapor phase. Partial evidence that this might be true is shown by Figure 3 which relates the densities of 200 psia moist steams with quality.

FIGURE 3

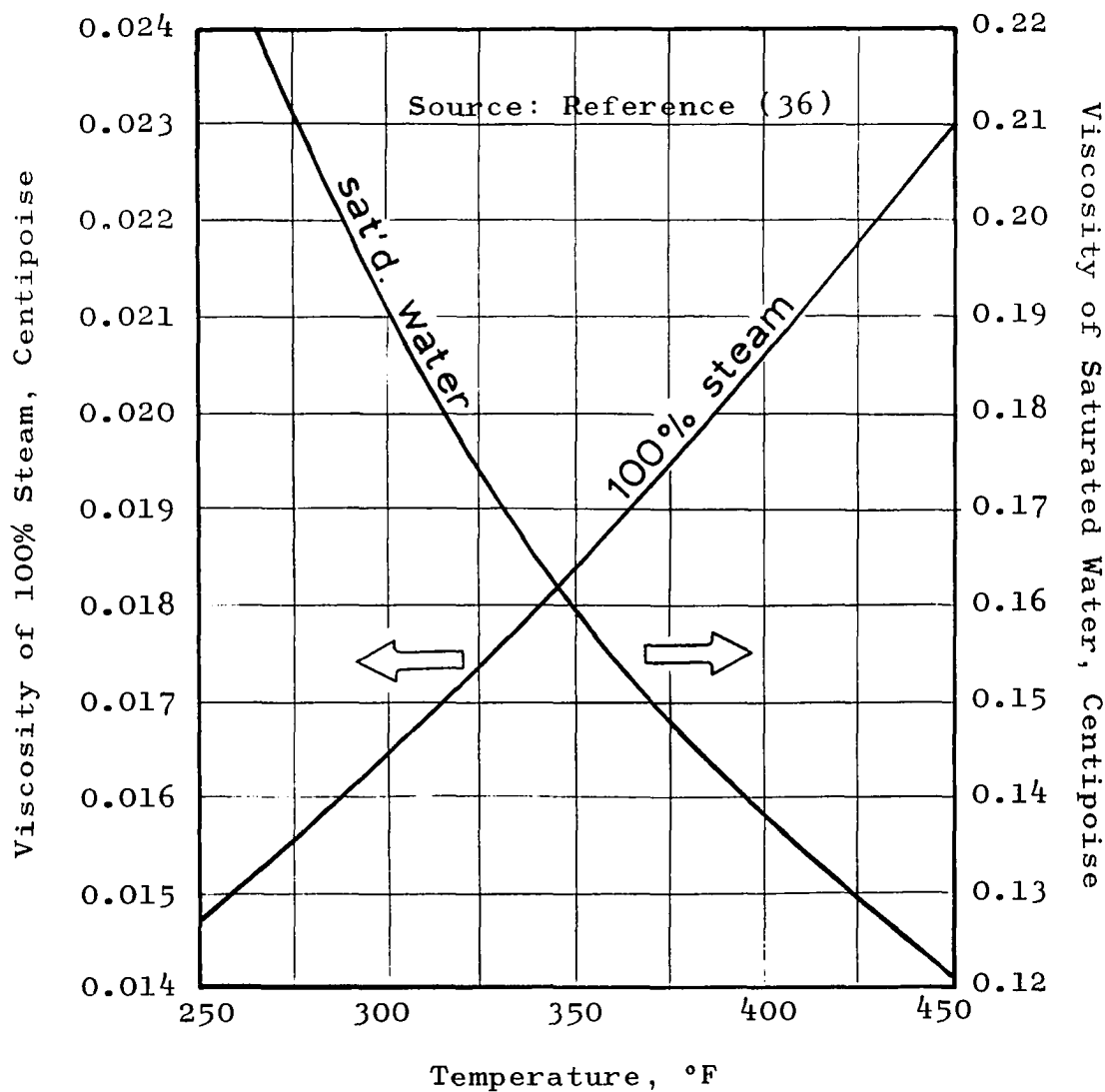
DENSITY OF 200 PSIA MOIST STEAM



The effective viscosity of moist steam is of prime interest in this investigation. Apparently, this property has not been determined. The viscosities of saturated water and 100 percent quality steam have been measured by Hawkins et al. (36). These data are shown by Figure 4.

FIGURE 4

VISCOSITIES OF SATURATED WATER AND STEAM



ANALYSIS OF STEAM FRONT PROPAGATION

While an examination of transient production response to steam injection is not of direct concern in this work, some discussion of the manner in which a steam front is thought to progress through a linear system is necessary in support of a theoretical basis which motivated this study.

Initial Velocity of A Steam Front

The velocity of a steam front exhibits a maximum value when there are no heat losses from the steamed zone.

A simple heat balance:

$$\begin{aligned} \text{Rate of heat injected} &= \text{Rate of heat flowing} \\ &= (\text{velocity})(\text{area})(\text{heat content}) \end{aligned}$$

yields:

$$H_i = v_{si} \cdot A \cdot \Omega \cdot \Delta T \quad (2)$$

where:

$$H_i = \text{BTU/minute injected into area } A, \text{ cm}^2$$

$$v_{si} = \text{initial velocity of front, cm/minute}$$

$$\Omega \cdot \Delta T = \text{heat capacity of steamed region, BTU/cm}^3.$$

In Equation (2), the steamed zone's heat capacity is presented as a specific heat (Ω , BTU/cc-°F) - Temperature increase (ΔT , °F) product.

Behind the front, it is assumed that steam is flowing in the presence of an immobile, nondistillable oil residue of saturation S_{or} , specific heat C_{or} , and density ρ_{or} . Considering the heat possessed by all phases within the steamed zone, the heat capacity behind the steam front is:

$$\Omega = (1 - \phi) \rho_r C_r + \phi \left[S_{or} \rho_{or} C_{or} + \frac{H(\lambda)}{\Delta T} \rho_s S_s \right] \quad (3)$$

where:

- ϕ = porosity of rock
- ρ_r = rock density, grams/cc
- C_r = specific heat of rock, BTU/gram-°F
- $H(\lambda)$ = enthalpy, BTU/gram, of λ quality steam
- ρ_s = density, grams/cc, of λ quality steam
- S_s = steam saturation = $1 - S_{or}$.

Experiments regarding the mobility of connate water have shown that essentially all of a rock's native saline water is replaced by injected water during displacement. It is presumed that the same effect is produced by any condensed steam ahead of the front (4,8).

Frontal Velocity Including Effects of External Heat Loss

When heat flows by conduction from the steamed region into the bounding media, the propagation of a plane saturation - temperature front can be described by Marx and Langenheim's equation (56).

$$v_f = v_{si} e^{\alpha^2} \operatorname{erfc}(\alpha) = v_{si} \bar{v}_s \quad (4)$$

where:

$$v_f = \text{velocity of front, cm/min}$$

$$v_{si} = \frac{H_i}{A \Omega \Delta T} \quad (\text{From Equation 2})$$

$$\alpha = \frac{4}{\Omega D_c} \sqrt{k_2 \rho_2 C_2} \sqrt{t}$$

$$D_c = \text{diameter of cylindrical core, cm}$$

$$k_2 = \text{thermal conductivity of surroundings,} \\ \text{BTU/cm-min-}^\circ\text{F}$$

$$\rho_2 C_2 = \text{heat capacity of surroundings, BTU/cc-}^\circ\text{F}$$

$$t = \text{time, minutes}$$

$$\bar{v}_s = \text{dimensionless velocity.}$$

Equation (4) is written for the dimensions of a cylindrical core; it represents a slight modification of the form presented by Marx and Langenheim.

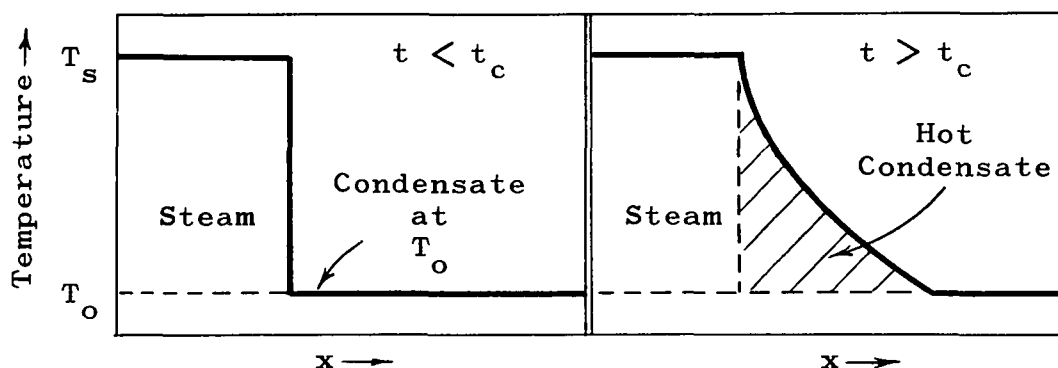
Convection Constraint on Frontal Velocity

As the front is propagated through the linear system, heat losses to the surroundings occur at all times. A diminution of frontal velocity with time is the immediate consequence. Marx and Langenheim (56) implicitly assumed that all of the heat arriving at the steam front is consumed there in heating the matrix and residual liquid from the original reservoir temperature to steam temperature. Hence, condensate is assumed to leave the steamed region, but the condensate's temperature is equal to that of the unheated reservoir. In effect, there is mass transfer through the front, but there is no heat transfer through the front.

It is postulated that when the steam front's velocity declines to some critical value, an additional process of heat transfer occurs - heat flow through the front by convective transport. This point signals the onset of hot condensate accumulation ahead of the front; a diffused temperature profile results. This concept is illustrated by Figure 5.

FIGURE 5

IDEALIZED TEMPERATURE PROFILES AT STEAM FRONTS



It is proposed that the condition at which heat begins to flow through the front may be deduced by examining an equivalent form of the Marx and Langenheim equation for frontal velocities. By writing the steamed region's heat capacity as an equivalent specific heat - density product:

$$\Omega = C_{eq} \cdot \rho_{eq} \quad (5)$$

the dimensionless frontal velocity may be expressed as follows:

$$\begin{aligned} \bar{V}_s &= \frac{v_f A C_{eq} \rho_{eq} \Delta T}{H_i} \\ &= \frac{C_{eq} \Delta T}{\frac{H_i}{v_f A \rho_{eq}}} \\ &= \frac{\text{Heat flowing, BTU/gram}}{\text{Available heat, BTU/gram}} \cdot \quad (6) \end{aligned}$$

With convective loss through the front, the fluid which flows just at the downstream side of the discontinuity is liquid water. By analogy with Equation (6), a dimensionless critical velocity is defined as:

$$\begin{aligned} \bar{V}_c &= \frac{\text{Heat contained by flowing fluid}}{\text{Maximum heat available}} \\ &= \frac{\text{Enthalpy of saturated liquid}}{\text{Enthalpy of vapor}} = \frac{H_{sw}}{H(\lambda)} \cdot \quad (7) \end{aligned}$$

The time at which convective heat transfer begins is found by equating \bar{V}_s and \bar{V}_c .

$$\exp(\alpha_c^2) \operatorname{erfc}(\alpha_c) = \frac{H_{sw}}{H(\lambda)} \quad (8)$$

where $\alpha_c = \alpha(t_c)$ is identified after Equation (4).

By Equation (8), it is seen that condensation is initiated more rapidly as moist steam's enthalpy or quality decreases.

In effect, an additional limit is imposed on the Marx and Langenheim development. Their analysis depends upon the flow of a temperature discontinuity. With condensation, however, a diffused temperature profile ahead of the steamed zone would be expected. With the onset of an additional mode of heat loss, the front's velocity will be less than that predicted by the Marx and Langenheim method.

Computation of Critical Distance

For a specified rate of steam injection (as BTU/min), the front's velocity within a given system declines to a critical value after flowing for a critical time, t_c . The spatial coordinate at which this condition arises is defined as the critical distance, x_c . Marx and Langenheim have derived an equation relating the volume of a steamed zone to elapsed injection time. Their equation may be modified to accommodate the basic dimensions of a cylindrical core. The modification is shown by Equation (9).

$$x_f = \frac{H_i \Omega}{4 \pi k_2 \rho_2 c_2} \left[\bar{v}_s + \frac{2\alpha}{\sqrt{\pi}} - 1 \right] \frac{1}{\Delta T} \quad (9)$$

When the critical state is achieved, $x_f = x_c$, $\bar{v}_s = \bar{v}_c$, and $t = t_c$. Equation (9) is modified accordingly.

$$x_c = \frac{H_i \Omega}{4 \pi k_2 \rho_2 c_2 \Delta T} \left[\frac{H_{sw}}{H(\lambda)} + \frac{8\sqrt{k_2 \rho_2 c_2}}{\sqrt{\pi} \Omega D_c} \sqrt{t_c} - 1 \right] \quad (10)$$

The transient response to steam injection is not of direct interest within the scope of this work. Little emphasis will be delegated to critical time, t_c ; however, the critical distance concept is of greater importance. Through convective heat losses, a change in the basic oil displacement mechanism apparently occurs at the system's critical state. Hence, total oil recovery from steam injection depends on the extent of the reservoir through which different processes operate. This is discussed in greater detail in the next section.

Equation (10) may be solved without direct knowledge of t_c . Data for $\left[\exp(z^2) \operatorname{erfc}(z) + 2z/\sqrt{\pi} - 1 \right]$ are known for given values of z and $\left[\exp(z^2) \operatorname{erfc}(z) \right]$ (56). In this study, $z_c^* = H_{sw}/H(\lambda) = \left[\exp(z_c^2) \operatorname{erfc}(z_c) \right]$ are known, and the term in brackets in Equation (10) may be evaluated from tabulated data.

THEORETICAL BASIS

The density of 200 psia steam is shown to vary significantly at low qualities by Figure 3. Assuming that changes in density with quality produce changes in the equilibrium mixture's effective viscosity, the effective mobility, k/μ , of an isothermal steam can be a function of its quality. The effective viscosities of moist steams apparently have not been measured. Consequently, the viscosity model developed by Andrade (58) is submitted as a means of calculating the effective viscosity of moist steam. Of the various viscosity models examined, the Andrade concept was especially appealing by virtue of its dependence on density.

Andrade's equation,

$$\mu = G \cdot \exp(J \rho/T) \cdot (\rho)^{1/3} \quad (11)$$

where G and J are constants, T is absolute temperature, and ρ is density, is said to be quite accurate for most liquids. Using an equation of the form

$$\frac{\mu_s}{\mu_w} = \frac{G_s}{G_w} \cdot \exp\left(\frac{J_s \rho_s - J_w \rho_w}{T}\right) \cdot (\rho_s/\rho_w)^{1/3}, \quad (12)$$

a regression analysis was performed on the single-phase viscosity data shown by Figure 4; the subscript "s" refers to steam, and "w" refers to liquid water. The approximation

$$\mu_s = \mu_w (0.00072T + 0.426) \left[\frac{\rho_s}{\rho_w} \right]^{1/3} \quad (13)$$

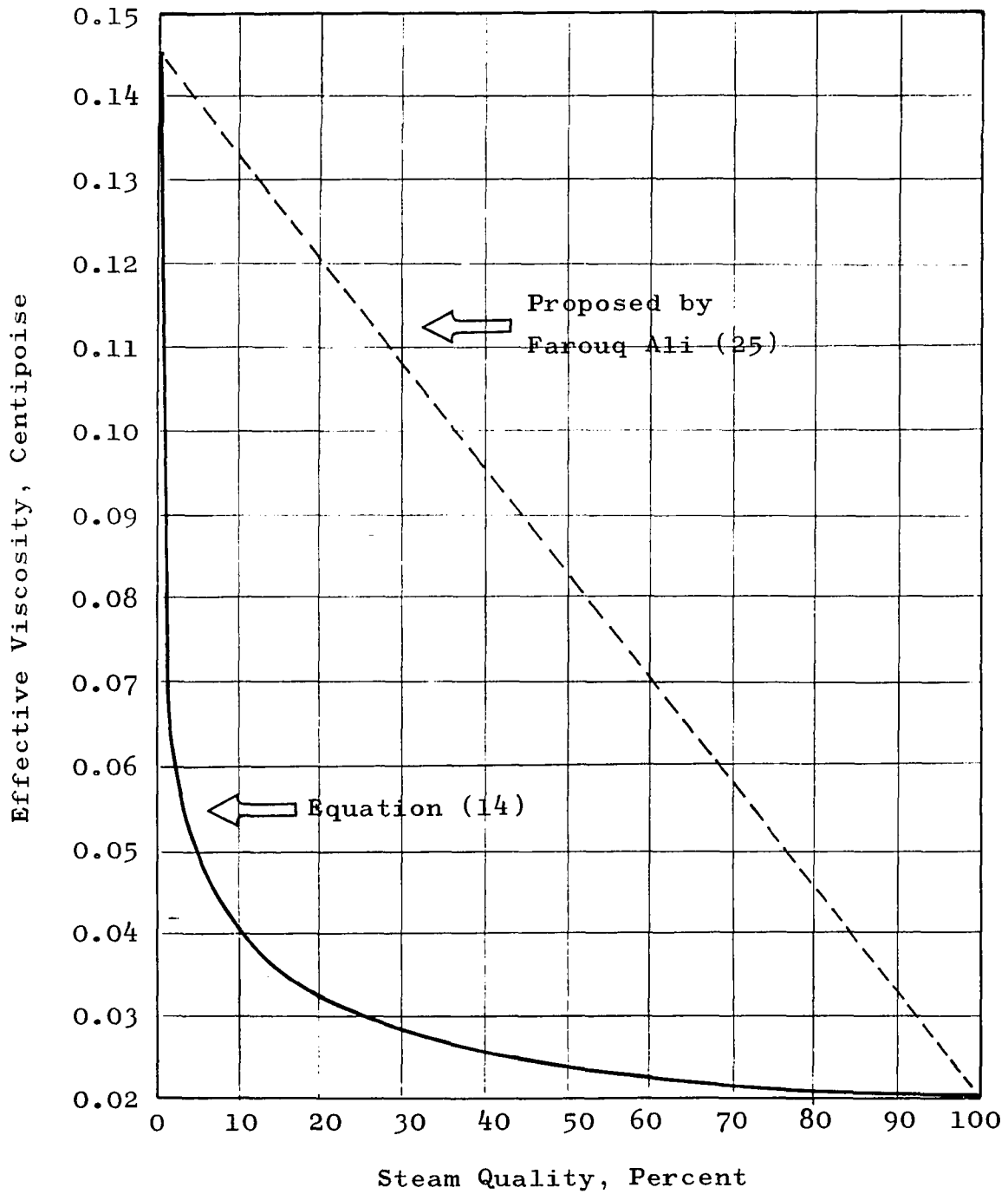
resulted. Limits are $250^\circ\text{F} < T < 450^\circ\text{F}$ and $0 < \rho < 1$. Having an expression which relates viscosity to density, it was assumed that Equation (13) could be extended to the case of isothermal moist steam. For 382°F moist steams, Equation (13) becomes

$$\left[\mu_s(\lambda) \right]_{\text{eff}} = 0.1064 \left[\rho_s(\lambda) \right]^{1/3} . \quad (14)$$

Using densities of 382°F moist steams, corresponding effective viscosities were computed. The results are summarized by Figure 6. These data are compared with a linear model proposed by Farouq Ali (25). Figure 6 shows that some 84 percent of the maximum change in estimated effective viscosity occurs between 0 and 10 percent steam qualities; 78 percent of the maximum variation occurs below 5 percent quality. These data are strictly empirical; they reveal possibility rather than fact. However, the moist steam mobility data reported by Kingelin (45) lend strength to this concept; mobilities are shown to vary in the manner implied by Figure 6 and Equation (13).

FIGURE 6

POSTULATED EFFECTIVE VISCOSITY OF 382°F MOIST STEAM



The concept of mobility ratio, defined as

$$M = \frac{k_{rd}}{k_{ro}} \frac{\mu_o}{\mu_d} \quad , \quad (15)$$

has been extensively used as a criterion for fluid displacement efficiency. Subscript "d" refers to the displacing phase while subscript "o" refers to the displaced phase, oil; k_r are the relative permeabilities to the respective phases. Above unity, mobility ratios are said to be unfavorable, and a very mobile fluid inefficiently displaces a less mobile fluid from a porous medium. In waterflooding, mobility ratio is a variable since displacement of oil by water persists after passage of a saturation discontinuity or front. Other than prescribing the nature of the flood's front, it is difficult to characterize a waterflood by a unique mobility ratio. With steam, however, the concept of a constant mobility ratio may be valid during a portion of the flood since there is evidence that steam is the only mobile phase within the steamed region.

At mobility ratios greater than unity, it has been observed that displacement efficiency is aggravated by the development of displacing-phase protuberances called viscous fingers. Van Meurs (84) has obtained photographic evidence that fingering is initiated at mobility ratios greater than unity; its severity was observed to increase with M.

The dynamics of viscous fingering are not fully understood, and presently there is no quantitative means for modifying analytical displacement models for this effect. Currently, it is only possible to show that fingering develops at mobility ratios greater than unity (14,61,70).

It has been proposed that a temperature-saturation discontinuity can be propagated through a porous medium for a critical length of time, the duration of which is a function of steam quality, temperature, and the thermal properties of the porous medium and its surroundings. Due to forward conduction, to convection of vaporized distillation products, and to possible mixing of connate water and steam's liquid phase at the zones' interface, the oil which exists at the steam front possibly has been preheated to steam temperature. Consequently, displacement of oil by steam may be characterized by the mobility contrast exhibited at steam temperature. Such a mobility ratio would be applicable until the critical steam velocity is reached. If there is negligible dilution of the oil by distillation products, oil's viscosity is subject only to responding to the temperature increase. Mobility ratio, being an apparent quality-dependent relationship by virtue of a possible quality-dependent effective viscosity for steam, could be stated as

$$M(T_s, \lambda) = \left[\frac{k_{rs}}{\mu_s} (T_s, \lambda) \right]_{\text{eff}} \cdot \frac{\mu_o}{k_{ro}} (T_s). \quad (16)$$

Currently, it is not possible to quantify relative permeability's response to temperature. Consequently, an effective oil-to-steam viscosity ratio is employed in discussing displacement's dependency upon mobility ratio. Figure 7 illustrates a mobility ratio-type spectrum for a 24.3°API oil and moist steam system at 382°F. A seven-fold increase in effective viscosity ratio is exhibited within a 0-80 percent quality range. Effective viscosity ratio at 0 percent quality and 382°F is 1.8; the measured oil-to-water viscosity ratio at 80°F is 147. Thus, steam would be expected to displace this oil more efficiently at 382°F than would water at 80°F. However, displacement efficiency by steaming would diminish as steam quality increased. It is postulated that low quality steam will displace oil more efficiently than will high quality steam at constant temperature.

As applied to total oil displacement, the pore volume through which steam displaces oil - the critical pore volume - is small at low qualities as indicated by Equation (10). For a constant area normal to the direction of flow, critical distance can be used to specify the critical pore volume. Figure 8 shows computed dimensionless critical distance as a function of steam quality for the experimental systems used in this study. Computations are illustrated in the Appendix. These curves are applicable only for the stated hardware and the imposed experimental conditions.

FIGURE 7

ISOTHERMAL MOIST STEAM - OIL VISCOSITY RATIO

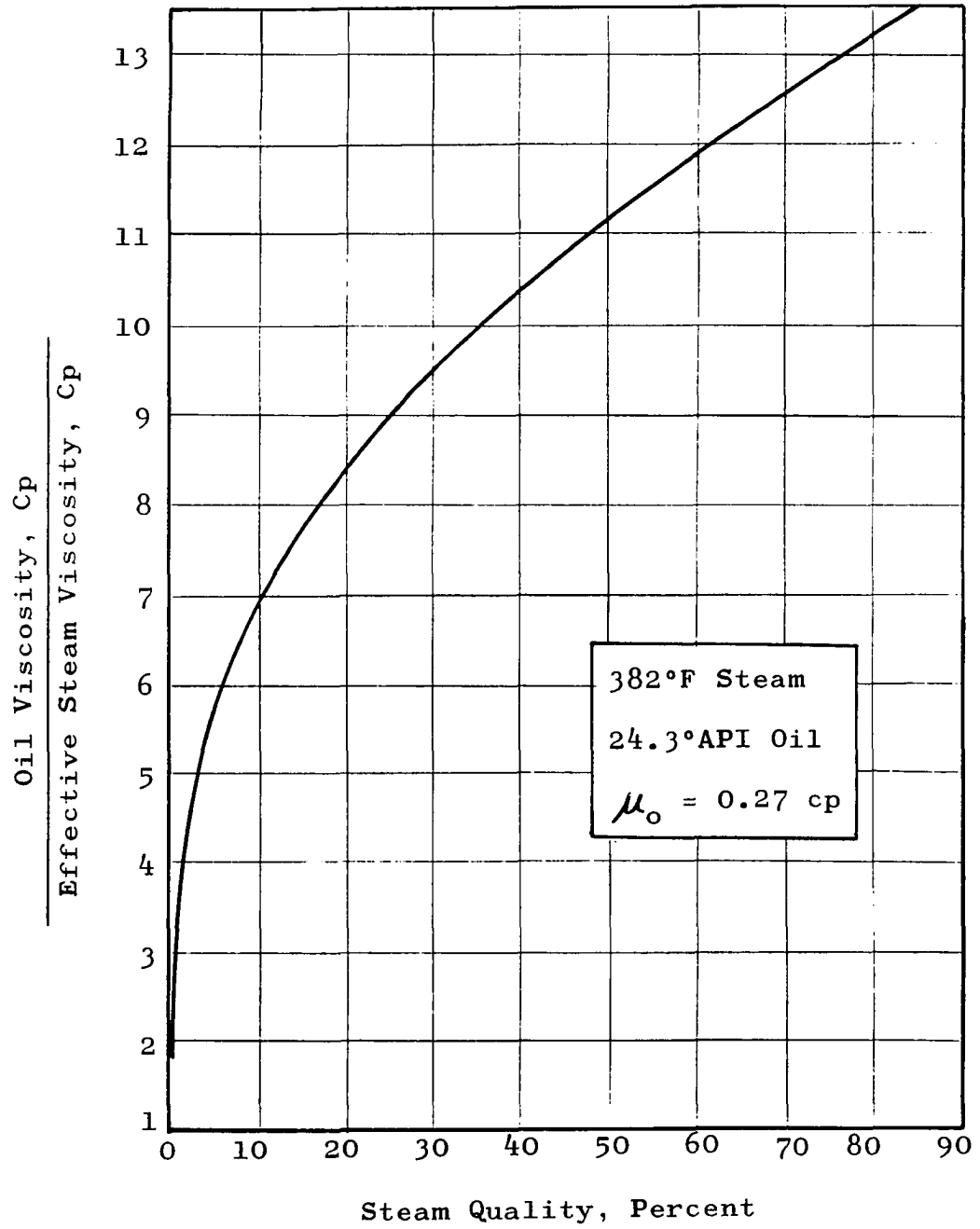
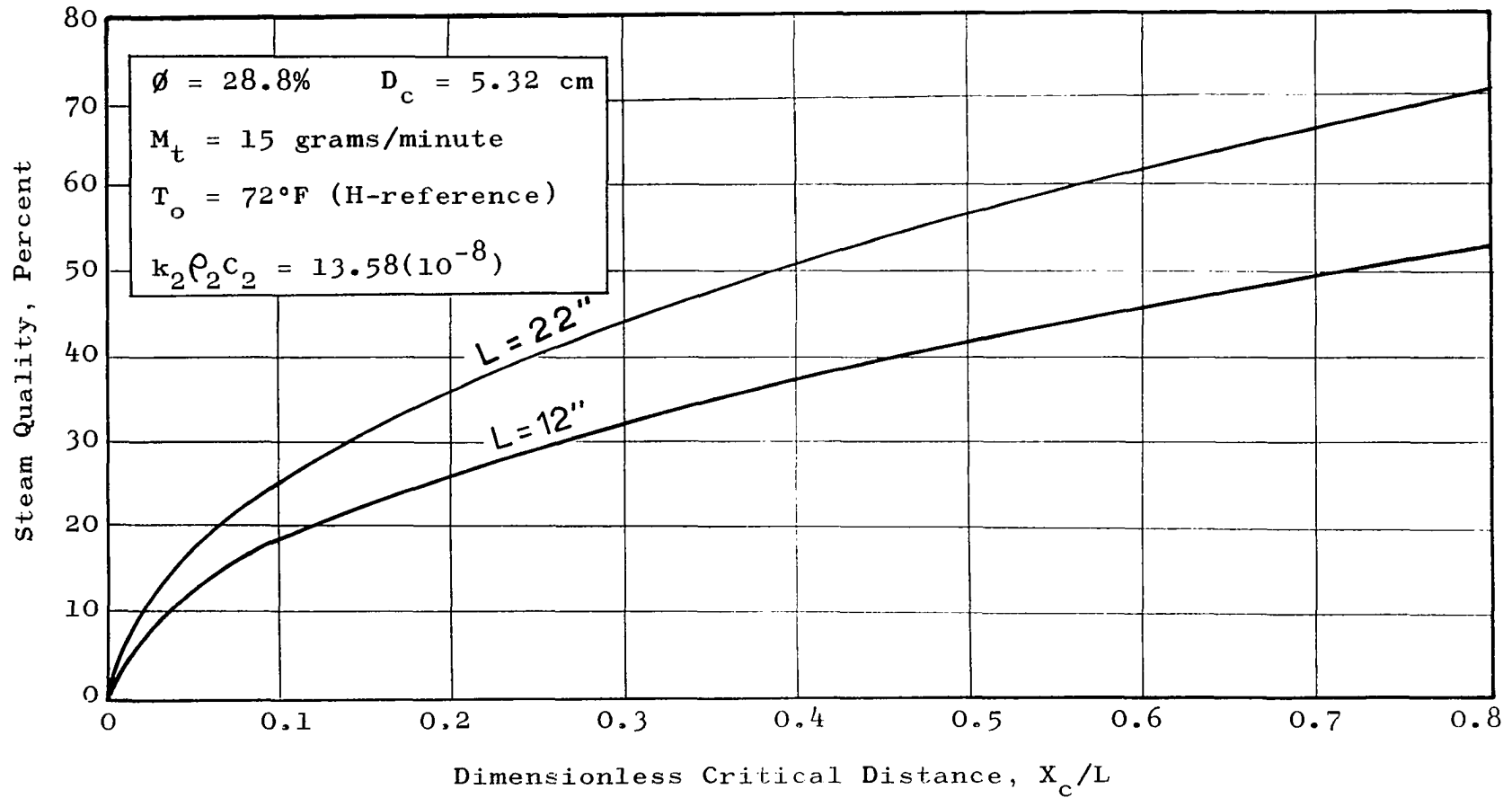


FIGURE 8

DIMENSIONLESS CRITICAL LENGTH, CYLINDRICAL CORE

382°F STEAM, BOISE SANDSTONE



During the time duration between the initiation of injection and the subsequent critical time, some oil displacement is caused by the flow of cool condensate ahead of the steam front. Additional oil displacement occurs as the advancing steam operates on the cool waterflood's residual oil saturation. From the point of view of total displacement, it is postulated that the ultimate desaturation may be examined on the basis of steam displacing oil.

After passage of the critical time, oil displacement within the balance of the conformable zone is postulated to be governed by liquid-liquid displacement principles. Although oil displacement evidently occurs within a temperature field, the magnitude of the total displacement should reflect that which is caused by the flow of saturated water. Since the effective viscosity argument permits greater oil displacement by saturated water than by a higher quality steam, the subsequent contact of the hot waterflood's residual oil saturation by steam should produce no further displacement.

Inasmuch as the apparent properties of moist steam approach those of liquid water as quality approaches zero, there is a tendency to suppose that total displacement efficiency improves with the change in ultimate displacement mechanism. However, a mobility discontinuity at the steam - liquid water phase boundary has been observed (45). Figure 9 shows that the nature of this discontinuity favors oil

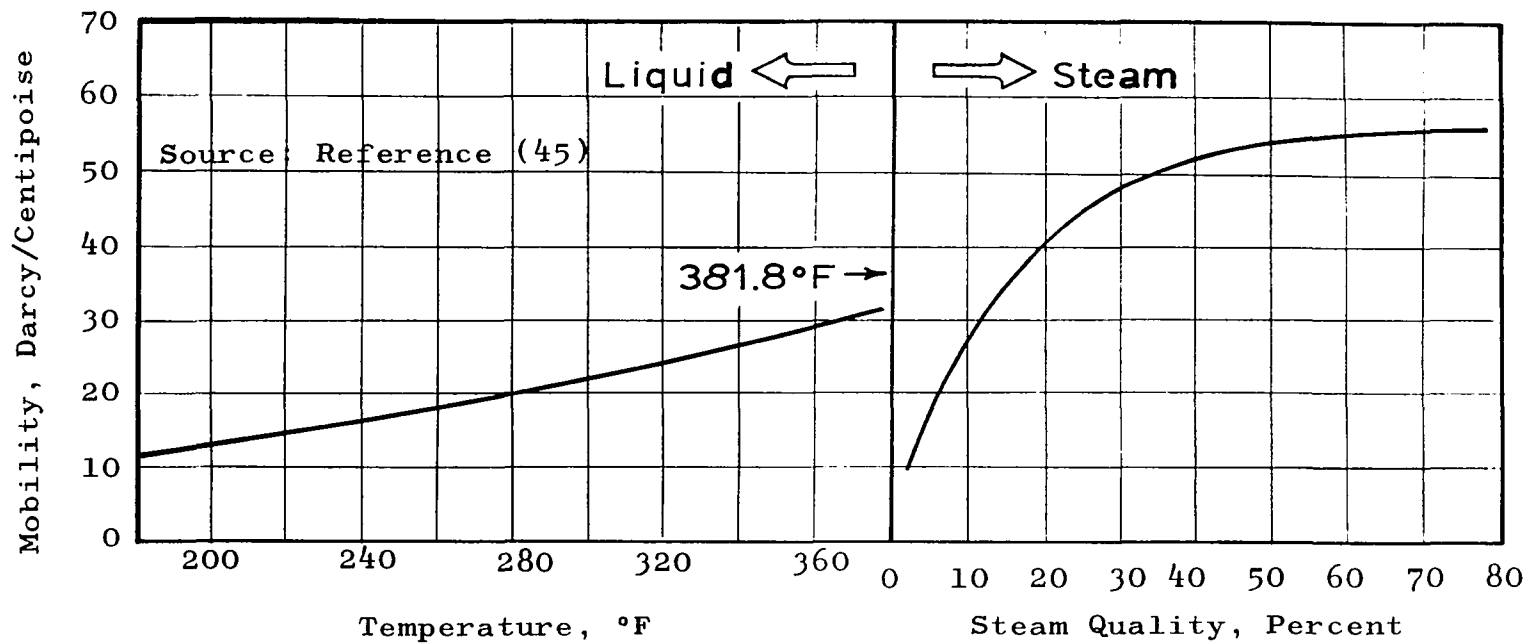


FIGURE 9

ABSOLUTE MOBILITIES OF 200 PSIA SYSTEM WATER

IN BOISE SANDSTONE

displacement by low quality 382°F steam compared with that which undersaturated water might displace.

The theoretically-based apparent change in displacement mechanism combined with a suspected quality-dependent steam-to-oil mobility ratio constitutes the basis for anticipating that ultimate oil displacement can be sensitive to the isothermal quality of the injected steam.

OBSERVED CHARACTERISTICS OF LINEAR STEAM FLOODS

The experimental investigations reported by Willman et al. (90) constitute the most thorough analysis of linear steam drives published to date. The authors proposed that the following mechanisms contributed toward oil recovery:

- a) Steam distillation of oil;
- b) Reduction in oil viscosity due to temperature increase and to dilution by condensing products of distillation;
- c) Thermal expansion of oil.

The authors also attributed some benefit to a mechanism which they categorized as a gas drive effect; this process was not clearly described.

The role of steam in their study was shown to be three-fold:

- a) Added volume flux is provided by steam;
- b) System temperature is significantly raised above its original level;
- c) Hydrocarbons exhibiting a high partial pressure are subject to vaporization upon being contacted by steam.

Experiments were performed at 330°F using 100 percent

quality steam. Conventional and hot waterfloods were executed to demonstrate the benefits of heat injection and the superiority of steam over liquid injection.

Using a refined oil enriched with a volatile component, the authors show that a small zone of distillate can accumulate immediately ahead of an advancing steam front.

Willman et al. observed that ultimate oil production was essentially established upon achieving breakthrough of the steam front. Transient recovery performances of conventional and hot waterfloods and steam floods followed the same depletion history during early stages of each process. Water breakthrough with hot water injection occurred at the same stage of depletion as that with cold waterfloods. Earlier water breakthrough was reported for steamfloods, but this phenomenon was not explained. Conversely, Abbasov et al. (1) observed that water-free oil production persisted for a greater duration with steam injection than with waterflooding.

A sequence of temperature profiles submitted by Willman et al. indicate that a fairly large condensate bank formed ahead of their laboratory steam fronts. Some five hours were required to steam flood their three-foot length core; evidently, conditions were in effect which would permit condensation of steam with relative ease due to an apparent high rate of heat loss. Liquid rather than vapor displacement of oil was induced.

Based on data submitted by Willman et al., Figures 10 and 11 are included to summarize the saturation and temperature profiles which apparently prevailed during their experiments with steam injection.

FIGURE 10

SATURATION PROFILE: WILLMAN EXPERIMENTS

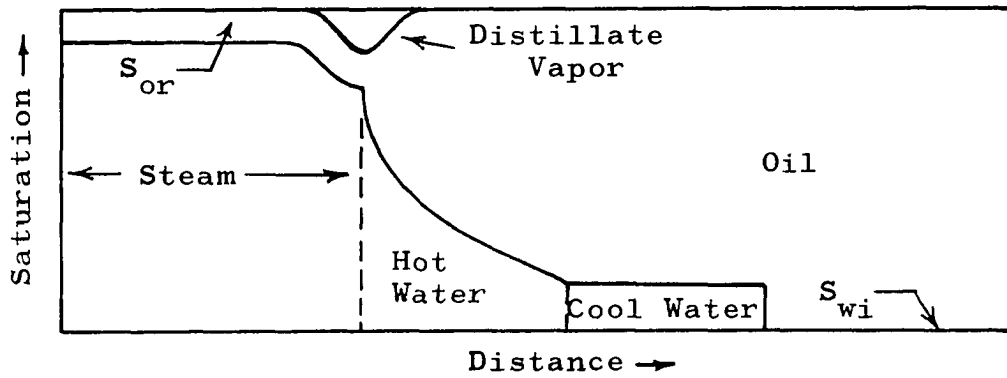
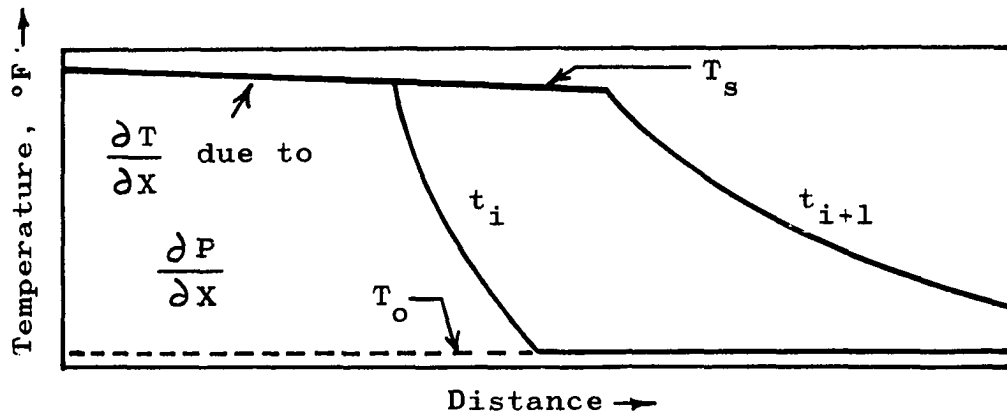


FIGURE 11

TEMPERATURE PROFILES: WILLMAN EXPERIMENTS



EXPERIMENTAL EQUIPMENT, CORE AND OILS' PROPERTIES

Basis For Equipment Design

The primary aim of this research was to identify a possible effect on oil recovery caused by injecting isothermal steam at various qualities. A laboratory system was employed which permitted control of the primary variables and which allowed variables of no interest to this study to be held constant while accommodating the imposed temperatures and pressures. The basic requirement was the construction of a steam generation apparatus capable of delivering isothermal steam of a determinable quality.

Core Holder

The core holder employed is a Hassler-type apparatus capable of accommodating maximum conditions of 500 psia and 500°F. A cross-sectional view of the Hassler system containing a core is presented by Figure 12.

The outer pipe shell and its threaded closures are constructed of Monel steel. The sandstone core was inserted into a fluoro-elastomer rubber sleeve capable of accommodating design conditions. Monel steel manifolding

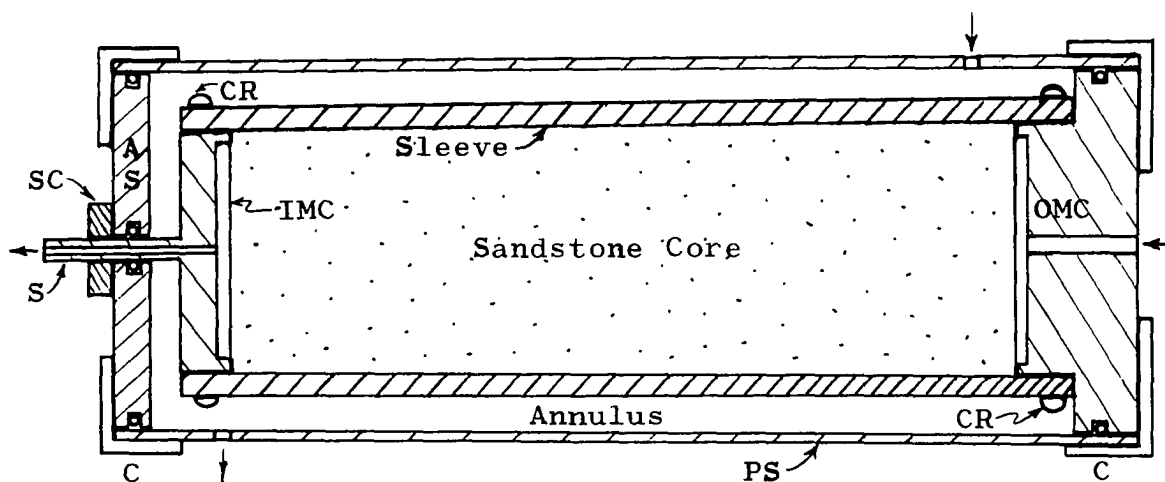
connectors were inserted into either end of the sleeve and abutting the core. The connectors were retained by steel clamp rings which were forced over the ends of the sleeve. Pressure sealing between the manifolding connector's stem and the annulus seal-plate is accomplished by using O-rings. Likewise, O-rings provided effective pressure confinement at the annulus seal-plate - pipe shell interface.

During preliminary testing of the core holder system, it was observed that pressure continuity between the Hassler annulus and the core was eliminated by maintaining at least 100 psi differential across the rubber sleeve. During all experiments, fluids were injected into the core at 200 psia while annulus pressure was maintained at 330 psi. The higher annulus pressure compressed the rubber sleeve tightly around the cylindrical core. It was observed that the rubber sleeve had a tendency to shrink and further compress around the core after being subjected to heat. An examination of recovered sleeves showed their inner surface to be clearly embossed by the sand grains contacted by rubber.

The core holder was tested for leaks and for communication between the annulus and the core before and after each experiment. It was observed that the O-rings tended to lose elasticity after repeated exposure to heat. These were replaced regularly to ensure safe operating conditions.

FIGURE 12

HASSLER-TYPE CORE HOLDER



- AS = Annulus seal-plate
 C = Closure cap (female threads)
 CR = Clamp ring
 OMC, IMC = Manifold connectors
 S = Stem, outlet manifold connector
 SC = Stem clamp
 PS = Pipe shell (male threads)

Equipment

Fluid injection to the core was provided by a double simplex metering pump. Precise control of volume rate was available through a variable stroke-length feature of each liquid end. Water for annulus pressure control was provided by a single simplex metering pump.

Constant back-pressures on the core and annulus systems were maintained by dome-loaded valves rated at 2000 psia and 150°F. Dome pressure was provided by nitrogen. On hot effluent lines, it was necessary to install heat exchangers ahead of these valves in order to cool the fluids to the valves' temperature rating.

Pressures were monitored using pressure transducers and a multi-channel chart recorder. Temperatures were monitored using thermocouples and a multi-channel chart recorder. Pressures could be recorded to the nearest 0.5 psig; recorded temperatures could be read to the nearest 1°F. Occasional checks during the course of calibration showed that recorded steam saturation conditions were in excellent agreement with published data.

Hot fluids were prepared by pumping water through electrically heated stainless steel tubing. By applying voltage across the tubing, a heating effect was produced which is analogous to the operating principle of the incandescent light bulb. One heat generator was used to

supply superheated steam to the core's inlet manifold; an identical generator was employed to provide hot water at steam temperature to the Hassler annulus. Manual control of temperatures was provided by variable transformers for each heat circuit. Sensitivity was improved by installing 3.58:1 voltage step-down transformers in series with the variable transformers. For the stainless steel tubing used as heating elements, it was determined that a 0-140 volt, 50 amp variable transformer (Powerstat) would adequately serve heating requirements for water injected into the Hassler annulus. A 0-115 volt, 15 amp variable transformer was adequate for generating superheated steam for core injection lines.

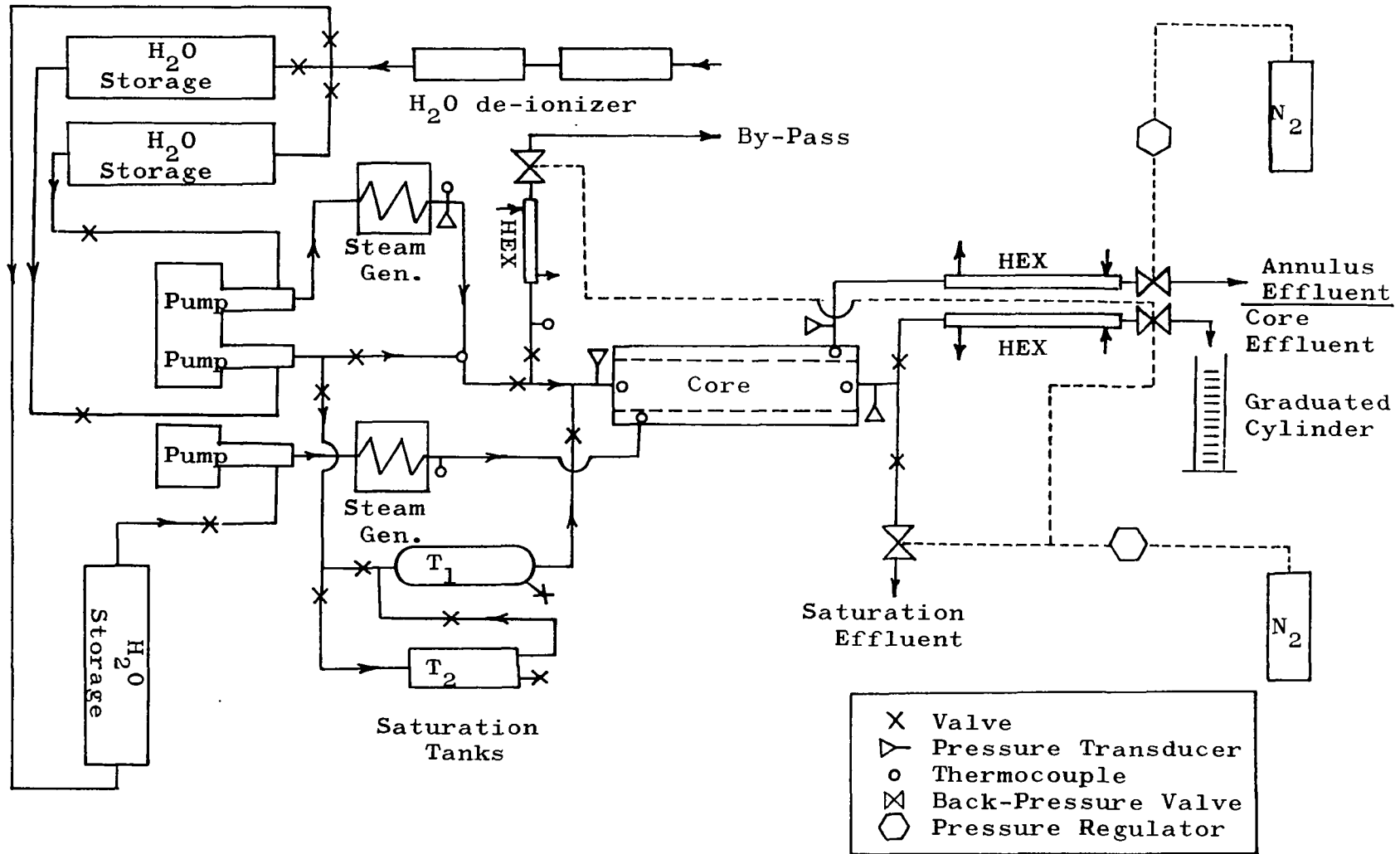
The volume of all saturation, injection, and efflux lines were measured for use in material balance computations. Stainless steel tubing and fittings were used throughout the system.

All heated lines and the Hassler core holder were insulated with Urethane non-burning insulation. This commercial insulation has a density of 1.9 lb/ft³ and a thermal conductivity of 0.15 BTU/ft²-hour per °F/inch temperature gradient.

A schematic of the experimental apparatus showing all fluid circuits and storage vessels is shown by Figure 13.

FIGURE 13

DIAGRAM OF EXPERIMENTAL EQUIPMENT

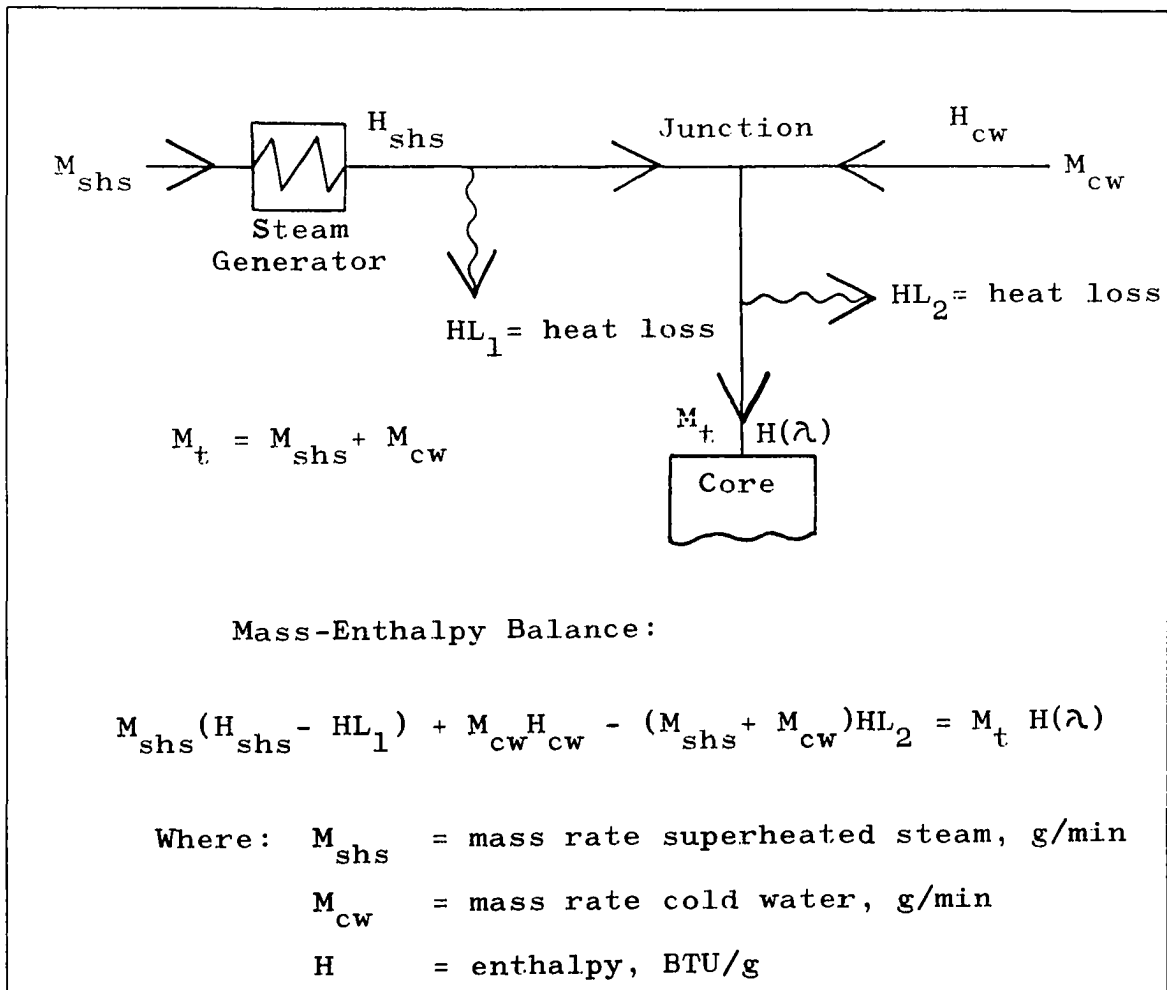


Preparation of Isothermal Moist Steam

Moist steam at 382°F (200 psia) was prepared by commingling cold water at 200 psia and 450°F-600°F superheated steam at 200 psia in proper mass-enthalpy proportions. Heat loss data were measured, and steam quality was computed. This process is summarized by Figure 14.

FIGURE 14

DETERMINATION OF INJECTED ENTHALPY, $H(\lambda)$



Enthalpy of the superheated steam leaving the steam generator was determined by noting its temperature and pressure and by referring to published data(21,42). The enthalpy of cold, compressed water was determined in a like manner. Heat losses, HL_1 and HL_2 , were measured by flowing superheated steam or hot water through the indicated lines and observing the temperature drops; the corresponding heat losses were obtained from published data (21,42). Steam quality, λ , was calculated by using Equation (1).

Porous Medium

Linear flow experiments were conducted using Boise sandstone as the consolidated porous medium. The sandstone was obtained from an Idaho quarry. Cylindrical cores were machined to accommodate the core holder's dimensions. The two cores used in this study were steamed repeatedly prior to initiating oil recovery experiments.

Porosity of the sandstone cores was 28.8 percent. Permeability at 200 psia proved to be sensitive to temperature. Figure 15 shows that permeability to water at 200 psia increased from 3.436 darcies at 80°F to 4.356 darcies at 380°F.

Boise sandstone - a medium grained, yellowish-gray, well-cemented micaceous and feldspathic sandstone - was chosen because of its low clay content and absence of soluble carbonates. Mineralogical properties are presented in Table 2.

FIGURE 15

PERMEABILITY VARIATION WITH TEMPERATURE, BOISE SANDSTONE

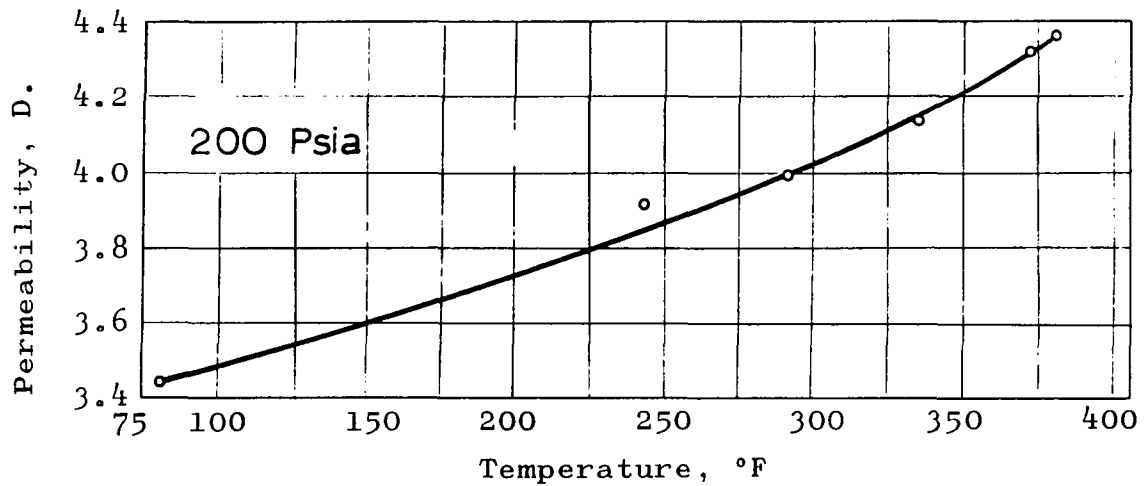


TABLE 2

MINERALOGICAL PROPERTIES OF BOISE SANDSTONE

Composition, Percent By Weight

<u>Quartz</u>	<u>Feldspar</u>	<u>Carbonates</u>	<u>Clays</u>	<u>Fe-Ti Minerals</u>
45*	45*	0*	9*	1*
40**	35**	NR**	NR**	NR**

* Reference (73)

** Reference (76)

NR = Not Reported

Crude Oils

The response to moist steam injection exhibited by three crude oils was examined. In order to obtain performance data for both relatively light and heavy crudes, it was initially surmised that samples within a 15°API to 30°API gravity range would suffice. It was felt that a light crude might amplify distillation effects while benefits due to viscosity reduction would be made apparent by a heavy crude. The oils used in this study have gravities of 27.8°, 24.3°, and 15.4° API. Densities were measured, and the corresponding gravities were corrected to the 60°F reference (30).

The manner in which each oil's viscosity responds to temperature is shown by Figure 16. Viscosities at temperatures in excess of 200°F are estimated by extrapolation on Figure 16 (26). The oils' density characteristics with temperature are summarized by Figure 17; densities in excess of 200°F are obtained by extrapolation. Distillation characteristics at atmospheric pressure are shown by Figure 18. These data were obtained according to the ASTM standard procedure (62).

FIGURE 16

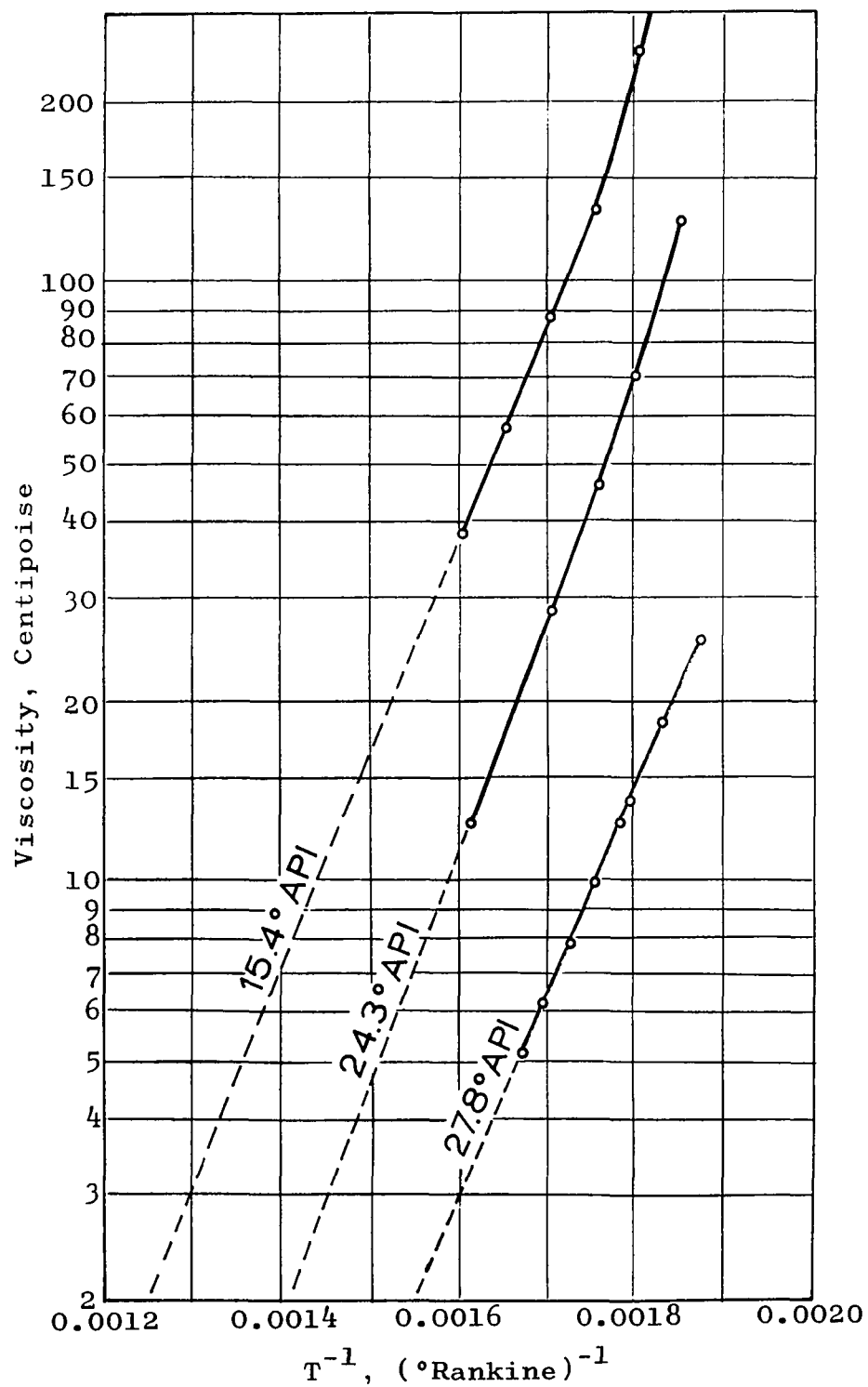
OIL VISCOSITY, CP., VS. T^{-1} , $^{\circ}\text{R}^{-1}$ 

FIGURE 17

OIL DENSITY VS. TEMPERATURE

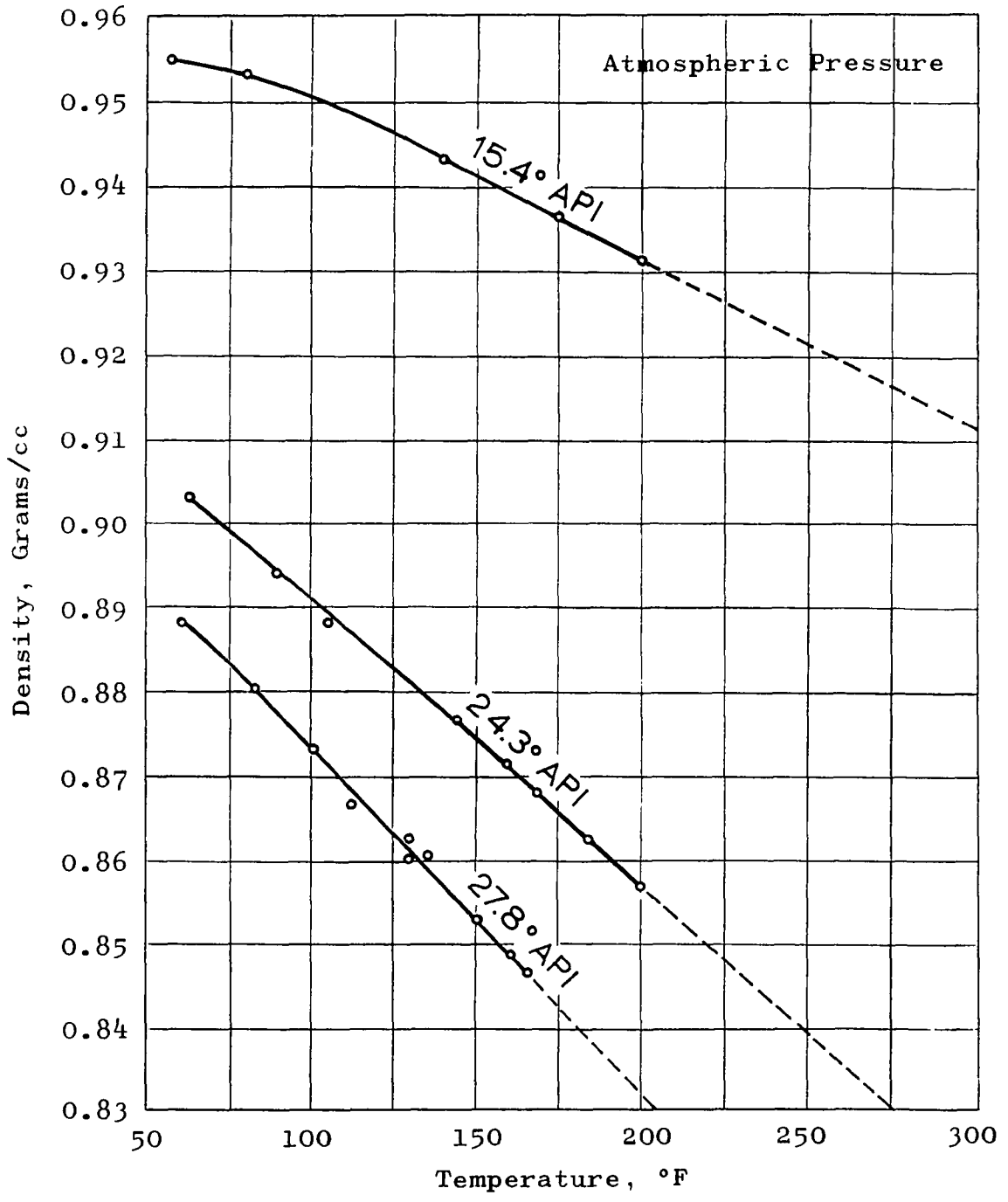
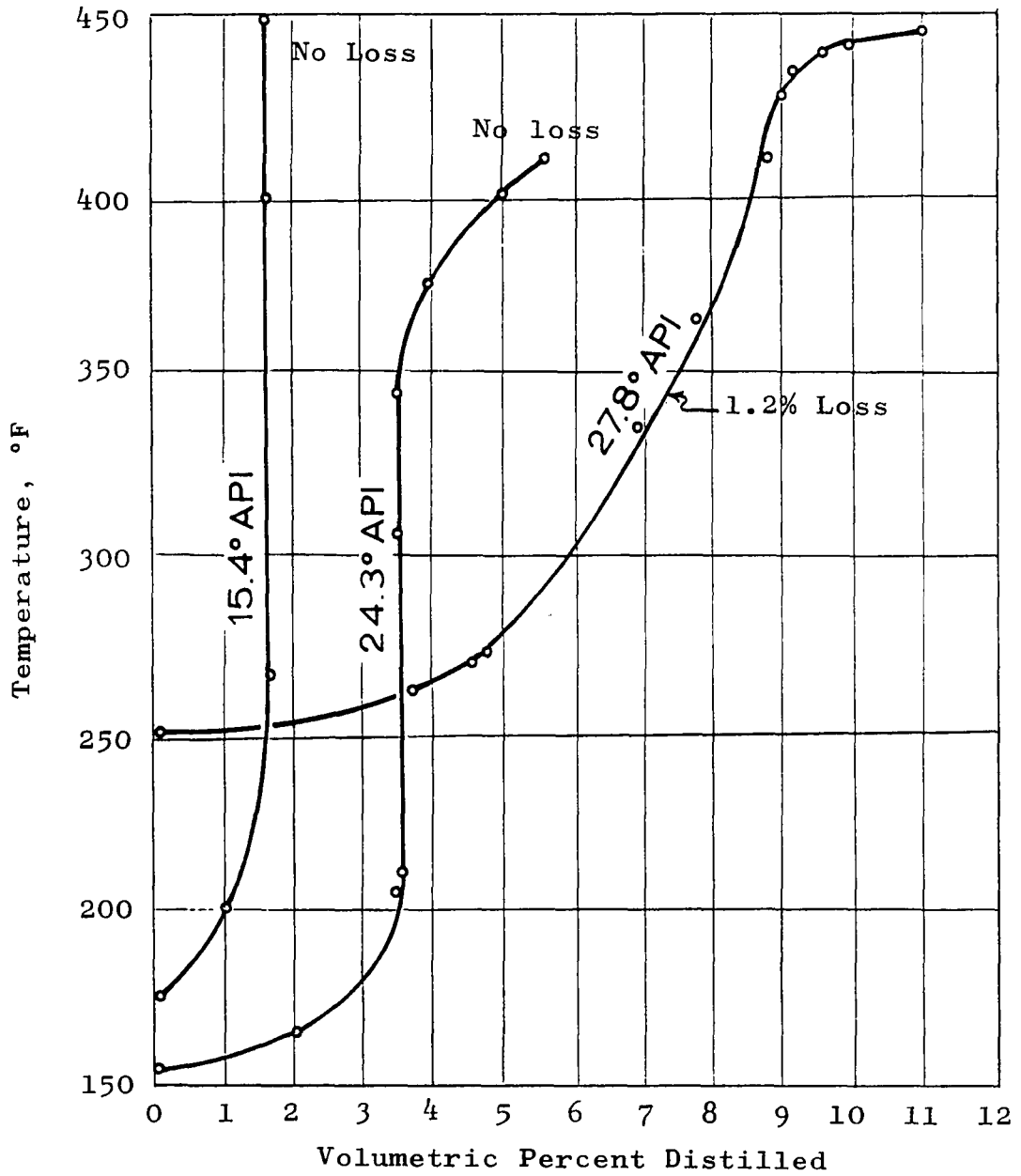


FIGURE 18

ASTM DISTILLATION CURVES



EXPERIMENTAL PROCEDURE

Preparation

Prior to each experiment, the Hassler system was tested to ensure that there was no pressure communication between the annulus and the core.

The core was initially saturated with distilled, de-ionized and deaerated water by applying a partial vacuum on the downstream side and slowly injecting water. Injection of water was continued until all lines and manifolding were filled. Crude oil was then pumped into the core by displacing the crude from an auxiliary vessel with water. During each oil saturation maneuver, pressure in the Hassler annulus was maintained at least 130 psi higher than the core injection pressure.

Coincident with initiating oil injection, the core's effluent was collected in graduated cylinders. Oil injection was continued until no water could be detected in the core effluent. Saturation was determined by material balance.

The saturated core was isolated from the injection lines, and conditioning of steam was initiated. To ensure that steam rather than liquid would be injected, steam was circulated through the inlet manifolding until temperature

at the steam-water mixing tee had stabilized at 382°F. Final mass rate adjustments were then made to assure that steam of the desired quality was available.

Prior to injecting steam into the core, the heat loss between the steam generator and the steam-water mixing tee, HL_1 (See Figure 14), was evaluated. Cold water injection to the mixing tee was temporarily suspended. This caused the temperature at the mixing tee to respond to the superheated steam flowing from the steam generator. Mixing tee and generator temperatures were continuously recorded until a constant differential was established. The difference in corresponding enthalpies constituted HL_1 . Cold water pumping was resumed, causing the mixing tee temperature to revert to 382°F.

Execution

Simultaneously with the introduction of steam into the core, the temperature of water entering the annulus was raised from room temperature to 382°F. An annular injection rate which would permit a realistic rate of heat loss from the steam-bearing core had been established during preliminary experiments. For example, from a zone bounded by strata having a thermal conductivity of 1.5 BTU/ft-hr-°F and a thermal diffusivity of 0.048 ft²/hr (56), an initial heat loss flux of 0.02 BTU/min-cm² could occur for a 310°F temperature increase. As illustrated in the

Appendix, the imposed annular injection rate, 98 cc/min, permitted an apparent average heat loss flux from the steamed core of 0.025 BTU/min-cm².

Incremental oil production arising from steam injection was recorded until the core's effluent became emulsified. Direct observation of oil and water volumes was impossible thereafter. The balance of the production was collected in a number of graduated cylinders. The oil-in-water emulsions were treated by adding concentrated H₂SO₄ such that its concentration in the oil-water mixture was two percent by volume. Preliminary work with artificially produced emulsions indicated this to be an optimum treatment for the three crude oils employed.

During all experiments, steam injection was maintained until it was evident that oil production had ceased. At least two pore volumes of liquid water were injected as steam following steam breakthrough to ensure that the experiment's maximum oil recovery had been achieved.

Prior to terminating steam injection, the heat loss between the mixing tee and the core inlet, HL₂ (Figure 14), was evaluated. As with HL₁, this was determined by noting the temperature difference exhibited by a single-phase fluid of known enthalpy between these two control points. Because of its relatively low specific heat, superheated steam could not be maintained between the mixing tee and the core's inlet for an injection rate of 15 g/minute. Hence,

it was necessary to employ hot water. Cold water pumping was suspended, and the discharge rate to the steam generator was increased such that a rate equivalent to the experiment's total mass rate resulted. Core and annulus pressures were raised until the temperature of liquid water at the mixing tee was 382°F. Injection of water was maintained until mixing tee and core inlet temperatures stabilized. The resulting temperature drop was used in calculating HL_2 .

After heat injection was terminated, the system was permitted to equilibrate with room temperature. Five pore volumes of Chloroethene (CH_2Cl_2 ; density 1.437 g/cc @ 20°C; boiling point 74°-76.5°F @ 14.7 psia) were injected through the core. The system was allowed to stand overnight, and the core was subjected to a 382°F high quality steam flood. Preliminary work had shown this procedure to be quite effective in removing residual oil from the core.

Water saturation, oil saturation, steam injection and cleaning manuevers were repeated for each experiment. The heat losses, likewise, were measured during each experiment.

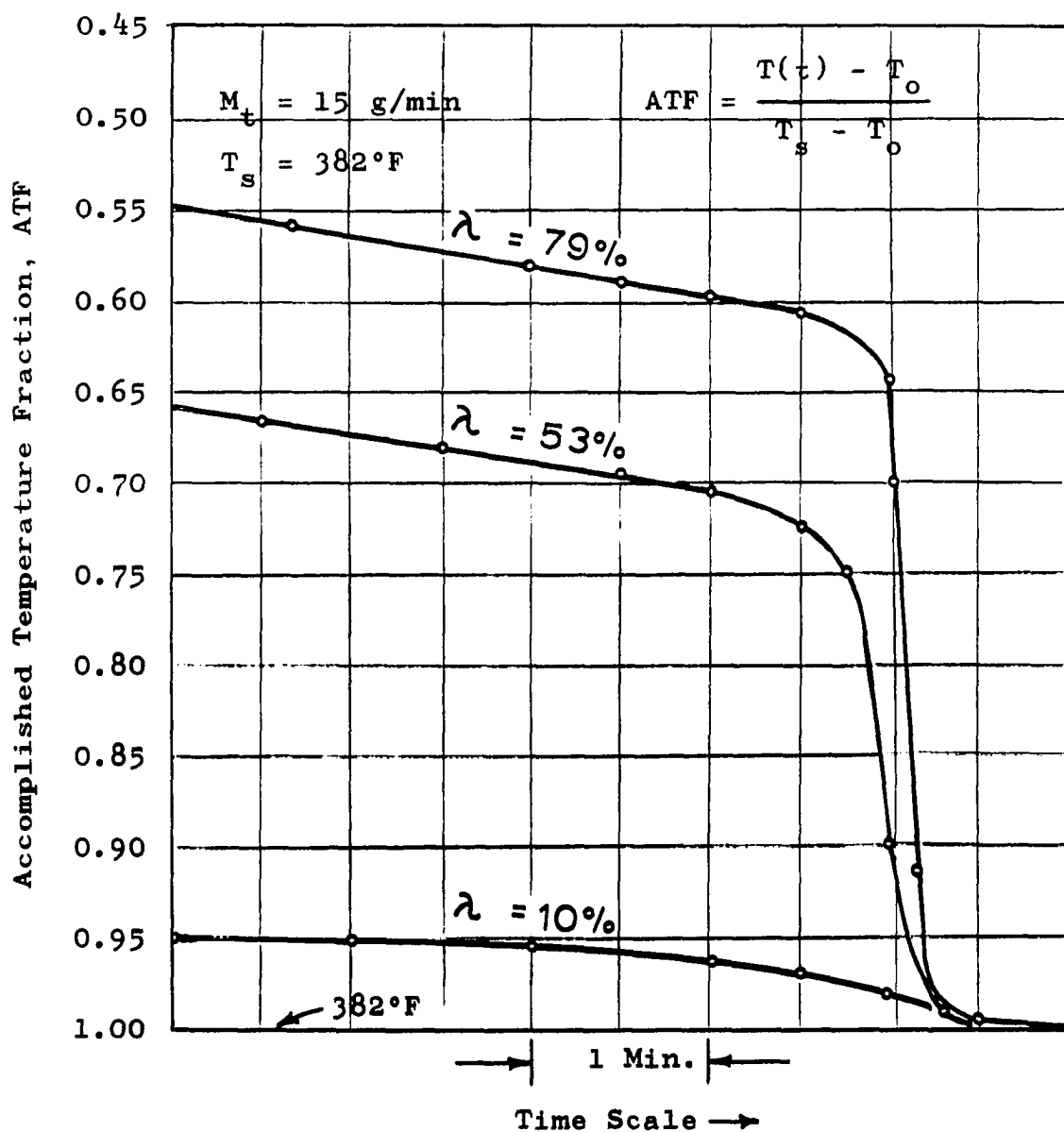
SUPPLEMENTARY EXPERIMENTS AND OBSERVATIONS

Inasmuch as the core's bounding media consisted of a rubber sleeve, annulus water, and the core holder shell, it was necessary to determine an equivalent heat parameter, $k_2 \rho_2 C_2$, for the core's surroundings. The equivalent heat parameter is used in association with Equation (10) in quantifying the system's critical lengths. Experiments designed to obtain this quantity and heat loss data were performed by injecting moist steam into the core saturated with water. The computation of $k_2 \rho_2 C_2$ is illustrated in the Appendix.

During the course of preliminary experimentation, some characteristics of effluent temperatures were observed which tended to enforce the presuppositions regarding the postulated convective heat loss characteristic of steam flow. Figure 19 shows that a diffused effluent temperature profile occurred for low quality steam injection. At higher qualities, the temperature history tended to approach that of the idealized shock concept employed by Marx and Langenheim (56). Effluent temperature histories for steam qualities in excess of 80 percent were virtually identical; those at lower qualities tended to be diffused.

FIGURE 19

EFFLUENT TEMPERATURE HISTORIES



Although Willman et al. (90) presented experimental evidence in the form of effluent compositions that products of distillation apparently accumulate immediately ahead of an advancing steam front, complementary thermal evidence was not submitted. Figure 20 shows several effluent temperature histories which were recorded during cleaning maneuvers. Histories of this type were observed at breakthrough of steam-chloroethene fronts. These data indicate that a mixture of water and chloroethene boils at 302° - 305° F at a pressure of 200 psia. A small slug of solvent was produced in association with each front; on the curve identified as Number 8, 2.5 cc of chloroethene were collected at breakthrough. These data indicate that the composition of the steam-chloroethene front can be as depicted by the following sketch.

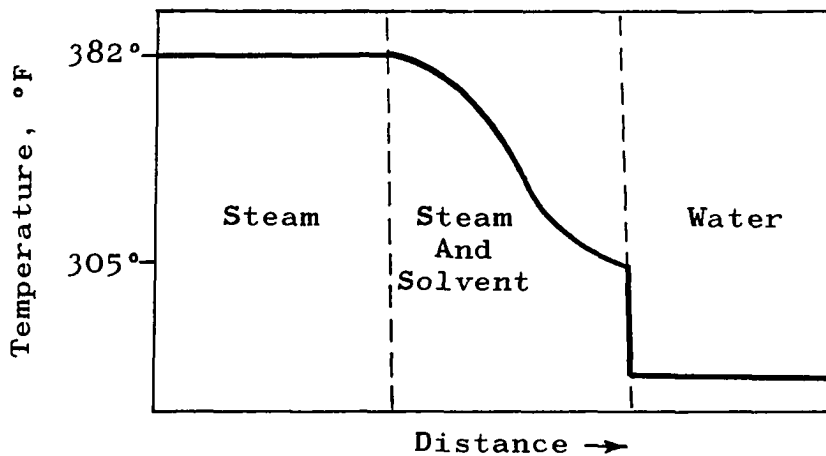


FIGURE 20

TEMPERATURE PROFILES OF STEAM-SOLVENT BREAKTHROUGH

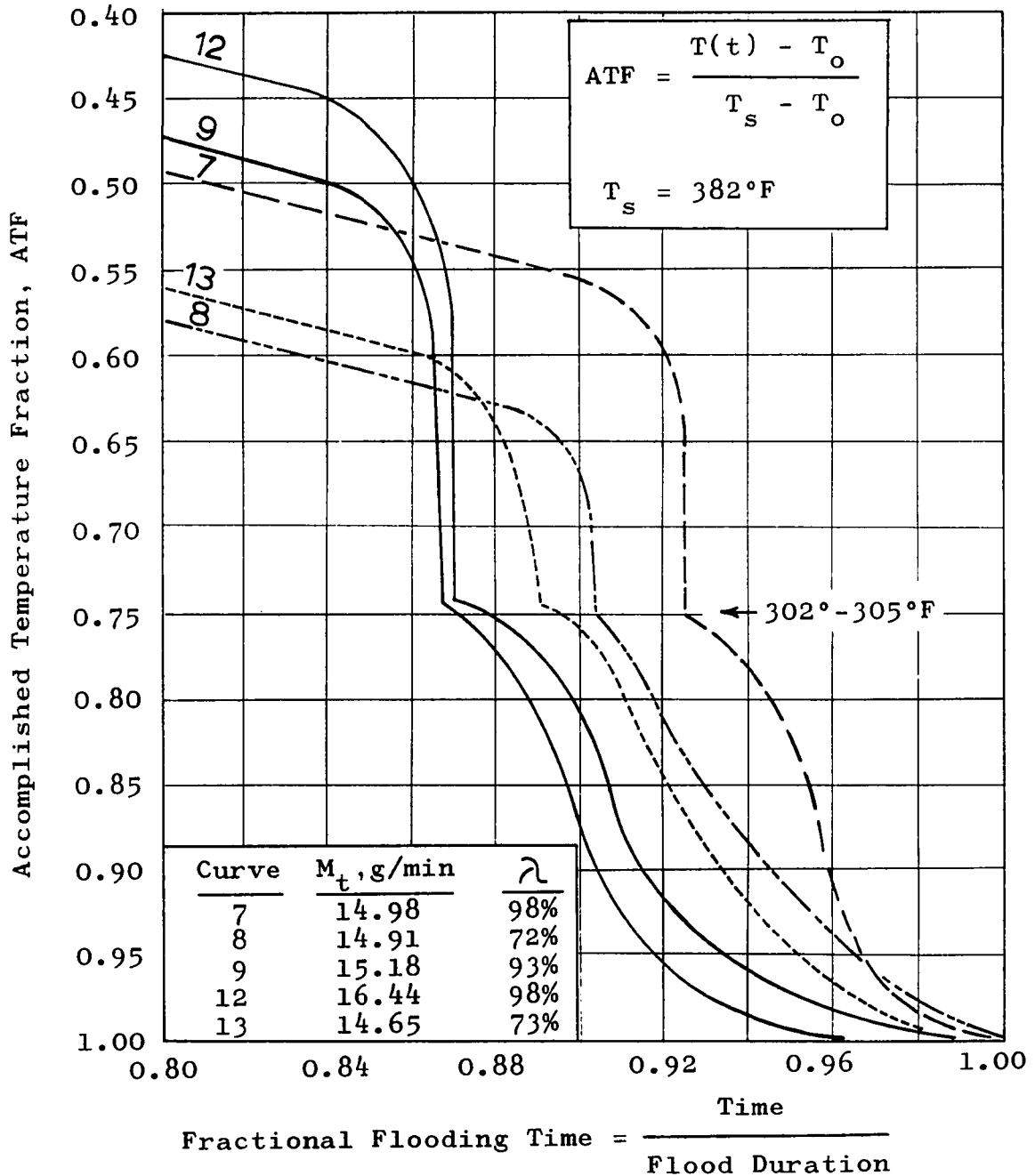
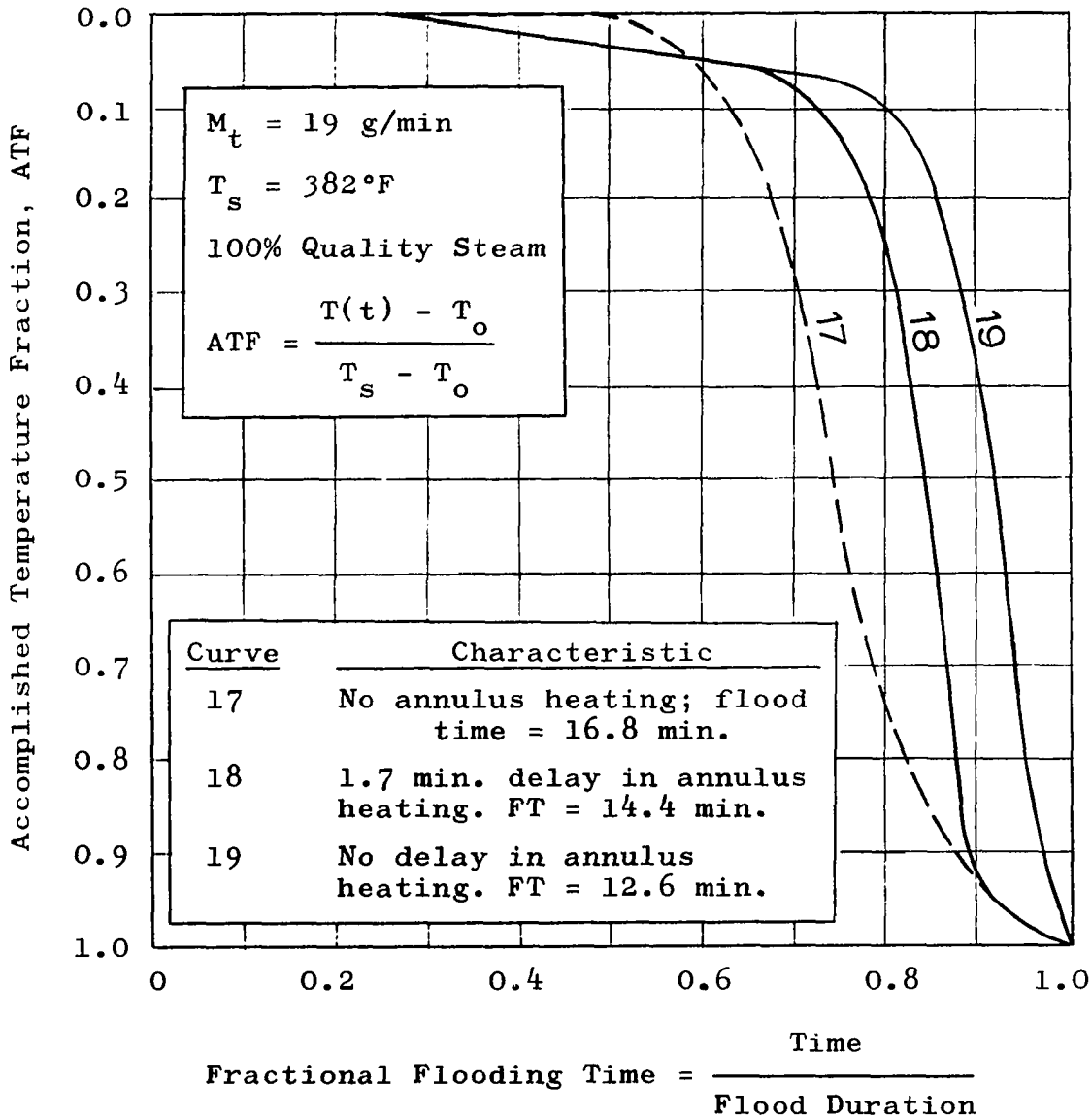


Figure 21 shows why it was necessary to inject hot water at steam temperature into the Hassler annulus simultaneously as steam was injected into the core. Curve 17 shows that 100 percent quality steam could not be injected using a cold annulus without forming a bank of condensate ahead of the front. Curve 18 shows that a 0.118 of flooding time delay in annulus heating extended flooding time by an equal amount; a small bank of condensate is indicated.

The response shown by Curve 17 of Figure 21 illustrates the consequence of imposing a higher thermal conductivity on the core's bounding media. Reference to Equation (10) reveals that a linear system's critical distance is approximately proportional to the inverse of the adjacent media's thermal conductivity. By injecting hot water into the core holder's annulus during oil recovery experiments, a lower effective thermal conductivity for the core's adjacent media was induced. This permitted a steam front to be propagated through the core without forming a hot water bank as specified by the critical distance concept.

FIGURE 21

EFFECT OF ANNULUS HEATING ON FLOODING TIME



PRESENTATION AND DISCUSSION OF RESULTS

Types of Data Presented

The primary objective of this study was to assess the possible influence of isothermal steam's quality on steam's ability to displace crude oil from a consolidated porous medium. The basic data illustrating this and accompanying effects are presented graphically as Percent Oil Recovery versus Quality of 382°F injected steam. Oil recovery applies strictly to that which was removed from a conformable zone - a ratio of volume removed to original volume contained by the conformable zone.

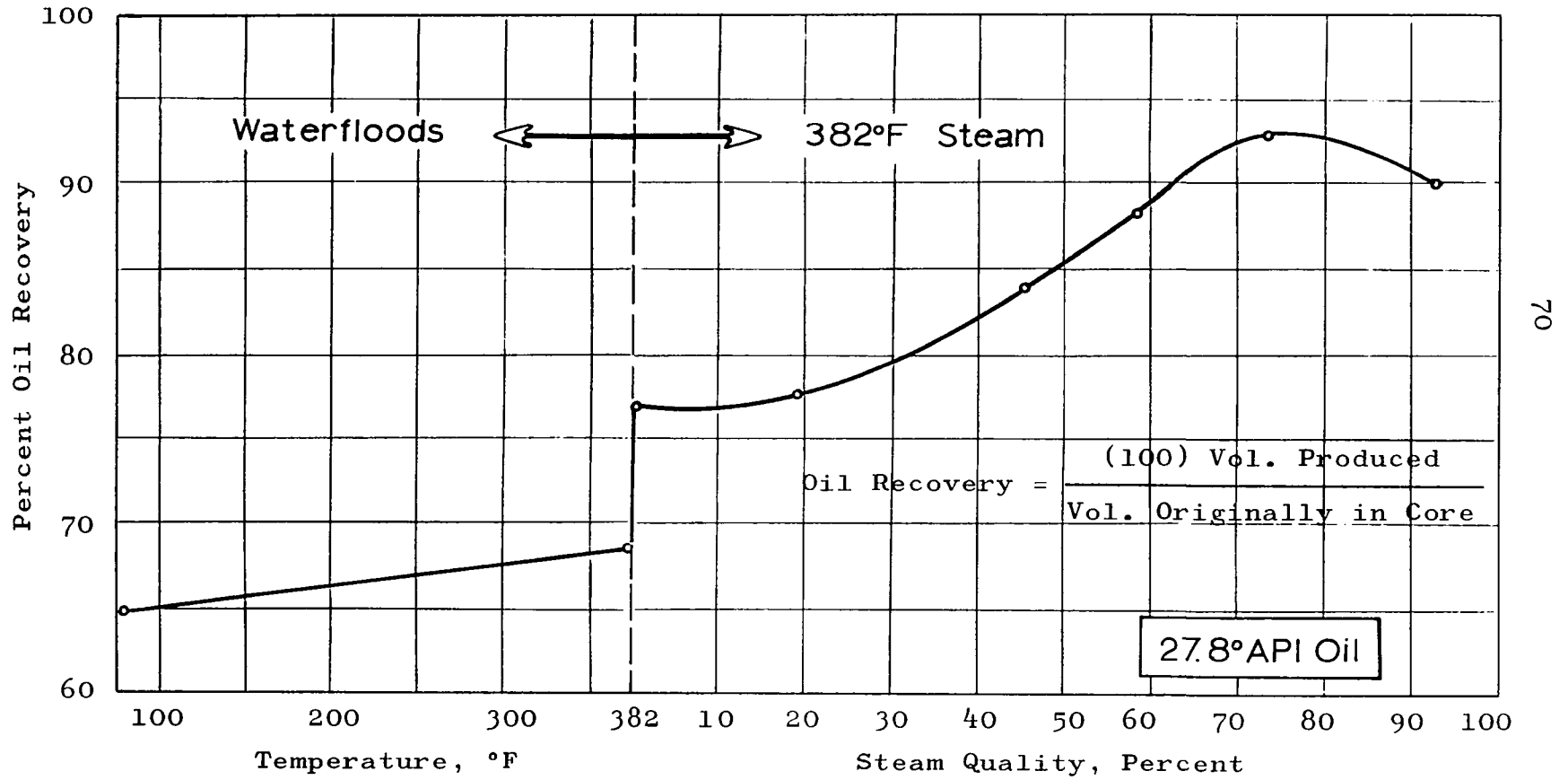
Incremental production data are presented as: (a) Percent Oil Recovery versus Pore Volumes of Liquid Production; and (b) Cumulative Water-Oil Ratio (WOR) versus Percent Oil Recovery. These data apply to a conformable zone.

Experimental Results: 27.8°API Crude Oil

Figure 22 is a composite presentation of waterflood and steam flood recoveries. While most industrial applications of steam injection have been devoted to oils within a 10°-20°API gravity range, the 27.8°API oil was tested on the premise that distillation effects would be amplified.

FIGURE 22

OIL RECOVERY BY HOT FLUID INJECTION: 27.8 API OIL



By the ASTM technique(62), 8.2 volume percent oil was distilled at 382°F; a loss of 1.2 volume percent occurred in this test. (See Figure 18) Viscosity at 80°F was 21 centipoise; estimated viscosity at 382°F is 0.12 centipoise. (See Figure 16) Oil-to-water viscosity ratios at these temperatures are 24.4 and 0.86, respectively.

Waterflood recovery at 79°F was 64.7 percent compared with 68.3 percent at 374°F. Although a 175-fold decrease in oil viscosity occurs as its temperature is raised from 79°F to 374°F, oil recovery by waterflooding exhibited only slight response to temperature. It will be shown in a subsequent section that a diminution of k_{ro}/k_{rw} with temperature increase tended to counteract the apparent benefit of viscosity reduction.

The oil recovery discontinuity at 382°F (0% steam) shown by Figure 22 is attributed to steam distillation. At 0 percent steam quality, 76.8 percent oil recovery was realized. Compared with the 374°F waterflood's recovery, an additional 8.5 percent was recovered by steam injection relative to waterflooding at approximately the same temperature. That this figure is in good agreement with ASTM distillation recovery at 382°F may be fortuitous; no such correspondence was observed with the two other crudes.

With moist steam injection, oil recovery increased as quality increased from 0 percent to 73.4 percent. At 92.9 percent quality, recovery was 2.9 percent less than

that at 73.4 percent quality steam. This trend was verified by duplicate experiments. Reproducibility was 0.5 recovery percent. It should be emphasized that the data points shown by Figure 22 represent individual experiments.

According to proposed theory, a 73.4 percent quality steam front can be propagated through 85 percent of the linear extent of the employed core before formation of a hot water bank is initiated. (See Figure 8) Likewise, steams of 85 percent and higher qualities can travel through the subject system without convective heat loss. Hence, oil recoveries at 73.4 and 92.9 percent qualities reflect essentially oil displacement by steam with little intermediate waterflooding at 80°F. As it has been observed that moist steam's mobility can increase with quality (45), a more unfavorable steam-to-oil mobility ratio occurs as steam's quality increases. The decrease in oil recovery at 92.9 percent quality is thought to reflect the consequences of the mobility ratio becoming more unfavorable.

Kingelin's observations regarding the mobility of moist steam indicate that oil recovery should decline as steam quality increases (45). Figure 22, however, shows that oil recovery increased as the quality of injected steam was increased. The present data do not refute Kingelin's contention, however, since two different displacement mechanisms operating according to the critical distance concept are thought to have produced the results shown by Figure 22.

In a subsequent section of this report, it is shown that when incremental recoveries attributed to steam-oil and water-oil displacements are weighted according to the critical distance concept, a total recovery curve very similar to that illustrated by Figure 22 results. Further evidence that a transition in basic displacement mechanism occurred at low steam qualities is provided by incremental oil recovery data. Figure 23 relates fractional oil recovery to pore volumes of produced liquid for the various steam qualities and waterfloods. Slightly greater water-free oil production occurred with steam injection relative to waterflood performance; this is consistent with Abbasov's observations (1) but contrary to Willman's results (90). During all experiments, oil production ceased at breakthrough of the steam front. That production performance improved as steam quality increased from 0 percent to 73.4 percent is indicative of a corresponding increase in the system's extent which was subjected to liquid-free steam displacement.

The same production data expressed as cumulative WOR versus oil recovery are illustrated by Figure 24. At a given cumulative WOR, higher recovery was achieved as steam quality increased from 0 to 73.4 percent. As steam quality decreases, the performance curves are shown to approach that of a pure waterflood. The position of the 92.9 percent quality curve is indicative of the type performance expected for a pure steam flood; the influence of mobility

FIGURE 23

LIQUID PRODUCTION PERFORMANCE: 27.8°API OIL

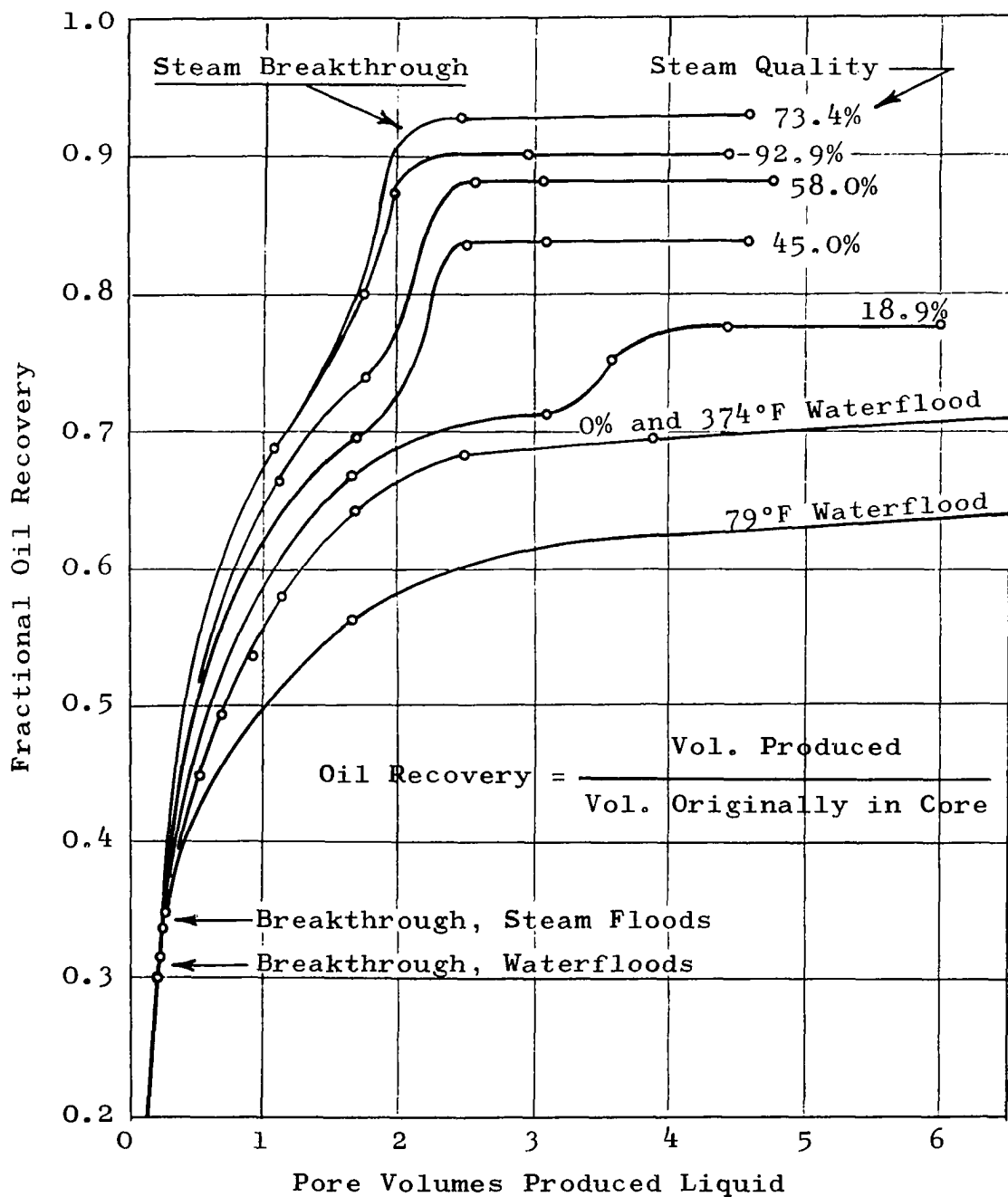
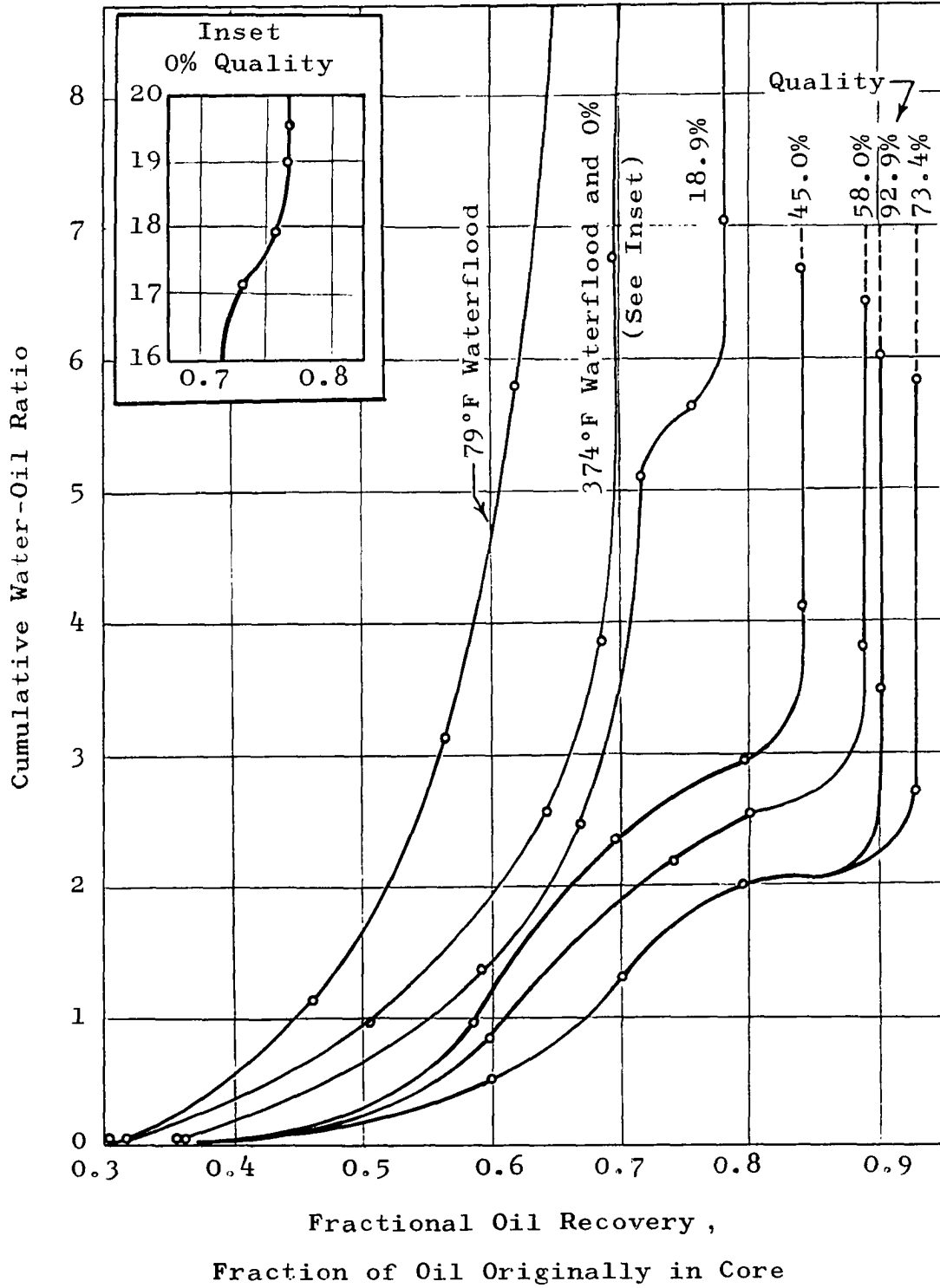


FIGURE 24

CUMULATIVE WOR VS. OIL RECOVERY: 27.8°API OIL



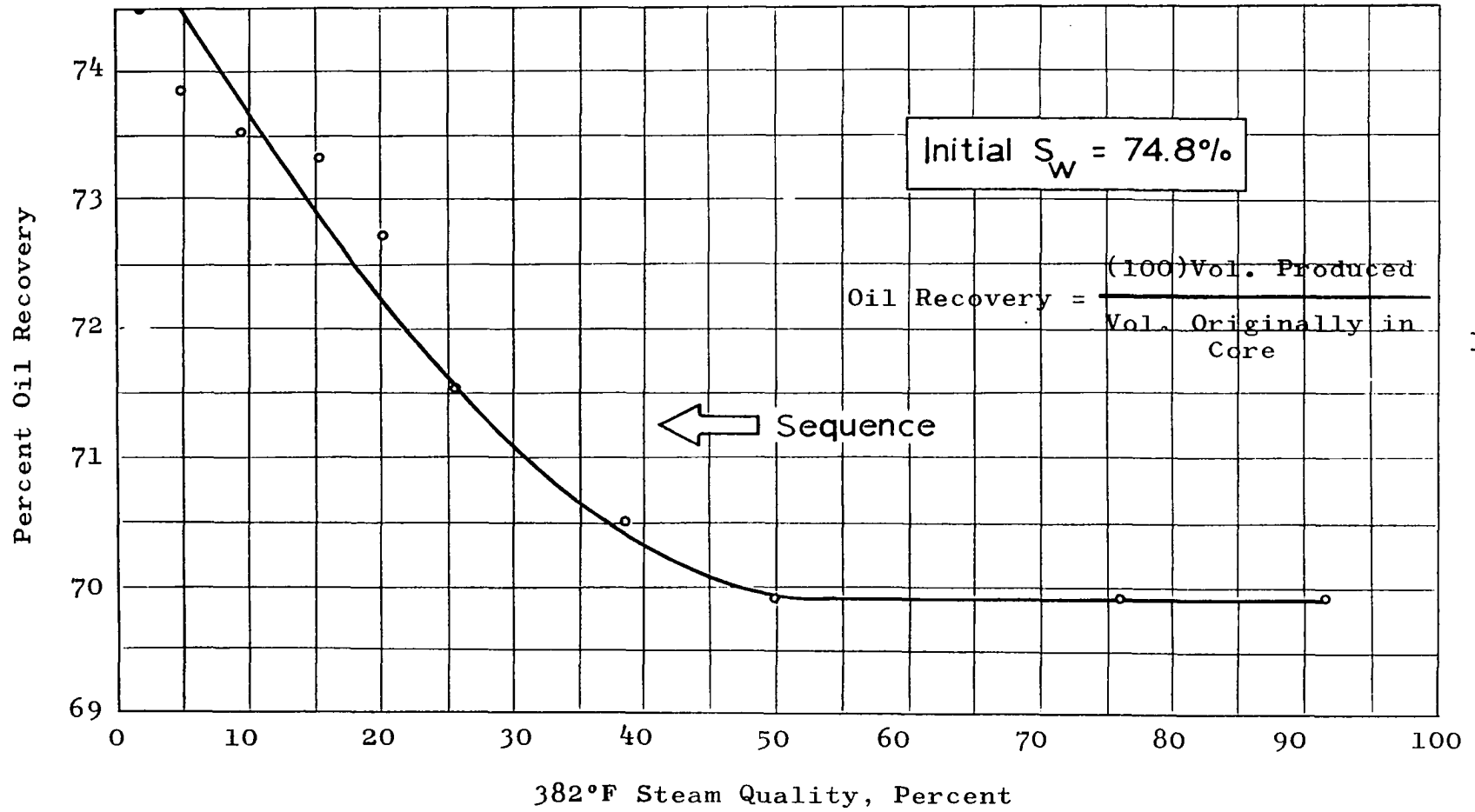
ratio rather than a sequential combination of two displacement mechanisms is thought to dictate the position of this quality's production curve.

Although greater oil recovery with hot water injection was realized compared with that for a 79°F waterflood, the additional recovery was produced at the expense of higher water production. This behavior is explained by a less favorable oil-to-water relative permeability ratio at the higher temperature. In a subsequent section, Figure 34 shows that approximately a ten-fold decrease in k_{ro}/k_{rw} occurred for a temperature increase of 250°F.

In order to investigate changes in oil recovery due to changes in the quality of steam flowing through the core, two additional experiments were performed. The first was executed at the termination of the 79°F waterflood; water saturation at this point was 74.8 percent of pore volume. Steam at 91.8 percent quality was introduced into the core, the additional oil recovery was noted, and quality was decreased without interruption of flow. The continuous flow process was repeated until the terminal quality of 1.8 percent had been achieved. Results are summarized by Figure 25. These data show that under continuous flow conditions, oil recovery increased as steam quality was decreased. A possible point of confusion lies in attempts to compare continuous flow, variable quality data (Figure 25) with constant-quality-per-experiment data (Figure 22). It should

FIGURE 25

EFFECT OF CONTINUOUS FLOW QUALITY CHANGE ON OIL RECOVERY: 27.8°API OIL



be recognized that Figure 22's data represent a series of steam injection experiments while Figure 25's data summarize the results of but one experiment. The latter constitutes a series of steady-state conditions whereas the former illustrates comparisons between individual, unsteady-state results.

A second continuous flow, variable quality experiment was performed wherein steam quality was incrementally increased from 2.1 percent to 92 percent. These maneuvers were executed following the completion of the 374°F water-flood. An additional 8.5 percent oil recovery resulted by converting the injected fluid from water into steam. No further recovery increase was observed as steam quality was incrementally increased.

The recovery responses to these two experiments suggest that an isothermal moist steam's effective mobility may be comprised of two variables, effective permeability and effective viscosity. A theoretical basis for this work considered only effective viscosity in producing a variable mobility. Assuming that a moist steam's liquid and vapor phases tend to distribute themselves in a porous media characterized by a variety of pore sizes according to relative permeability concepts (93), two separate but interconnected flow paths arise. Vapor tends to flow through the largest pores while a liquid tends to flow from the smaller into the larger pores. As the quantity of liquid

is increased, a proportionately larger volumetric flow from small pores through successively larger pores would result. Increasing the quantity of flow from small into large pores increases the probability that oil contained by these pores will be displaced by the liquid phase of moist steam. The maximum liquid concentration possessed by steam occurs at 0 percent quality; hence, maximum displacement of a non-wetting phase (oil) should occur at this quality. As quality increases, the quantity of liquid in equilibrium with its vapor decreases as shown by Figure 2. Flow in the form of vapor tends to concentrate in the largest pores as steam quality increases. Consequently, oil displacement efficiency should decrease as an isothermal steam's quality is decreased.

The experiment whose data are summarized by Figure 25 produced evidence that the initial oil saturation may not be process variable at constant steam quality. These data are based on an initial oil saturation of 25.2 percent. Recovery at 91.8 percent steam quality was 69.9 percent, corresponding to a residual oil saturation of 7.6 percent. Figure 22 shows that when 92.9 percent quality steam was injected into a core containing 72.8 percent oil, 90.0 percent of the oil was recovered; this corresponds to a residual oil saturation of 7.3 percent. Willman et al. (90) submit similar evidence, but their conclusion in this respect is not qualified by a constant-quality restriction.

Initial water saturations applicable to the primary data (Figure 22) varied between 27.2 and 28.7 percent of pore volume; average initial water saturation was 27.8 percent. These data along with experimental conditions, oil recoveries, and corresponding steam qualities are summarized by Table A-1 in the Appendix.

Experimental Results: 24.3°API Crude Oil

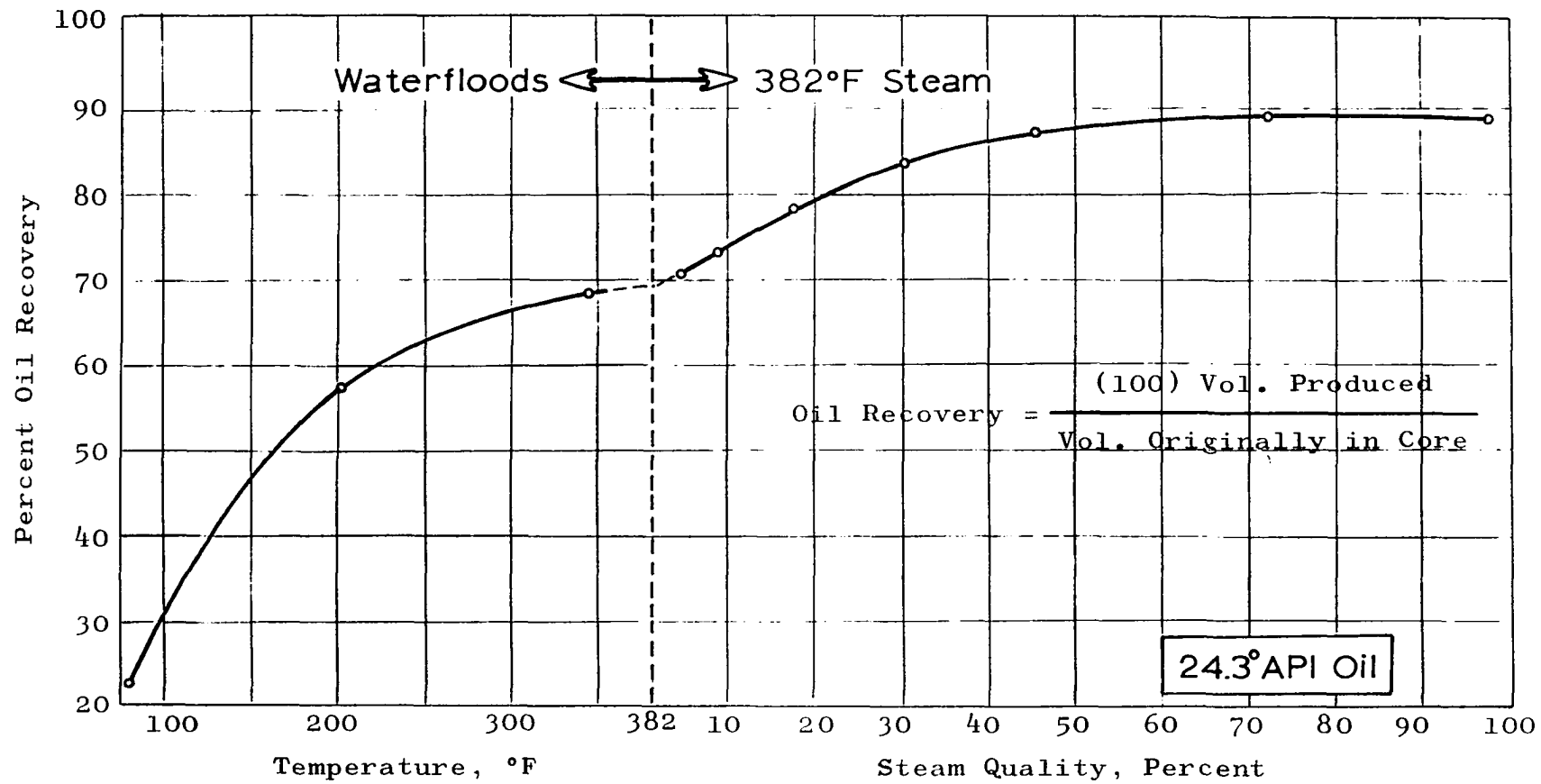
Oil recoveries obtained from waterfloods and 382°F steam floods are shown by Figure 26. Viscosity of the 24.3°API oil is 124 centipoise at 80°F; estimated viscosity at 382°F is 0.26 centipoise. A 477-fold change in oil viscosity occurs within this temperature range compared with 175 for the 27.8°API oil. From Figure 18, the 24.3° API oil is 4.1 percent distillable at 382°F by the ASTM test. For waterflood and steam injection experiments, initial water saturations varied between 22.6 percent and 27.3 percent, averaging 24.4 percent of pore volume.

The manner in which the waterflood and steam flood oil recovery curves join indicates that this oil was non-distillable in the presence of 200 psia steam.

The role of viscosity reduction in the recovery process appears quite significant in the present case. Oil recovery at 79°F was 22.9 percent whereas that at 345°F was 68.2 percent. A 203°F waterflood yielded 57.5 percent oil recovery.

FIGURE 26

OIL RECOVERY BY HOT FLUID INJECTION: 24.3° API OIL



Fractional oil recovery due to steam injection is shown to be dependent upon the quality of injected steam. The experimental minimum recovery of 70.6 percent occurred by injecting 4.8 percent quality steam. Maximum oil recovery, 88.9 percent, corresponds to 71.9 percent quality steam. Although recovery at 97.8 percent quality is shown to be 0.4 recovery percent less than that at 71.9 percent quality steam, it cannot be stated conclusively that oil recovery decreased at the higher quality; reproducibility of these experiments was 0.6 recovery percent.

Figures 27 and 28 summarize depletion histories for each experiment. Consistent with the trends exhibited by the 27.8°API oil, these curves show that greater oil recovery at the expense of less water production was realized as steam quality increased from 4.8 percent to 71.9 percent. The superiority of steam injection over waterfloods, both from total recovery and production performance vantages, is again demonstrated.

The position of the 97.8 percent quality's depletion curves relative to that of 71.9 percent quality gives some indication of the role of a quality-dependent displacement mobility ratio. Stratification of the performance curves for the lower qualities are interpreted as reflecting the degrees to which sequential displacement mechanisms were in operation. During each steam injection experiment, the cessation of oil production was coincident with steam breakthrough.

FIGURE 27

LIQUID PRODUCTION PERFORMANCE: 24.3°API OIL

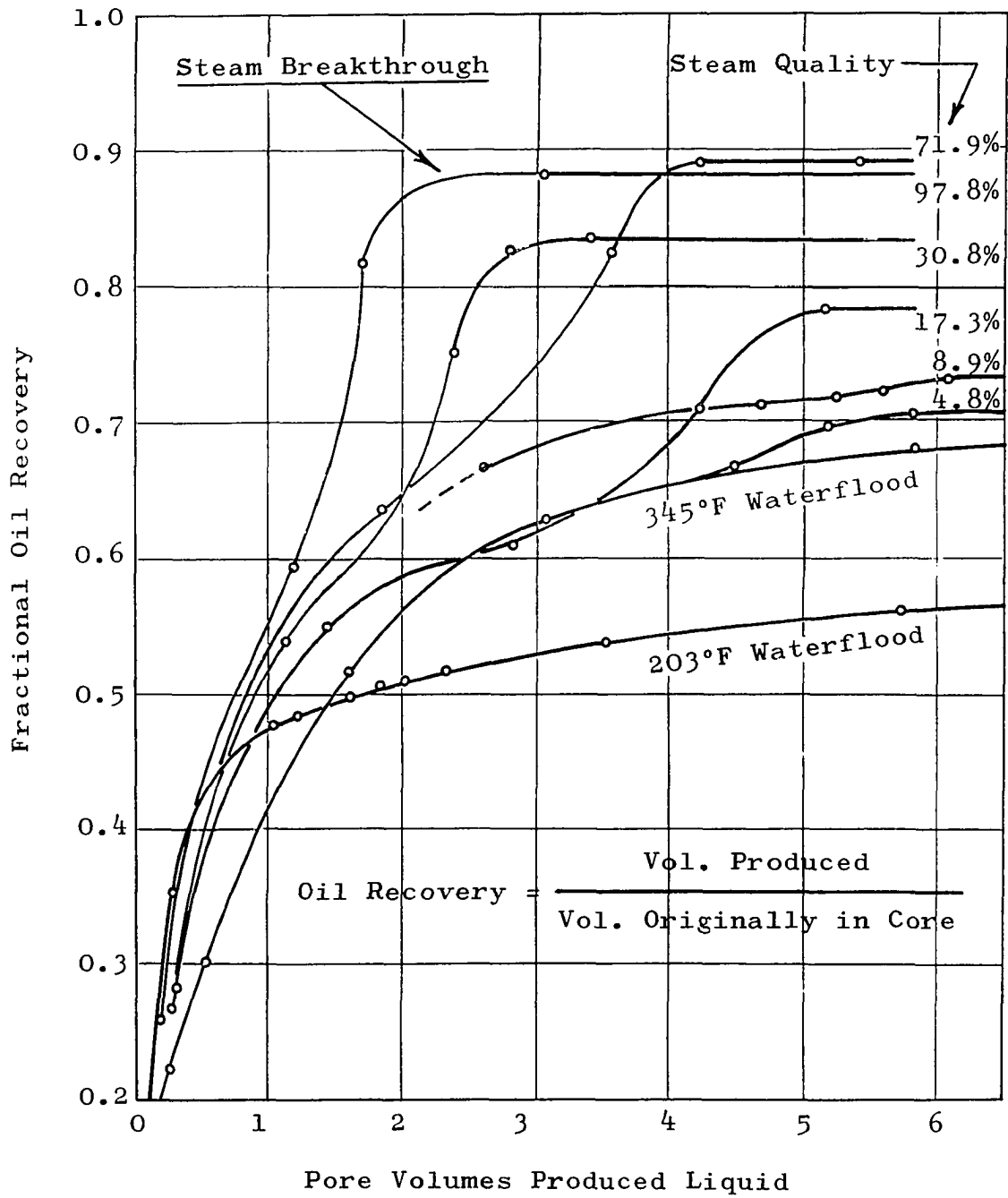
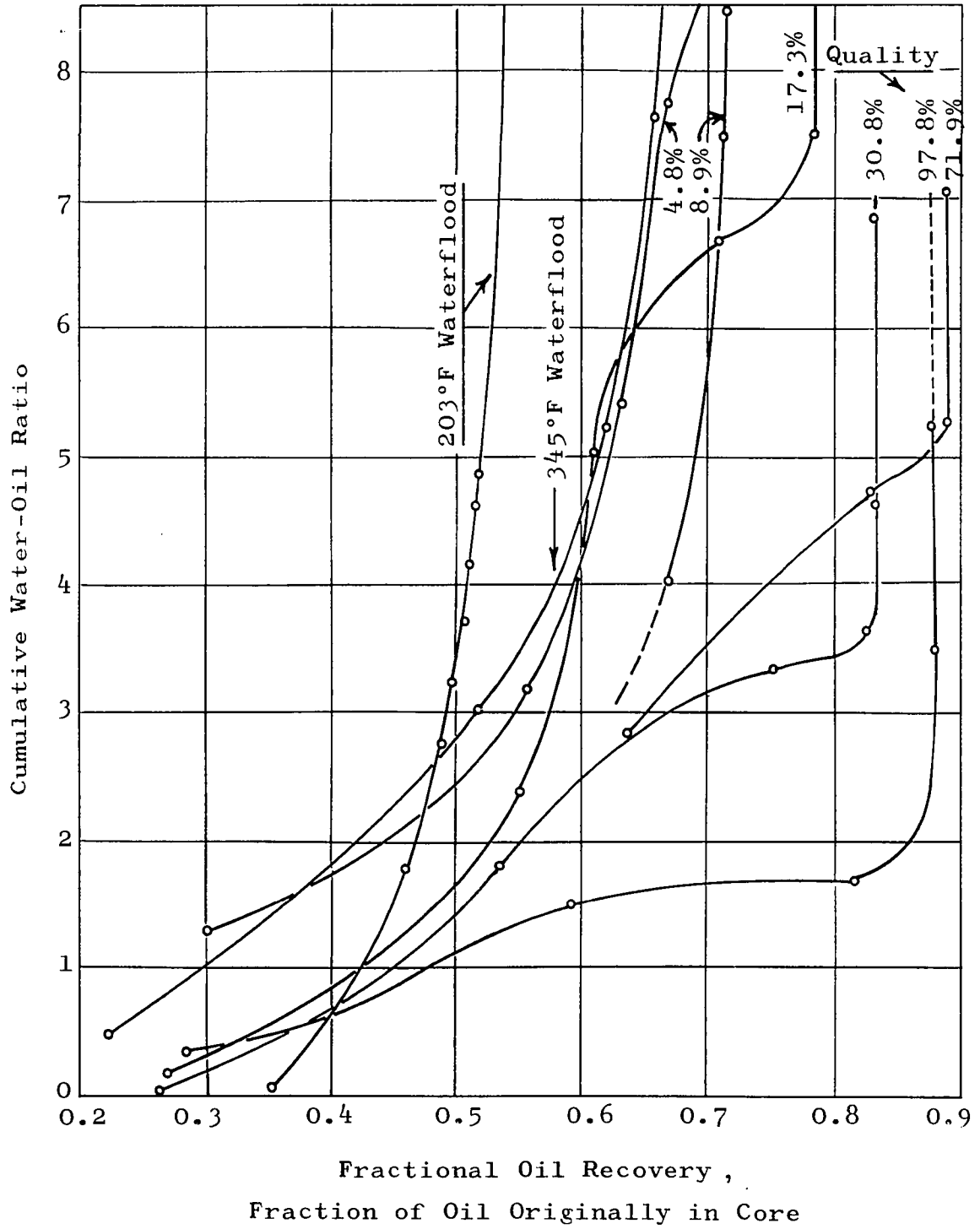


FIGURE 28

CUMULATIVE WOR VS. OIL RECOVERY: 24.3°API OIL



Theory suggests that critical distance depends only upon the rate of heat injection into a specified system and for a given temperature increase. Hence a steam front free of convective heat loss should be capable of traveling some distance X_c by injecting λ quality steam regardless of the degree to which the linear system's extent exceeds X_c . Both total recovery and depletion performance will be extensive properties of the system provided that $1-X_c$ is finite relative to X_c . A further test of the critical distance supposition was performed by substituting a shorter core for one of the experiments with the 24.3°API oil. A 21.45-inch length core was employed in evaluating the 27.8°API oil; the same core was employed for experiments using the 24.3°API oil except for the experiment wherein 71.9 percent quality steam was injected. For this particular experiment, an 11.75-inch length core was substituted. Figures 27 and 28 show that the position of the 71.9 percent quality's performance curve reflects some change in depletion history. These data show that the unsteady-state results submitted within this report must be interpreted as being extensive rather than intensive experimental data.

To illustrate the importance of performing a solvent clean out after each experiment, one experiment was performed without prior cleaning. Water was injected into the core containing 21.9 percent residual oil saturation. Oil was injected until its saturation was increased to

63.9 percent of pore volume. Subsequent steaming at 17 percent quality yielded 97.5 percent oil recovery. In contrast, a 17.3 percent quality experiment was performed following the usual clean out; initial oil saturation was 77.4 percent, and 78.5 percent of this amount was recovered by steam injection.

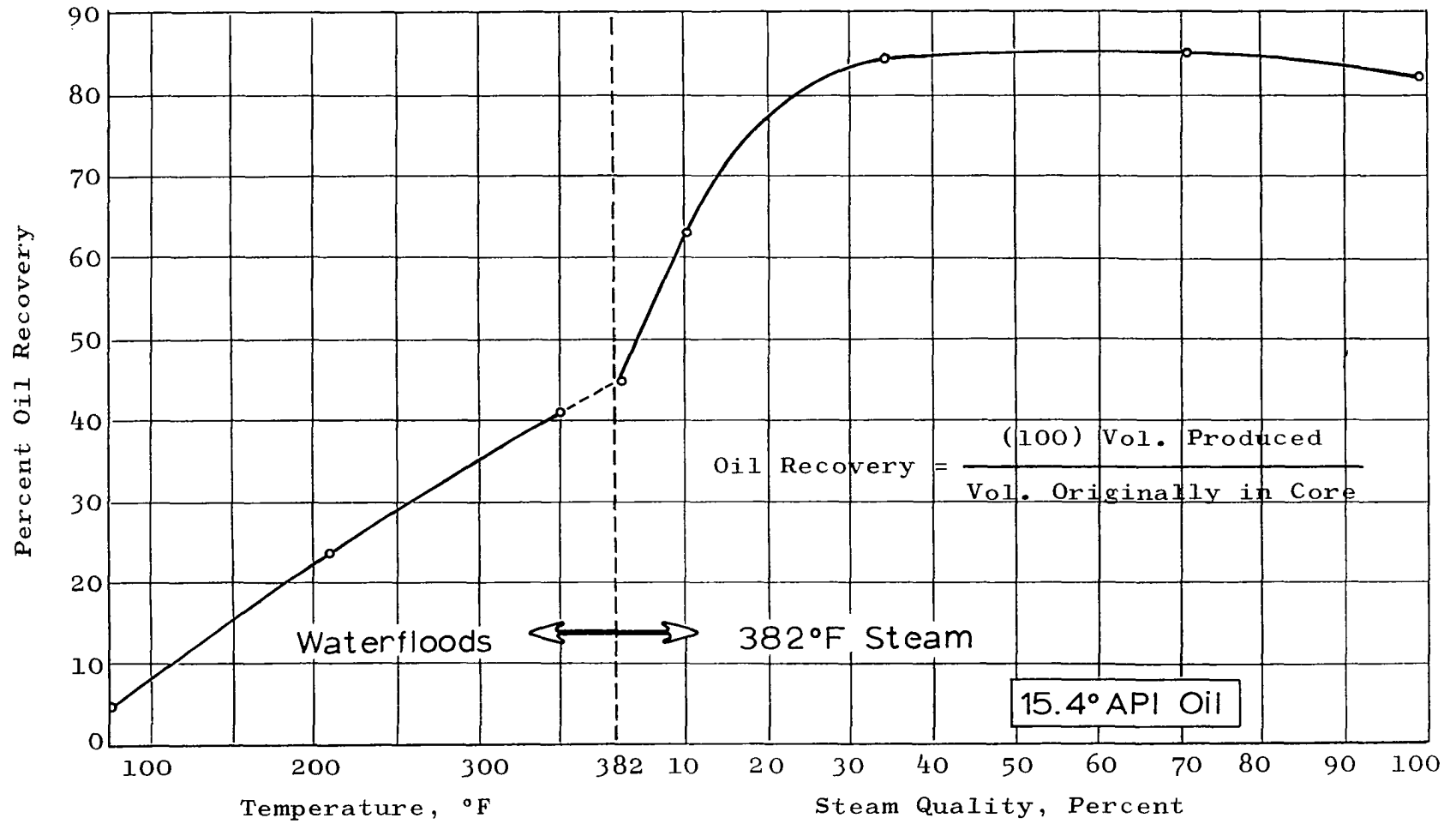
As with the 27.8°API oil, the initial water production accompanying the flow of 24.3°API oil occurred in the form of fine particles distributed within the oil phase. The 24.3°API oil was sufficiently opaque to prevent visual identification of the point of initial water production. Data from the 17.3 and 30.8 percent quality experiments indicate that water production was initiated at about 0.26 fractional oil recovery. With 345°F waterflooding, water was being produced prior to achieving 0.22 fractional oil recovery.

Experimental Results: 15.4°API Crude Oil

The measured viscosity of the 15.4°API oil at 87°F was 1050 centipoise; anticipated viscosity at 382°F is 1.2 centipoise representing an 880-fold reduction. Corresponding oil-to-water viscosity ratios are 1330 and 8.6, respectively. These data suggest that this oil should respond favorably to flooding with heat-laden fluids. Figure 29 summarizes experimental results for three water-floods and five moist steam floods.

FIGURE 29

OIL RECOVERY BY HOT FLUID INJECTION: 15.4°API OIL



By waterflooding, recovery at 75°F was only 4.9 percent; corresponding recoveries at 209°F and 350°F were 23.3 percent and 41.0 percent, respectively. Recoveries by steam injection ranged from 45.1 percent at 1.2 percent quality to 85.2 percent using 70.9 percent quality. At the highest experimental steam quality, 99 percent, oil recovery was 82.3 percent.

The greatest variation in oil recovery with steam quality is shown to occur between 0 and 35 percent qualities. The apparent insensitivity of oil recovery to quality at qualities in excess of 35 percent initially cast doubt on the reliability of the measured data at 34.4 percent quality. Its validity was verified by performing a second experiment. Experimental reproducibility was 0.6 recovery percent.

Initial water saturations varied between 9.0 and 15.0 percent. The arithmetic average initial water saturation for all experiments using this oil was 12.7 percent.

By ASTM analysis, the 15.4°API oil is 1.6 percent distillable at 382°F. By extrapolating the steam injection and waterflood recovery curves to 0 percent quality, there is no indication that the oil was steam distillable at 382°F and 200 psia.

Consistent with recovery characteristics exhibited by the two lighter oils, no additional 15.4°API oil production occurred after steam breakthrough.

A preliminary computation indicated that the 15.4°API oil's high viscosity would prevent injection of steam at a mass rate of 15 grams per minute and at 200 psia if the 22-inch length core were employed. Consequently, experiments with this oil were executed using a 12-inch length core. It was necessary to modify experimental initiation procedure in order to retain the standardized rate and pressure. Just prior to introducing steam into the oil saturated core, the duplex pump's discharge rate was lowered by reducing the pump's motor speed. The core's artificially induced back-pressure was removed, and moist steam at a low mass rate was introduced. Having established injectivity, the back-pressure and the pump's stroking speed were alternately increased such that 200 psia steam was available at the core's inlet face. Mass injection rate could be raised to 15 grams per minute after only a short delay.

A further experimental difficulty occurred because of the oil's high viscosity. At room temperature, the extreme contrast between oil and water viscosities permitted severe channeling of produced water through oil in the efflux lines. This problem was partially remedied by regulating the flow of cooling water through the down-stream heat exchangers such that the back-pressure valve's temperature limitation, 150°F, was just achieved.

Depletion data are presented by Figures 30 and 31. The above-mentioned liquid holdup may have influenced their reliability.

FIGURE 30

LIQUID PRODUCTION PERFORMANCE: 15.4°API OIL

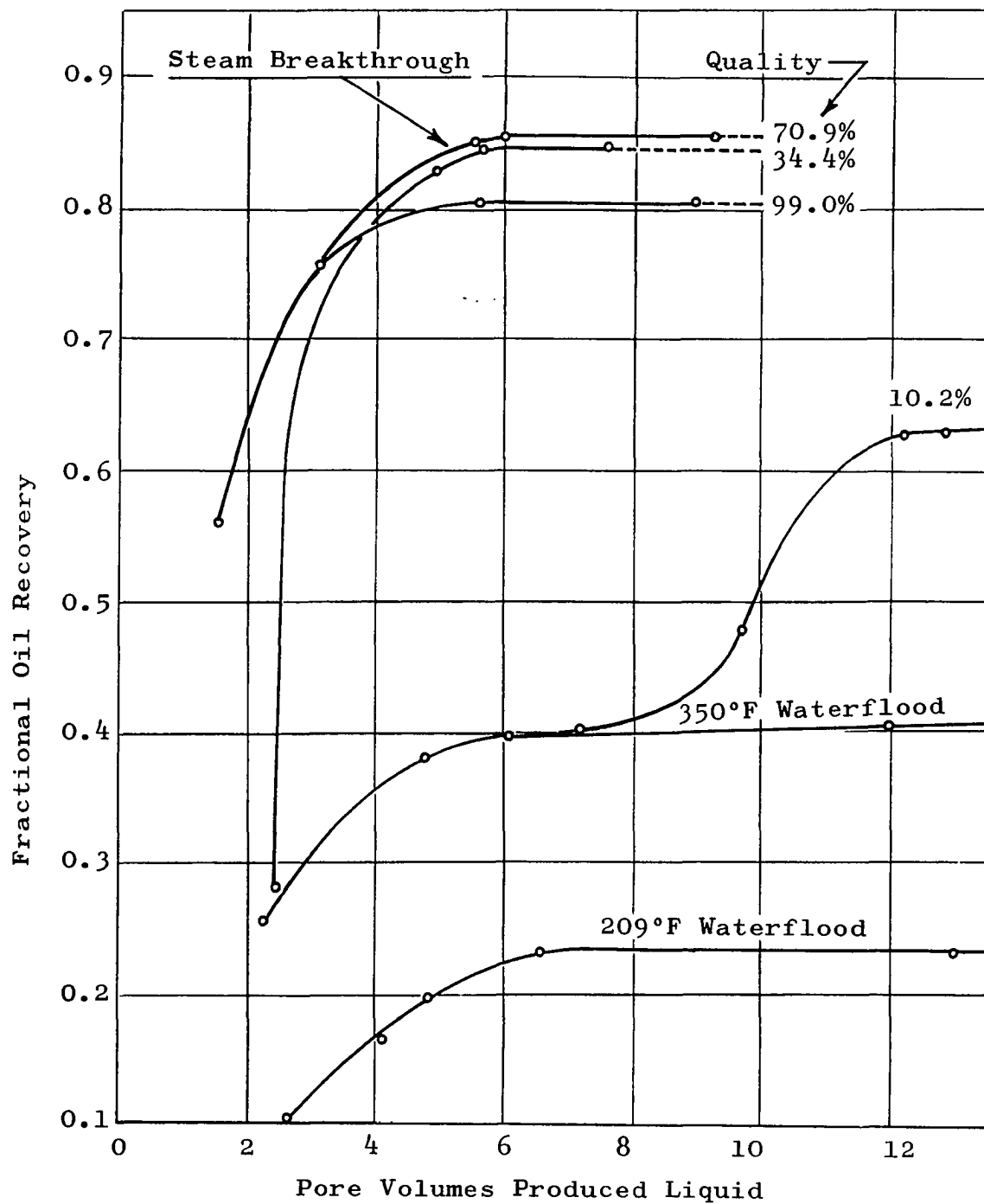
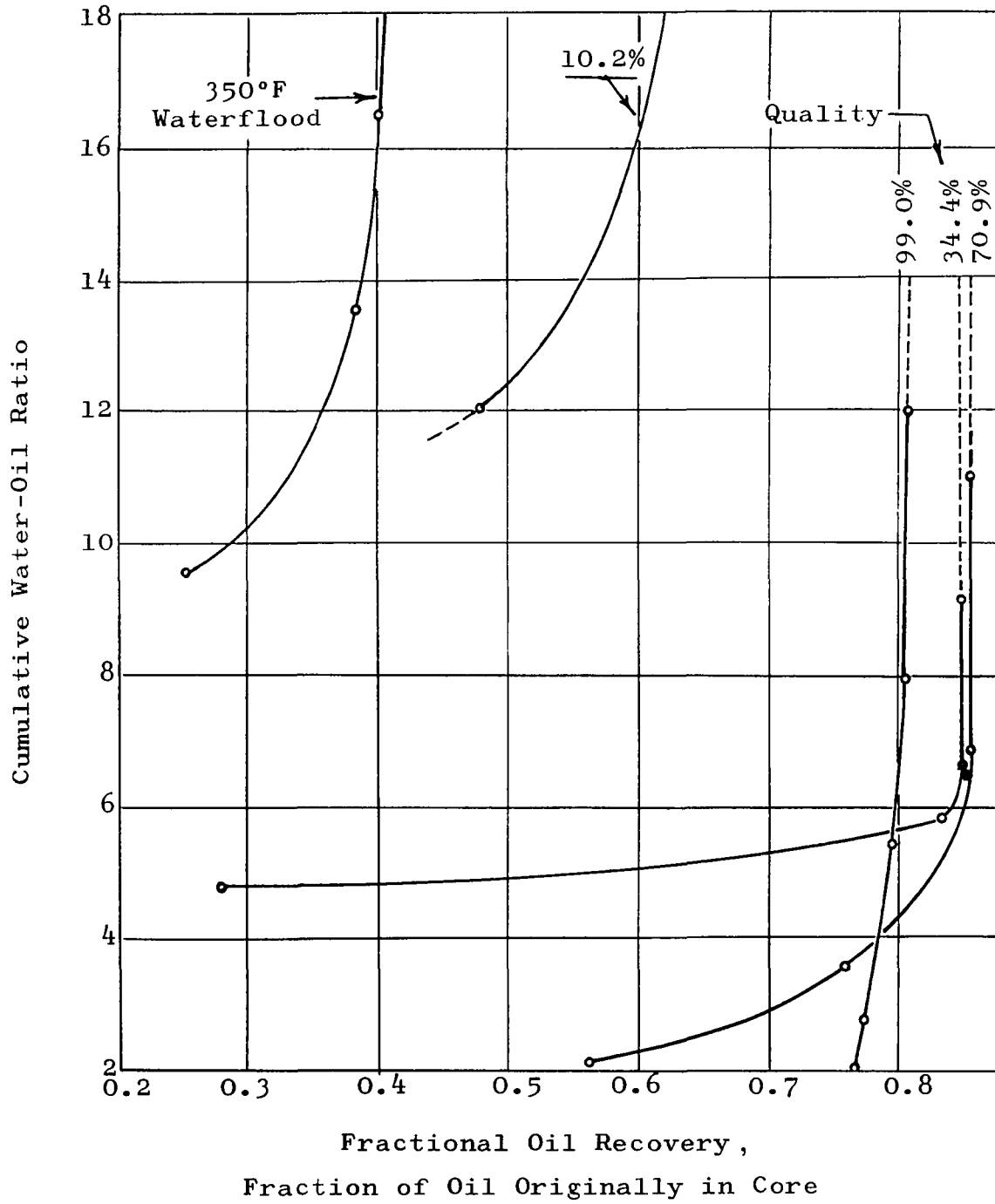


FIGURE 31

CUMULATIVE WOR VS. OIL RECOVERY: 15.4° API OIL



The fractional depletion data qualitatively show characteristics similar to those exhibited by the lighter oils. 382°F steam at approximately 70 percent quality produces the most favorable results.

According to the critical distance concept, any 382°F steam in excess of 60 percent quality which is injected into the subject system at a mass rate of 15 g/min can flow through the 12-inch length core without forming a hot water bank. Hence, the 70.9 and 99.0 percent quality recovery data should reflect the consequences of steam displacing oil. Due to the oil's high viscosity, the mobility ratio is large at either of these qualities; little difference between oil recoveries at 70.9 percent quality and 99 percent quality was anticipated.

The surprisingly high recovery at 34.4 percent quality was not anticipated. Observed recovery was 83.9 percent; some 75 percent recovery had been expected. This result may cast some doubts on the reliability of the critical distance concept as applied to high viscosity oils. That a pronounced variation in recovery with steam quality occurred within the 0-35 percent quality range, however, is indicative that sequential displacement mechanisms occurred. A variation of about 40 recovery percent is shown for the 0-35 percent quality range.

Comparison of Experiments and Data

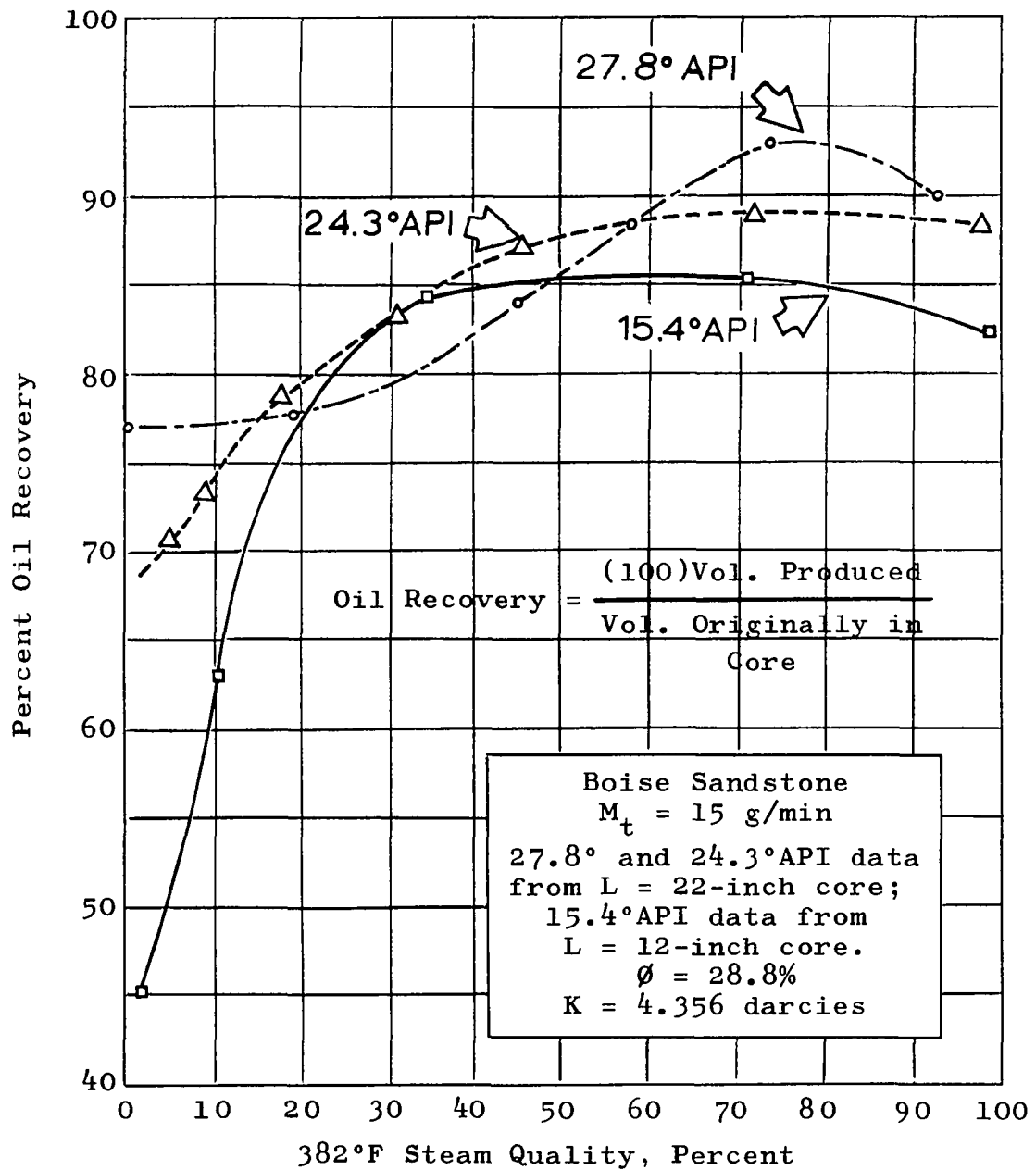
Minor changes in experimental procedure which were invoked have been discussed within data presentations. As denoted, a 12-inch length core was employed in obtaining results using 15.4°API oil; a 22-inch length core was used in examining the 27.8°API and 24.3°API crudes.

Figure 32 presents a comparison of the oil recoveries realized by injecting 382°F steam at various qualities. Data are stratified according to oil density (or viscosity) only where a single displacement mechanism, either by steam or by liquid water, was thought to dominate the total recovery process. The absence of ordered characteristics within a 20-60 percent quality range is attributed primarily to the relative magnitude of waterflooded and steamflooded pore volumes as a function of core extent.

At low steam qualities, greater sensitivity to the quality of injected steam is exhibited as oil density or viscosity increases. While the curves' shapes are thought to be indicative of sequential displacement processes, the sensitivity of oil recovery to small changes in steam quality at low qualities with the heavy oils seemingly reflects the contrasts between steam-oil and water-oil mobility ratios. For example, the absolute mobility ratio of steam and 15.4°API oil is 4.7 at 5 percent quality and 9.7 at 15 percent quality; 382°F water-oil mobility ratio is 8.5 . Smaller contrasts occur with the lighter oils.

FIGURE 32

COMPARISON OF OIL RECOVERIES BY STEAM INJECTION



With the 24.3°API oil, mobility ratio at 5 percent quality is 1 while that at 15 percent quality is 2; water-oil mobility at 382°F is 1.8 . With 5 percent quality injection, the 15.4°API oil's mobility ratio changes from 4.7 to 8.5 as steam displacement reverts to water displacement; with 24.3°API oil, the corresponding change is from 1 to 1.8 . Using 15 percent quality steam, the 15.4°API oil's mobility ratio changes from 9.7 to 8.5 as a condensate bank forms; with 24.3°API oil, the corresponding change is from 2 to 1.8 . These values are based on Kingelin's absolute mobility data (45), estimated oil viscosities at 382°F, and Boise sandstone's absolute permeability.

As expected, the ASTM distillation curves offered little other than qualitative data. These data indicate that if steam distillation at 200 psia were to occur, the 27.8°API oil would undergo a greater amount of distillation than the two heavier oils. ASTM data apply to atmospheric pressure; at this pressure the equilibrium K-values for C_6-C_{10} hydrocarbons are approximately ten-times greater than K-values at 200 psia. Hence, ASTM data, at best, are liberal estimates of steam distillability at higher pressure. The actual contrast would be less than ten-fold since mixtures of paraffin hydrocarbons and water can boil at 200 psia at temperatures below 382°F. For example, a mixture of water and hexane at 200 psia boils at 315°F.

Some distillation, however, occurred as evidenced by oil density measurements. Samples of each oil were collected at steam breakthrough, and the density of each was measured. These data are summarized by Table 3.

TABLE 3

DENSITIES OF STEAMED AND UNSTEAMED OILS

<u>Oil</u>	<u>Original Density, 77°F</u>	<u>Steamed Oil Density, 77°F</u>
27.8°API	0.883 g/cc	0.866 g/cc
24.3°API	0.898 g/cc	0.880 g/cc
15.4°API	0.953 g/cc	0.936 g/cc

The lower densities of the steamed oils are indicative of enrichment by lighter ends as a consequence of distillation. The indicated density changes (-19.3%, -20.0%, and -17.8%, respectively) do not necessarily signify the degree to which distillation proceeded. The ASTM distillate densities at 77°F for the above oils were 0.792 g/cc, 0.666 g/cc, and 0.665 g/cc, respectively. A simple material balance using ASTM distillate densities and those listed in Table 3 shows that greater volumetric dilution of the 27.8°API oil relative to the heavier oils is necessary to yield the indicated density change. Table 4 summarizes these computations.

TABLE 4

DILUTION REQUIREMENTS TO YIELD
MEASURED OIL DENSITY CHANGES

Basis: Unit volume of mixture (Perfect Mixing)
of ASTM distillate and unsteamed oil, cc

<u>Oil</u>	<u>Vol. Distillate/Vol. Oil</u>	<u>Vol. Distillate</u>
27.8°API	0.230	0.187 cc
24.3°API	0.084	0.078 cc
15.4°API	0.063	0.059 cc

While some distillation apparently occurred with each crude oil, the vaporized fractions evidently condensed ahead of the steam front. No gas was produced during experiments with the three oils; this was ascertained by collecting the core's effluent in a cylinder which was inverted in a tank of water, the cylinder being initially filled with water. This maneuver was performed with the first experiment with each oil wherein steam was injected.

At the point of steam breakthrough, maximum oil recovery had been achieved. Maximum recovery of 27.8°API and 24.3°API crudes was achieved at the expense of less water production compared with that for the 15.4°API oil. Cumulative water-oil ratios at steam breakthrough for the 27.8°API and 24.3°API oils were very similar ; this is attributed to the numerical similarity of their mobility ratios. Figure 33 summarizes these results.

FIGURE 33

CUMULATIVE WATER-OIL RATIO AT STEAM BREAKTHROUGH VS. STEAM QUALITY

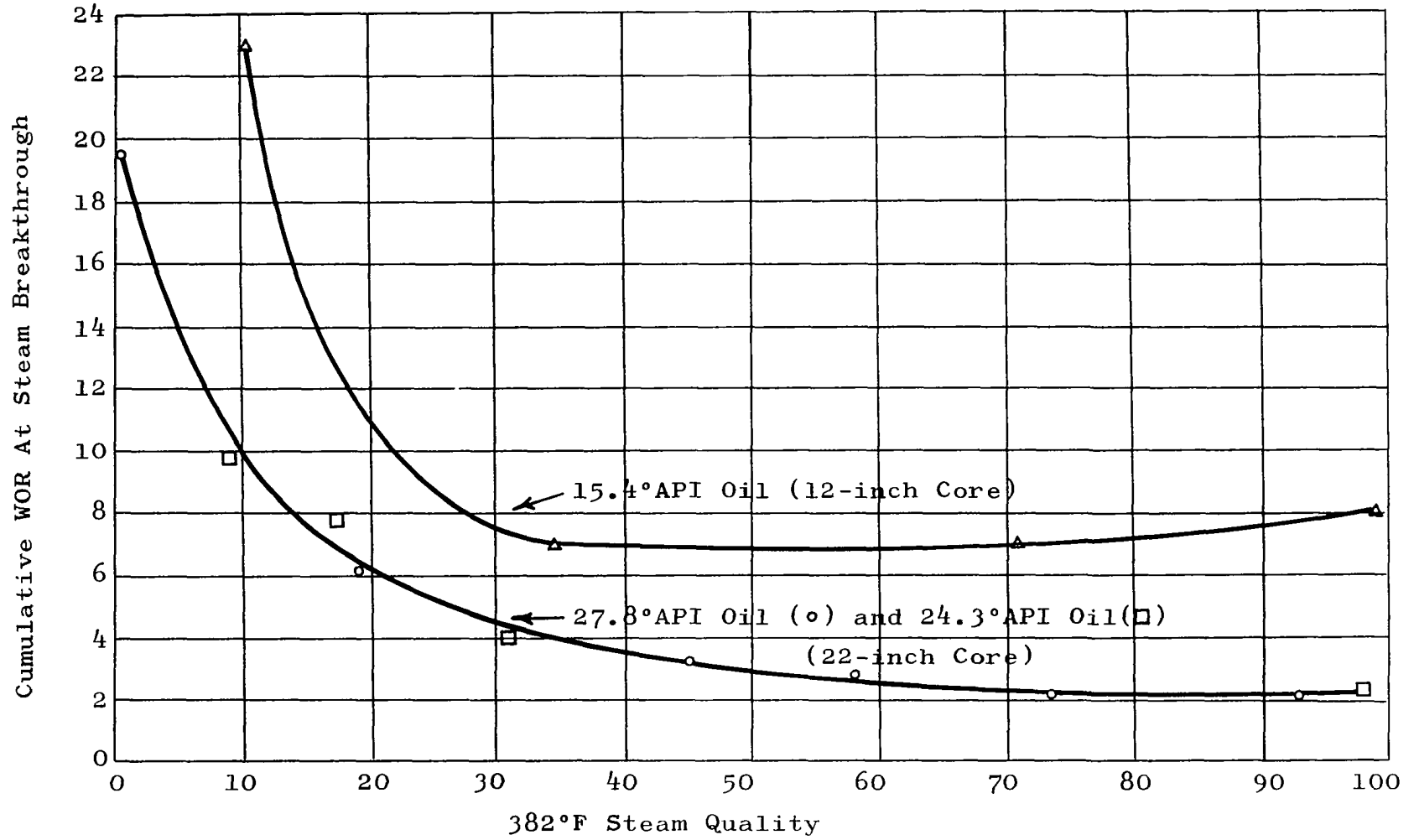
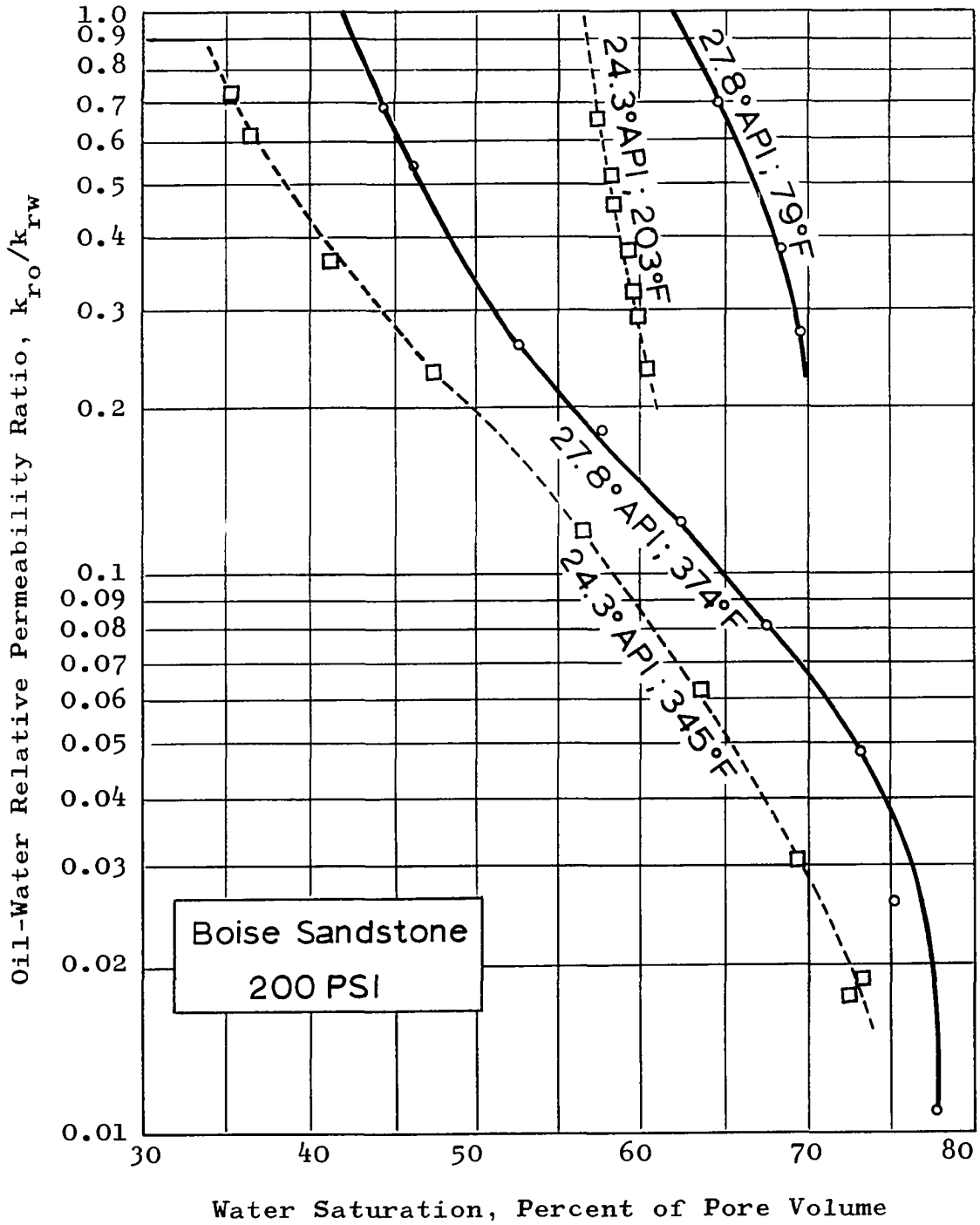


Figure 34 relates imbibition-type relative permeability ratios to water saturation for various temperatures. These data show a diminution of k_{ro}/k_{rw} as temperature increases. Edmondson (20) observed that k_{ro}/k_{rw} can increase with temperature for crude oil - sandstone systems. Hossain's experiments with a refined oil and an unconsolidated rock agree in trend with Edmondson's data (38). These data were computed from waterflood performance curves using Welge's method (87). The similarity between the 27.8°API data and those for the 24.3°API oil indicates that consistent wettability was retained. 15.4°API data were computed, also, but they are not presented since it is felt that liquid holdup in production lines rendered these data useless. The displayed response to temperature indicates that the additional oil recovered by hot waterflooding was due to viscosity reduction, thermal expansion, and improvement in absolute permeability; k_{ro}/k_{rw} acted in opposition.

Prior to steam breakthrough but after water production had begun, production consisted of a water-in-oil emulsion. This is attributed to mixing incurred as the fluids flowed through the back-pressure diaphragm valve; no emulsions occurred during saturation maneuvers where effluents were not subjected to flow restrictions. With the onset of heat production, an oil-in-water emulsion was produced. The size of the dispersed phase (oil) droplets was evidently between 1.4 and 10 microns diameter. The emulsion could

FIGURE 34

EFFECT OF TEMPERATURE ON k_{ro}/k_{rw}



be passed through a 10-14 micron filter; only the water phase could be forced through a 0.9-1.4 micron filter. The ability of acid pH to break the oil-in-water emulsions provides further confirmation of Strassner's observations(79). Noting that oil-and-water emulsions are thought to be stabilized primarily by film-forming asphaltines and resins containing organic acids and bases, Strassner showed that for a particular oil-water system, there exists an optimum pH range within which the phases may be best separated. Resin-induced emulsions were observed to respond favorably to acid pH while the asphaltine-type emulsions were effectively broken with basic pH.

Since the emulsions which occurred during steam injection responded favorably to acid pH, they could be classified as resin-type emulsions by Strassner's criterion. Inasmuch as asphaltines are thought to promote strong oil-wetting of silica surfaces while resins do not (79), the apparently resinous characteristic of each of the three oils implicitly indicates that water-wet conditions within the core prevailed with each oil.

INFLUENCE OF VARIABLES WHICH WERE HELD CONSTANT

With the exception of using a shorter core to obtain 15.4°API recovery data, all experiments were performed under identical experimental conditions. The variables of this study were 382°F steam quality and crude oil. Individual and collective changes in imposed conditions could possibly yield different oil recovery data. Possible consequences are examined in the discussions which follow.

Mass Rate of Steam Injection

The mass rate of steam injection employed in this study was 15 grams per minute. Had a lower throughput been employed, a greater amount of heat would have been lost by steam in the injection lines since residence time would be extended. Steam at lower qualities would be available for injection. The immediate effect of using a lower mass rate would be that of causing lower oil recovery.

By Equation (4), the velocity of a non-condensing front is directly proportional to the rate of isothermal heat injection. As mass rate is reduced, residence time within the core increases, external heat losses increase,

and steam quality decreases. The net effect is a decrease in oil recovery.

Although it has been demonstrated that low quality steam causes greater oil displacement than high quality steam, it is submitted that oil recovery should decrease as mass injection rate decreases even though steams of lower quality result. This is because the critical parameters (velocity, time, distance) approach zero as steam quality approaches zero. As mass injection rate is lowered, ultimate oil recovery becomes independent of the quality of steam available for injection.

It is felt that the oil recovery data submitted by Willman et al. (90) would have been constant for any isothermal steam quality that they could have employed. The mass rate of injection was sufficiently low that formation of a hot condensate bank probably occurred at $t = 0$.

Steam Temperature

Steam temperature employed within this study was 382°F. It has been shown that moist steam mobility in Boise sandstone is inversely proportional to its temperature (45). Since oil recovery is inversely related to the displacing phase's mobility, increasing steam temperature operates toward improving the efficiency in which steam can displace oil. With condensation, however, the opposite effect might occur due to a decrease in k_{ro}/k_{rw} .

Porosity

The average porosity at 80°F exhibited by the Boise sandstone employed in these experiments was 28.8 percent. The effect of increasing porosity for invariant permeability is to extend steam's residence time within a specified pore volume. Lower frontal velocities result, and the critical parameters decrease as does steam quality. Displacement of oil by steam improves, but the areal extent of this process decreases. The effect of porosity change must be examined on the basis of the reservoir's areal extent.

Permeability

Permeability of the Boise sandstone used in this study was 4.356 darcies at 200 psia and 382°F. On a microscopic basis, the oil recovery contrast between low and high quality steams could be greater than that exhibited by the high permeability Boise sandstone. Permeability reflects not only pore sizes but also the degree to which the pores are interconnected. The preponderance of small pore sizes that a low permeability rock can exhibit may force an increase in $k_{r(\text{water})}/k_{r(\text{gas})}$, where water is the wetting phase. The greater quantity of liquid carried by low quality steam may afford a greater degree of small-pore flooding relative to that by vapor

which is thought to flow in the largest pores. Hence, there exists the possibility that low quality steam may displace oil from a low permeability rock more efficiently than would a high quality steam.

The existence of low permeability, however, may disturb the maintenance of low qualities. Since low quality steams evidently have a relatively high effective viscosity, flowing such a fluid through low permeability will produce a sizeable pressure drop. A corresponding temperature drop occurs. If the temperature decline can occur adiabatically, Figure 1 shows that quality will increase.

Convection In Bounding Media

Since hot water was injected into the core holder's annulus, the experimental results are further confined as to their generality. The necessity of this maneuver has been discussed. Referred to 80°F, an annular flux of 5.36 centimeters per minute prevailed during all experiments. Steam front velocities varied between 1 and 2 centimeters per minute. Figure 21 shows that the region ahead of a steam front within the core was subjected to a slight degree of pre-heating. Thomas (81) has discussed heat transfer by this process for in situ combustion.

With pre-heating arising from a relatively high

flow diffusivity within a bounding medium, a larger volume of reservoir fluids will be subjected to viscosity reduction and thermal expansion. Some improvement in steam and water displacement mobility ratios would occur. An improvement in oil recovery would be anticipated.

Gravity

It is known that natural convection can cause channeling in vertical directions (92). In downward flow, a dense fluid can channel through a lighter fluid. The opposite occurs for upward flow. Natural convection effects are often correlated by either the Grashof number or the Rayleigh number (19,32); the Rayleigh number is a product of the Grashof number and the Prandtl number.

These concepts are difficult to apply to a consolidated porous medium since their evaluation requires knowledge of some characteristic length. With unconsolidated media, sand grain diameter is usually chosen as the characteristic length (32).

In the absence of the capillary gradient effect, the fractional gas-flow equation is

$$f_g = \frac{1 - (K_o g \Delta \rho \sin \theta) / \mu_o q_t}{1 + 1/M} \quad (17)$$

where M is the mobility ratio, $\Delta \rho = \rho_g - \rho_o$, and the angle θ is positive for up-dip flow. Since $\Delta \rho$ normally

is negative, f_g assumes larger values for up-dip flow than for downward flow. Lower oil recovery by upward flow is implied. The penalty for flowing upward can be partially alleviated by increasing the injection rate. In this manner, viscous forces become dominant relative to gravity forces.

The experiments performed herein were executed with the core oriented vertically. In view of the oils' viscosities and the mass rate of injection employed, the viscous forces within the oil zone were appreciably greater than the gravity force existing between the steam and oil zones. The ratio of viscous to gravity forces can be expressed as

$$\frac{F_{\mu}}{F_g} = \frac{\frac{Q_t \mu_o}{AK_o}}{g(\rho_o - \rho_s) \sin \theta} \approx \frac{\frac{v_f \mu_o}{K_o}}{0.00097 \rho_o} \quad (18)$$

for upward flow of steam. The maximum viscous force occurred at the beginning of the experiment while the oil's viscosity reflected room temperature. The minimum viscous force occurred at the completion of each experiment since the oil's temperature corresponded to that of steam. Using as an example the 24.3°API oil and a conservative frontal velocity of 1 cm/min, the following calculations indicate that viscous forces exceeded gravity forces throughout the experiment.

(a) Maximum gravity force, maximum viscous force

Condition: Beginning of steam injection

24.3°API oil at 80°F

$$\frac{F_{\mu}}{F_g} = \frac{(1/60)(124)(1/4.356 k_{ro})}{0.00097(0.897)} = \frac{545}{k_{ro}}$$

(b) Minimum gravity force, minimum viscous force

Condition: Just prior to steam breakthrough

24.3°API oil at 382°F

$$\frac{F_{\mu}}{F_g} = \frac{(1/60)(0.26)(1/4.356 k_{ro})}{0.00097(792)} = \frac{1.3}{k_{ro}}$$

Since k_{ro} was less than unity, the ratio of viscous to gravity forces for either extreme was numerically greater than unity. This indicates that the magnitude of the gravity forces was less than the magnitude of the opposing viscous forces. Hence, it is felt that the core's orientation and the direction flooded had little influence on the observed oil recoveries.

Had a lower injection rate been employed, a lower rate of frontal advance would have occurred. The magnitude of the viscous forces would be correspondingly lower while gravity forces remain as stated above. Less oil recovery would be anticipated.

PREDICTION OF OIL RECOVERY

A method for computing total oil recovery resulting from the injection of isothermal moist steam at a constant mass rate is submitted. An objective of this presentation is to assess the applicability of conventional fluid displacement concepts as applied to the mechanisms which are postulated to occur with steam injection.

The analytical oil recovery model is constructed around three basic principles:

- (1) Two flow regions exist whose mutual interface is the steam front (not to be confused with temperature front); condensate and native reservoir fluids flow ahead of the front while only steam is mobile behind the front;
- (2) The mobility of isothermal moist steam changes with variations in quality;
- (3) Successive or sequential displacement mechanisms occur in accordance with the critical distance concept. Initially, displacement is characterized by piston-like removal of oil by steam. After the onset of condensation at the steam front, displacement of oil by condensate (water) occurs

ahead of the steam front; no displacement of oil by steam occurs.

Statement (1) is based on the observation that no additional oil was produced after steam breakthrough during experiments reported herein. Statement (2) is based on the experimental observations reported by Kingelin (45). Statement (3) is theoretically-based, but evidence is submitted within this report which experimentally supports the critical distance concept.

The Buckley-Leverett or fractional flow equation,

$$f_d = \left[1 + \frac{k_{rd}}{\mu_d} \frac{\mu_o}{k_{ro}} \right]^{-1}, \quad (19)$$

is an accepted tool for quantifying the simultaneous flow of immiscible fluids. The value of f_d , the volumetric fraction of displacing fluid contained by the two-fluid stream, can assume any numerical value between zero and unity. For piston-like displacement of oil by steam, however, $f_d = f_s$ must be zero on the liquid side of the steam front and unity on the steam side of the front. Hence, a series of oil saturations may be assumed, their corresponding relative permeabilities determined, and a curve relating f_s to S_o (or S_s) can be constructed. The curve is physically meaningless in view of Statement (1), serving only as a device for extrapolating to $f_s = 1$.

After a hot water bank forms, Equation (19) is written for the condition wherein steam displaces a multi-phase liquid bank composed of oil and steam condensate. As in the previous case, $f_s = 0$ on the liquid-side of the front and $f_s = 1$ on the steam-side. Water saturation on the liquid side of the interface is evaluated by expressing f_s in terms of oil, water, and effective steam mobilities; curves relating the quality-dependent f_s to S_w are constructed for an arbitrary series of saturations, and the curves are extrapolated to $f_s = 0$.

An example calculation wherein these mechanics are illustrated is included in the Appendix. The applicable equations are presented in that illustration on the presumption that associations of relationships with their mechanical treatment may eliminate interpretation problems.

Suggested methods for estimating the recovery contributions attributed to thermal expansion and distillation are presented in the example calculation, also. These techniques represent practical means-to-ends; the concepts used do not necessarily indicate that the thermal expansion and distillation processes have been properly identified.

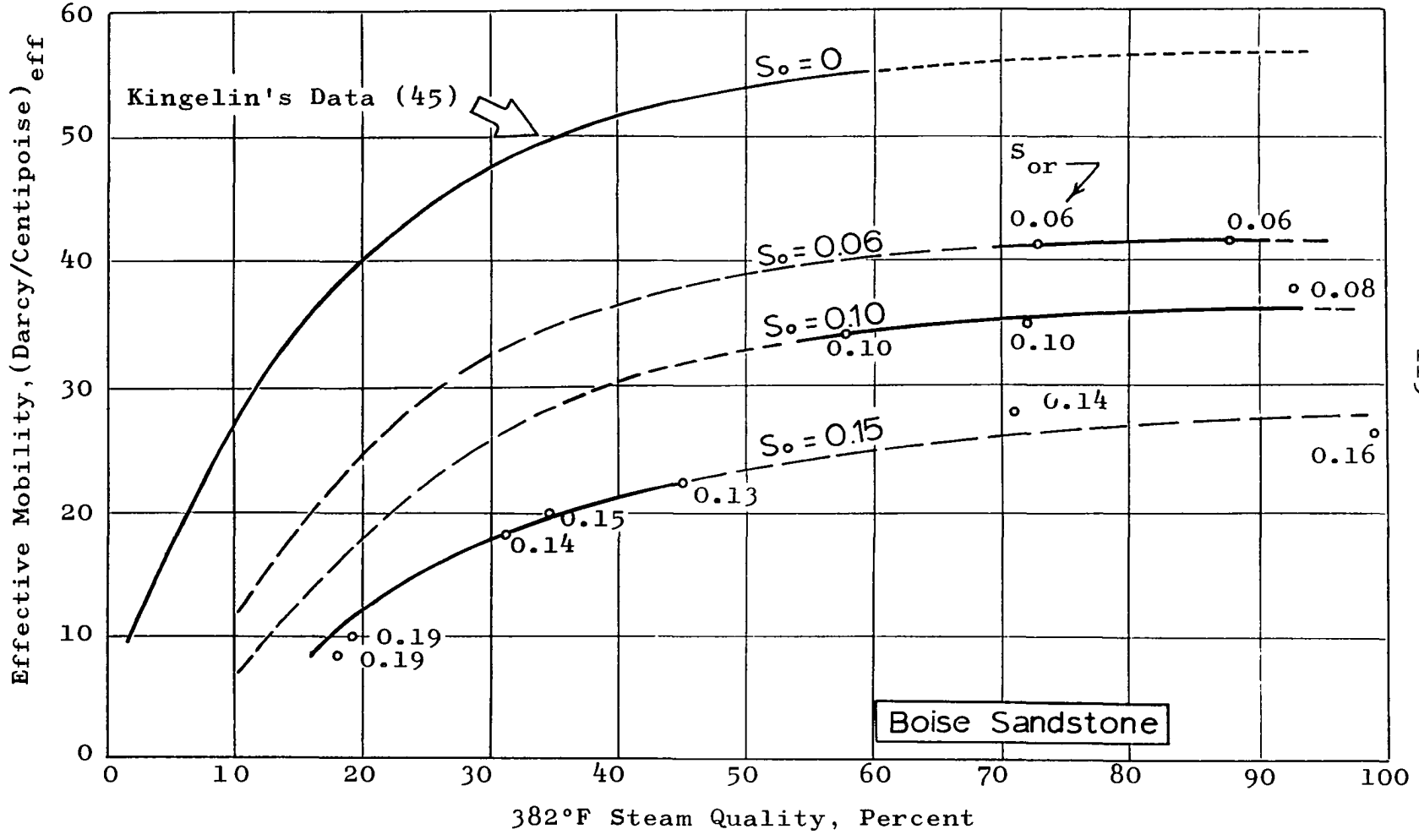
The displacement equations are written in the forms in which laboratory-derived data usually appear. One difficulty arises in that relative permeability to oil, k_{ro} , occurs as an individual variable rather than as a ratio to, say, k_{rw} . While k_{ro}/k_{rw} data may be extracted

from basic waterflood performance data, specially designed experiments are necessary to evaluate the phase permeabilities. In the numerical example presented in the Appendix, k_{ro} data are estimated using empirical equations developed by Corey (15). These relationships were constructed by Corey for the drainage rather than the imbibition saturation process (93); in the present treatment, however, they are applied to an imbibition process. This disparity operates to favor the effects of high temperature. In general, k_{ro}/k_{rw} for the drainage cycle are numerically greater than those for imbibition. Hossain submits evidence that both k_{ro} and k_{rw} increase with temperature (38). Thus, the use of drainage cycle k_{ro} equations may offer some compensation for the present inability to increase imbibition k_{ro} data for temperature effects.

Of paramount importance in solving the displacement equations is an accurate knowledge of moist steam's effective relative mobility, $(k_{rs}/\mu_s)_{eff}$. Kingelin (45) has measured some absolute mobilities of moist steams in Boise sandstone; conclusive evidence regarding the influence of residual oil saturation on the magnitude of steam mobility was not demonstrated. Figure 35 shows Kingelin's absolute mobility data for 382°F moist steams. Superimposed on this figure are some steam mobility data with residual oil which were derived from experimental data.

FIGURE 35

MOIST STEAM MOBILITY AT RESIDUAL OIL SATURATIONS



The superimposed mobility data at residual oil saturation were derived as follows:

(a) After steam breakthrough, steam injection was continued until stabilization of core inlet and core outlet temperatures was assured. These data were translated into the corresponding saturation pressures of steam.

(b) Knowing the core's dimensions, the mass rate of injection, the estimated steam quality (expressed in terms of specific volume), and the pressure drop across the core (From (a)), effective mobilities were computed using Darcy's equation:

$$\left[\frac{K_s}{\mu_s} (S_s, 382^\circ\text{F}, \lambda) \right]_{\text{eff}} = \frac{M_t \cdot \bar{v}_s(\lambda) \cdot L}{A \cdot \Delta P} \quad (20)$$

Residual oil saturation was estimated by material balance using recovery data and oil densities. The computed data were plotted on Figure 35, and curves for constant S_{or} were constructed using Kingelin's curve for extrapolation control.

These experimentally derived mobility data indicate that moist steam's effective mobility in Boise sandstone can be highly sensitive to the magnitude of the residual oil saturation. Hence, effective mobilities at residual oil saturation were employed in displacement computations.

Comparison Between Computed and Experimental Results

27.8°API Crude Oil

Two sets of computations were performed which illustrate the consequences of using effective steam mobilities (a) which reflect residual oil saturations and (b) which were measured in an oil-free core. The results are summarized graphically by Figure 36.

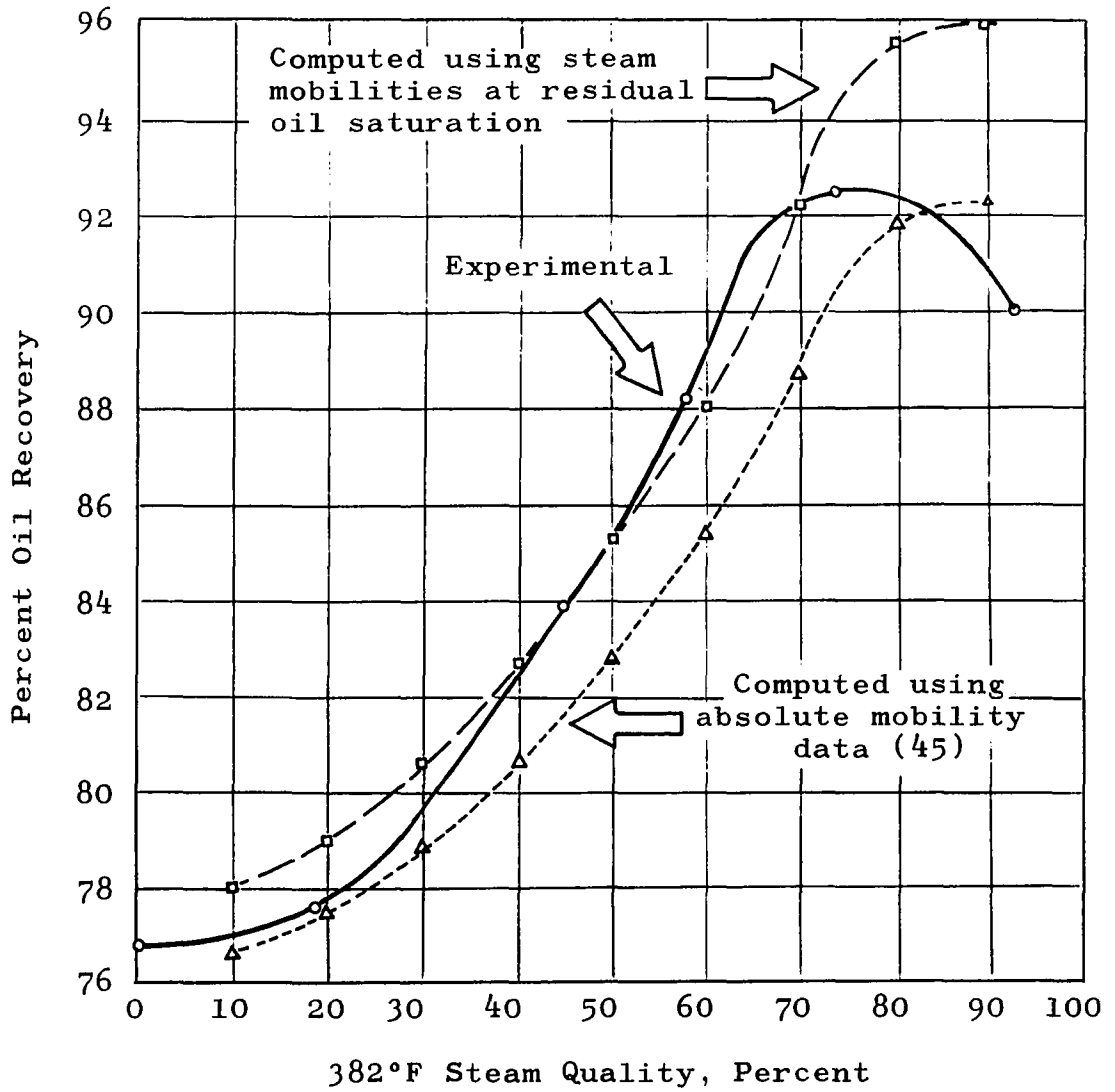
Very good agreement between experimental and computed results is shown where effective steam mobilities in the presence of residual oil are used. Computed results using oil-free mobilities tend to be conservative. The good correspondence between computed and experimental data tends to justify further the presuppositions regarding critical distance and the associated change in displacement mechanism. A maximum error of +5.7 percent occurs at 90 percent quality steam.

Data which were used in performing the computations were: effective steam mobilities, absolute permeability, oil-to-water relative permeability ratios, empirical relative permeabilities to oil, dimensionless critical distances, water and oil viscosities, water and oil densities, and an average initial water saturation.

FIGURE 36

COMPUTED AND EXPERIMENTAL

RECOVERIES: 27.8°API OIL



24.3°API Crude Oil

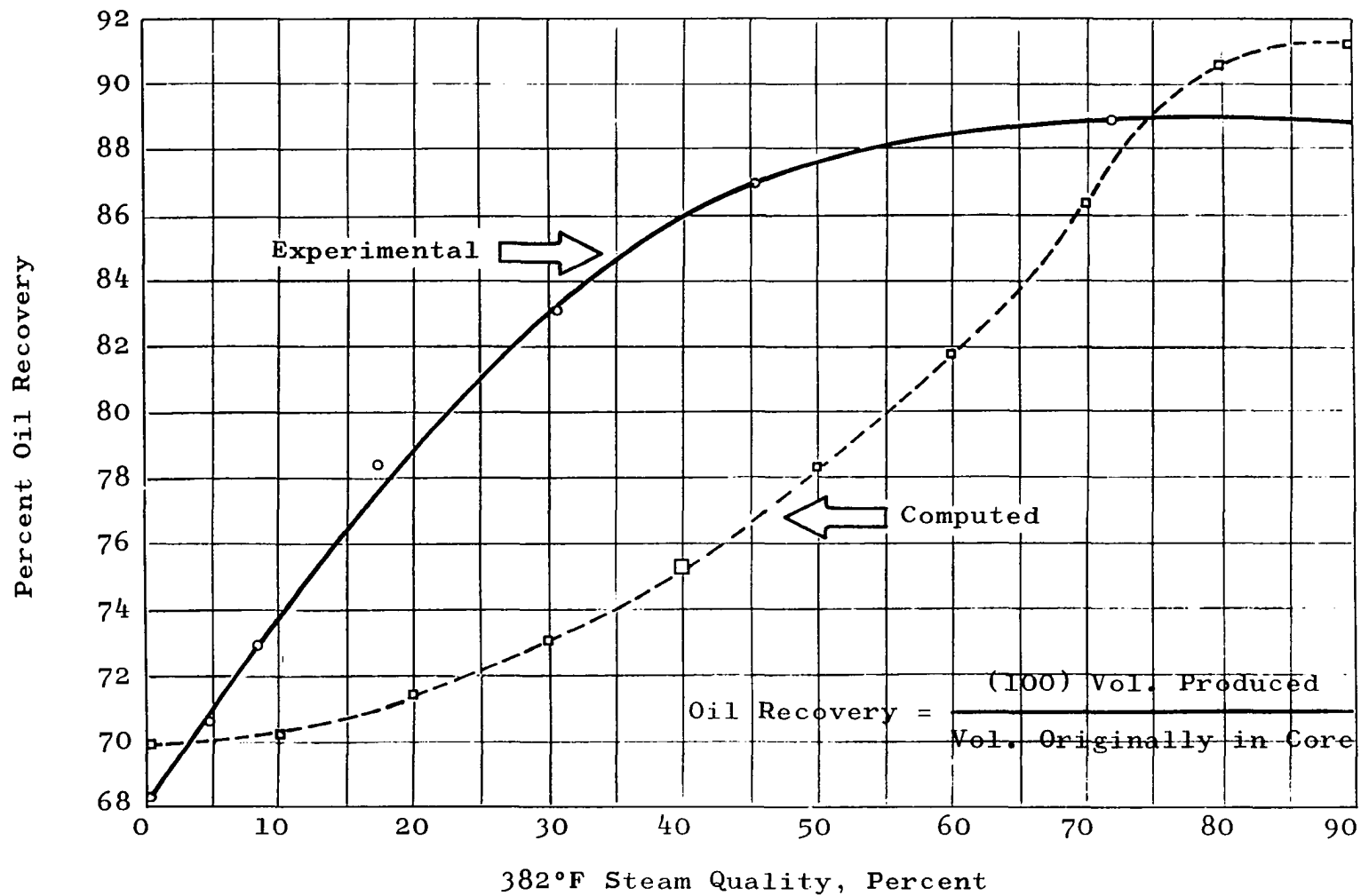
The comparison between experimental and computed data is presented on Figure 37. The analytical model forecasts a recovery increase as the quality of injected steam increases; however, the computational scheme does not adequately explain the shape of the experimental curve. Water-oil displacement has been properly identified, and steam-oil displacement at high qualities is reasonably approximated. Computed errors at 0 and 90 percent qualities are +2.0 and +2.7 percent, respectively. The maximum error, -12.1 percent occurs at 40 percent steam quality.

Since the shape of the computed curve reflects the weights assigned to each of the displacement mechanisms, the difference between the computed and experimental results apparently lies in awarding a conservative weighting to the more efficient process - steam-oil displacement.

The magnitude of the critical distances were derived using data obtained from steam-water displacements. These data reflect the consequences of 100 percent displacement efficiency. Using the maximum oil recoveries observed for the 27.8°API and 24.3°API oils - the apparent points where the displacement mechanism transition occurred - and the corresponding steam qualities, the mass of steam within the core following breakthrough was 2.94 grams and 2.90 grams, respectively. When steam displaces water, Figure 8 shows that X_c/L equals unity at about 80 percent quality. This

FIGURE 37

COMPUTED AND EXPERIMENTAL RECOVERIES: 24.3°API OIL



corresponds to 2.90 grams of steam within the 22-inch length core. Virtually equivalent masses of steam were in the core at the quality conditions where steam breakthrough was just achieved prior to the formation of a hot condensate bank. These computations indicate that steam-oil displacement efficiency contributes toward establishing a system's critical distance - as indicated by Equations (3) and (10). That the 100 percent displacement data were successful in verifying the 27.8°API oil's experimental recoveries may lie in the equivalence of oil and water viscosities at 382°F.

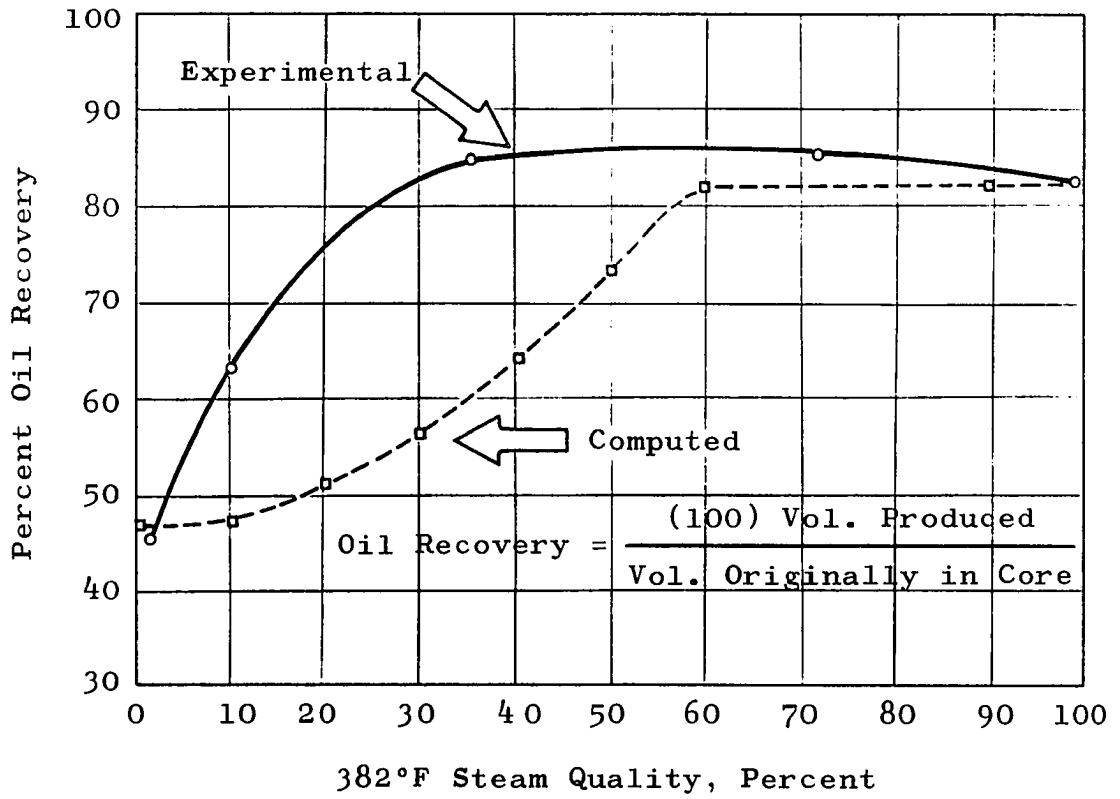
15.4°API Crude Oil

Similar to that observed with the 24.3°API oil, the computed 15.4°API recoveries fail to parallel experimental data within the quality spectrum where steam-oil and water-oil displacement mechanisms are thought to occur in varied amounts. Figure 38 summarizes computed and measured data. Performance was calculated using the critical distance curve for a 12-inch length core. The computed error at 0 percent quality is +4.5 percent. Above 60 percent quality, the error decreases from -3.6 percent to approximately 0 percent. A maximum error of -33 percent occurs at 30 percent steam quality.

As with the other oils, the individual displacements have been properly quantified. The manner in which they are combined apparently is in error.

FIGURE 38

COMPUTED AND EXPERIMENTAL
RECOVERIES: 15.4° API OIL



SUMMARY AND CONCLUSIONS

1. It is deduced that when a steam front's velocity declines to some critical value, heat loss through the front by convection is initiated. The formation of a bank of hot condensate evidently results, and a coincident change in displacement mechanism is thought to occur.
2. Evidence in the form of production history is presented which tends to support an implicit consequence of the Marx and Langenheim theory wherein mass (as condensate) can be transferred through a steam front without convective heat loss. For the experimental systems employed, 382°F steam was observed to displace oil more efficiently than did 80°F water. Thus, prior to the onset of convective heat loss, residual oil saturations were established by the flow of 382°F steam. It was observed that residual oil saturation was a function of the steam quality; most efficient displacement was caused by the flow of low quality steam. (See Figure 25, page 77)
3. After heat loss through the front is established, it is postulated that oil is displaced by a variable temperature waterflood whose maximum temperature is that of steam. This corresponds to displacement by 0 percent

quality steam. Since maximum displacement efficiency evidently occurs at 0 percent quality, it is postulated that subsequent contact of the hot waterflood's residual oil by steam will not produce further oil displacement.

4. In consequence of Conclusions 1, 2 and 3, it is submitted that the quantity of oil which can be removed from a conformable zone of known geometry is a function of: (a) The extent of the pore volume within which there is mass transfer but no heat transfer through the front; (b) The extent of the pore volume within which both heat and mass are transferred through the front; and (c) The mobility ratio which applies to each zone. A critical distance concept is submitted as a means of quantifying the extent of these zones for a linear system. Critical distance is analytically a function of steam quality while displacement efficiency within that zone was experimentally observed to be quality dependent.
5. The theoretical concepts were tested by comparing the results of some laboratory steam floods with computed data using a simplified analytical model. The experimental data show that conformable oil recovery can be sensitive to the quality of injected steam at 382°F. Good agreement between experimental and computed data is shown for a 27.8°API crude oil. The analytical model proved less accurate in reproducing the results of moist steam floods using 24.3°API and 15.4°API crude oils.

6. With each steam injection experiment, it was observed that oil production was terminated at steam breakthrough. This observation motivated the construction of an analytical model which employs piston-like displacement.
7. Experimental evidence is presented which shows that conformable oil recovery by steam injection exceeded that produced by waterflooding. Furthermore, oil recovered by steam injection was accompanied by a smaller quantity of produced water relative to waterfloods.
8. Experimental data are presented which indicate that the presence of residual oil caused an appreciable reduction of 382°F moist steams' mobilities in Boise sandstone.
9. Experimentally derived k_{ro}/k_{rw} data are submitted which indicate an unfavorable relative permeability response to increasing temperature in waterfloods.
10. The scope of this investigation required that all but two of the many heat and mass transfer variables which may control a steam displacement process be held constant. Isothermal steam quality and crude oils constituted the variables. Consequently, the results reported herein are applicable only for the experimental apparatus and procedures which were employed.
11. To apply the principles discussed herein to a field-scale operation, knowledge of areal sweep efficiency at steam breakthrough may be required. A dimensionless critical area could be defined as the ratio of critical

area to swept area at steam breakthrough. A suggested means of specifying critical area would be to subject Equation (2) in Reference (56) to the criterion related by Equation (7) of this study. Computations of residual oil saturations could be accomplished according to the principles enumerated in the Appendix. Laboratory data which are not easily obtained (e.g., effective mobility of moist steam within the subject rock and high temperature k_{ro}/k_{rw} data) would have to be available, and the quality of the steam entering the flooded zone would have to be known.

12. A combination of the postulated sequence of fluid zones along with experimentally observed oil depletion, effluent temperature, and recorded pressure histories may yield some insight into the injectivity behavior of a steam injection well. It is anticipated that injectivity would increase with time as low temperature, low mobility resistances are gradually removed from the flood pattern. Higher injectivity should be characteristic of higher quality steams, and the duration of a steamflood should increase as the quality of injected steam is decreased.

REFERENCES

1. Abbasov, A.A., Kasimov, S.A. and Tairov, N.D.: "Investigation of the Effect of Superheated Steam on Oil Recovery," Neft. Khoz. (1964) 42, 44.
2. Adivarahan, P., Kunii, D., and Smith, J.M.: "Heat Transfer in Porous Rocks Through Which Single-Phase Fluids Are Flowing," Trans., AIME (1962) 225, II-290.
3. Aronofsky, J.S. and Heller, J.P.: "A Diffusion Model to Explain Mixing of Flowing Miscible Fluids in Porous Media," Trans., AIME (1957) 210, 345.
4. Bagley, F.J. and Menzie, D.E.: "A Test of Connate Water Mobility," Producers Monthly (July, 1958) 22, No. 9, 21.
5. Bailey, H.R. and Larkin, B.K.: "Conduction-Convection In Underground Combustion," Trans., AIME (1960) 219, 320.
6. Bailey, H.R. and Larkin, B.K.: "Heat Conduction in Underground Combustion," Trans., AIME (1959) 216, 123.
7. Baker, P.E.: "Temperature Profiles in Underground Combustion," Trans., AIME (1962) 225, II-21.
8. Brown, W. O.: "The Mobility of Connate Water During a Water Flood," Trans., AIME (1957) 210, 190.
9. Carslaw, H.S. and Jaeger, J.C.: Conduction of Heat in Solids, Second Ed., Oxford At The Clarendon Press, London (1959), 388.
10. Carter, R. D.: Appendix to "Optimum Fluid Characteristics for Fracture Extension," Drill. and Prod. Prac., API (1957), 267.

11. Caudle, B.H. and Silberberg, I.H.: "Steam Injection as a Possible Stimulant for Water Injection Wells," Producers Monthly (October, 1963), 8.
12. Chu, Chieh: "Two-Dimensional Analysis of a Radial Heat Wave," Trans., AIME (1963) 228, I-1137.
13. Chu, Chieh: "The Vaporization-Condensation Phenomenon in a Linear Heat Wave," Trans., AIME (1964) 231, II-85.
14. Collins, R.E.: Flow of Fluids Through Porous Materials, Reinhold Publishing Corp., New York (1961), 196.
15. Corey, A.T.: "The Interrelation Between Gas and Oil Relative Permeabilities," Producers Monthly (November, 1954) 19, 38.
16. Craig, F.F., Jr. and Hujsak, K.L.: "Recovery of Heavy Oils by Steam Extraction," U.S. Patent 3,155,160 (November 3, 1964).
17. Crawford, P.B.: "Thermal Oil Recovery - The Big Payoff for Research," Petroleum Engineer (November, 1964), 72.
18. Davidson, L.B.: A Theoretical Analysis of Reservoir Behavior During the Intermittent Injection of Steam, Ph.D. Dissertation, Stanford University (1966).
19. Dirksen, C.: "Natural Convection in Porous Media and Its Effect on Segregated Forward Combustion," Trans., AIME (1966) 237, II-267.
20. Edmondson, T.A.: "Effect of Temperature on Waterflooding," Jour. Canadian Pet. Tech. (October-December, 1965), 236.
21. Ellenwood, F.O. and Mackey, C.O.: Thermodynamic Charts, John Wiley & Sons, Inc., New York (1964).
22. Farouq Ali, S.M.: "Effects of Differences in the Overburden and the Underburden on Steamflood Performance," Producers Monthly (December, 1966), 8.
23. Farouq Ali, S.M.: "Effects of Steam Pressure and Water Saturation On the Performance of a Steamflood," Producers Monthly (October, 1966), 8.

24. Farouq Ali, S.M.: "Oil Recovery by a Steamflood - Preliminary Considerations," Producers Monthly (June, 1966), 14.
25. Farouq Ali, S.M.: "Viscosity of Steam and Steam-Gas Mixtures," Producers Monthly (April, 1967), 10.
26. Farouq Ali, S.M.: "Estimation, Correlation and Measurement of Oil Viscosity at High Temperatures," Producers Monthly (February, 1967), 8.
27. Farouq Ali, S.M.: "Heat Losses to the Adjacent Formations," Producers Monthly (May, 1966), 4.
28. Fayers, F.J.: "Some Theoretical Results Concerning The Displacement of a Viscous Oil By A Hot Fluid In A Porous Medium," Jour. Fluid Mech. (1962) 13, Part 1, 65.
29. Fournier, K.P.: "A Numerical Method for Computing Recovery of Oil By Hot Water Injection in a Radial System," Trans., AIME (1965) 234, 131.
30. _____: "Measuring, Sampling, and Testing Crude Oil - API Standard 2500," Petroleum Production Handbook (T.C. Frick, Editor), McGraw-Hill Book Company, Inc., New York (1962) 1, 16-50.
31. Gottfried, B.S.: "A Mathematical Model of Thermal Oil Recovery in Linear Systems," Trans., AIME (1965) 234, 196.
32. Green, D.W.: Heat Transfer With A Flowing Fluid Through Porous Media, Ph.D. Dissertation, University of Oklahoma (1962).
33. Greenstein, R.I. and Preston, F.W.: "Heat Gain By Unconsolidated Sands During Hot Water Injection," Producers Monthly (February, 1953) 17, No. 4, 16.
34. Hadidi, T.A.R., Nielsen, R.F. and Calhoun, J.C., Jr.: "Studies On Heat Transfer During Linear Fluid Displacement In Porous Media," Producers Monthly (August, 1956) 20, No. 10, 38.
35. Harbert, W.D., Cain, D.C. and Huntington, R.L.: "Unsteady Flow of Heat Through Porous Media," Ind. and Eng. Chem. (February, 1941) 33, No. 2, 257.

36. Hawkins, G.A.: "The Viscosity of Superheated Steam," Trans., ASME (1940) 62.
37. Hester, D.V. and Menzie, D.E.: "Development of Sub-surface Combustion Drive," Petroleum Engineer (November, 1954) 26, No. 12, B-82.
38. Hossain, A.K.M.S.: The Displacement of Oil From Unconsolidated Sands by High Temperature Fluid Injection, M.S. Thesis, Texas A & M University (January, 1965).
39. Howard, F.A.: U. S. Patent 1,473,348 (Nov. 6, 1923).
40. _____: A Bibliography of Thermal Methods of Oil Recovery, Oil Recovery Committee, Independent Petroleum Association of America (March, 1965).
41. Jenkins, R. and Aronofsky, J.S.: "Analysis of Heat Transfer Processes in Porous Media - New concepts in Reservoir Heat Engineering," Bull. 64, Mineral Industries Experiment Station, Pennsylvania State University, State College, Pa. (1954), 69.
42. Keenan, J.H. and Keyes, G.F.: Thermodynamic Properties of Steam, John Wiley & Sons, Inc., New York (1964).
43. Keplinger, C.H. and Keplinger, H.F.: "Present Development of Steam Drive Oil Recovery and Results in the Mid-Continent Area," Producers Monthly (September, 1965), 2.
44. Khan, A.M. and Fatt, I.: "A Thermoelectric Device for Measuring Thermal Conductivity of Rock," Trans., AIME (1965) 234, 113.
45. Kingelin, G.F.R.: Unpublished PhD dissertation, University of Oklahoma (1968).
46. Klinkenberg, A.: "Numerical Evaluation of Equations Describing Transient Heat and Mass Transfer in Packed Solids," Ind. and Eng. Chem. (1948) 40, No. 10, 1992.
47. Kunii, D. and Smith, J.M.: "Thermal Conductivities of Porous Rocks Filled With Stagnant Fluids," Trans., AIME (1961) 222, II-37.
48. Landrum, B.L. et al.: "Calculated Temperature Distribution for Hot Water Floods in Ideal Reservoirs," Producers Monthly (March, 1958) 22, No. 5, 40.

49. Landrum, B.L., Smith, J.E., and Crawford, P.B.: "Calculation of Crude-Oil Recoveries by Steam Injection," Trans., AIME (1960) 219, 251.
50. Lauwerier, H.A.: "The Transport Of Heat In An Oil Layer Caused By The Injection Of Hot Fluid," Appl. Sci. Res. (1955) 5, Section A, 145.
51. Lesser, H.A., Bruce, G.H. and Stone, H.L.: "Conduction Heating of Formation with Limited Permeability by Condensing Gases," Trans., AIME (1966) 237, 372.
52. Lindsly, B.E.: "Oil Recovery By Use of Heated Gas," Oil and Gas Jour. (December 20, 1928) 27, No. 31, 27.
53. Malofeev, G.E. and Sheinman, A.B.: "Computation of Oil Recovery From a Reservoir Into Which Hot Water Is Injected," Neft. Khoz. (1963) 41, No. 3, 31.
54. Martin, J.C.: "A Theoretical Analysis of Steam Stimulation," Jour. Pet. Tech. (March, 1967), 411.
55. Martin, W.L., Alexander, J.D. and Dew, J.N.: "Process Variables of In Situ Combustion," Trans., AIME (1958) 213, 28.
56. Marx, J.W. and Langenheim, R.N.: "Reservoir Heating by Hot Fluid Injection," Trans., AIME (1959) 216, 312.
57. McAdams, W.H.: Heat Transmission, Second Ed., McGraw-Hill Book Co., Inc., New York (1942).
58. Moelwyn-Hughes, E.A.: Physical Chemistry, Pergamon Press, Oxford (1961), 726.
59. Munk, Walter: "The Delayed Hot Water Problem," Jour. Appl. Mech. (1954) 21, 193.
60. Payne, R.W. and Zambrano, G.: "Cyclic Steam Injection Helps Raise Venezuelan Production," Oil and Gas Jour. (May 24, 1965), 78.
61. Perkins, T.K., Johnston, O.C. and Hoffman, R.N.: "Mechanics of Viscous Fingering in Miscible Systems," Trans., AIME (1965) 234, 301.
62. Perry, J.H., Perry, R.H., Chilton, C.H. and Kirkpatrick, S.D.: Chemical Engineers' Handbook, Fourth Ed., McGraw-Hill Book Co., Inc., New York (1963), 13-45.

63. Preston, F.W. and Hazen, R.D.: "Further Studies on Heat Transfer In Unconsolidated Sands During Water Injection," Producers Monthly (Feb., 1953), 18, No. 4, 24.
64. Ramey, H.J., Jr.: Discussion of "Reservoir Heating by Hot Fluid Injection," Trans., AIME (1959) 216, 364.
65. Ramey, H.J., Jr.: "Transient Heat Conduction During Radial Movement of a Cylindrical Heat Source - Applications to the Thermal Recovery Process," Trans., AIME (1959) 216, 115.
66. Ramsey, P.E.: Recovery of Viscous Crude By Steam Injection, M.S. Thesis, University of Texas (May, 1958).
67. Sandrea, R.J. and Stahl, C.D.: "The Role of Some Physical Parameters In the Thermal Injection Process," Producers Monthly (June, 1966), 25.
68. Sarem, A.M. and Hawthorne, R.G.: "A Theoretical Comparison of Heat Transfer into Porous Media by the Injection of Steam or Hot Water," Jour. Canadian Pet. Tech. (April-June, 1966), 92.
69. Scheidegger, A.E.: The Physics of Flow Through Porous Media, The Macmillan Company, New York (1960), 231.
70. Ibid. (1960), 206.
71. Schild, A.: "A Theory for the Effect of Heating Oil Producing Wells," Trans., AIME (1957) 210, 1.
72. Schumann, T.E.W.: "Heat Transfer: A Fluid Flowing Through A Porous Prism," Jour. Franklin Inst. (September, 1929) 208, No. 1245-29, 405.
73. Somerton, W.H. and Boozer, G.D.: "Thermal Characteristics of Porous Rocks At Elevated Temperatures," Trans., AIME (1960) 219, 418.
74. Somerton, W.H., Mehta, M.M. and Dean, G.W.: "Thermal Alteration of Sandstones," Trans., AIME (1965) 234, 589.
75. Somerton, W.H. and Selim, M.A.: "Additional Thermal Data for Porous Rocks - Thermal Expansion and Heat of Reaction," Trans., AIME(1961) 222, 249.

76. Somerton, W.H. and Gupta, V.S.: "Role of Fluxing Agents in Thermal Alteration of Sandstones," Trans., AIME (1965) 234, I-585.
77. Spillette, A.G.: "Heat Transfer During Hot Fluid Injection Into an Oil Reservoir," Jour. Canadian Pet. Tech. (October-December, 1965), 213.
78. Stovall, S.L.: "Recovery of Oil from Depleted Sands by Means of Dry Steam," Oil Weekly (August 13, 1934) 74, No. 9, 17.
79. Strassner, J.E.: "Effect of pH on Interfacial Films and Stability of Crude Oil-Water Emulsions," SPE Paper 1939, Presented at 42nd Annual Fall Meeting of SPE of AIME, Houston (October, 1967).
80. Szasz, S.E. and Thomas, G.W.: "Principles of Heavy Oil Recovery," Jour. Canadian Pet. Tech. (October-December, 1965), 188.
81. Thomas, G.W.: "A Study of Forward Combustion in a Radial System Bounded by Permeable Media," Trans., AIME (1963) 228, II-1145.
82. Thomas, G.W.: "A Simplified Model of Conduction Heating in Systems of Limited Permeability," Trans., AIME (1964) 231, II-335.
83. _____: "U.S. Steamfloods and Firefloods and Their Status," Oil and Gas Jour. (April 4, 1965), 138B.
84. Van Meurs, P.: "The Use of Transparent Three-Dimensional Models for Studying the Mechanism of Flow Processes in Oil Reservoirs," Trans., AIME (1957) 210, 295.
85. Vogel, L.C. and Krueger, R.F.: "An Analog Computer for Studying Heat Transfer During a Thermal Recovery Process," Trans., AIME (1955) 204, 205.
86. Waldorf, D.M.: "Effect of Steam on Permeabilities of Water-Sensitive Formations," Trans., AIME (1965) 234, 1219.
87. Welge, H.: "A Simplified Method for Computing Oil Recoveries by Gas or Water Drive," Trans., AIME (1952) 195, 91.

88. Wertman, W.T., Caspero, N.A. and Sterner, T.E.:
Bibliography of Thermal Methods of Oil Recovery,
Bureau of Mines Information Circular 7958,
U.S. Dept. Interior, Washington (1960).
89. Willhite, G.P., Dranoff, J.S. and Smith, J.M.: "Heat
Transfer Perpendicular To Fluid Flow in Porous
Rocks," Trans., AIME (1963) 228, II-185.
90. Willman, B.T., Valleroy, V.V., Runberg, G.W.,
Cornelius, A.J. and Powers, L.W.: "Laboratory
Studies of Oil Recovery by Steam Injection,"
Trans., AIME (1961) 222, 681.
91. Wilson, L.A., Wygal, R.J., Reed, D.W., Gergins, R.L.
and Henderson, J.H.: "Fluid Dynamics During an
Underground Combustion Process," Trans., AIME
(1958) 213, 146.
92. Wooding, R.A.: "Instability of a Viscous Liquid of
Variable Density in a Vertical Hele-Shaw Cell,"
Jour. Fluid Mech. (1960) 7, 501.
93. Wyllie, M.R.J.: "Relative Permeability," Petroleum
Production Handbook (T.S. Frick, Ed.), McGraw-
Hill Book Co., Inc., New York (1962), 2, 25-1.

Uncited

Birdwell, B.F., Nowotny, M.B. and Silberberg, I.H.:
A Survey of Technical Literature Pertaining to the
Recovery of Oil by Thermal Methods, Bulletin 128,
Texas Petroleum Research Committee, Austin (1964).

APPENDIX

NOMENCLATURE

- A = Area normal to direction of fluid flow, cm^2
 $^\circ\text{API}$ = $\frac{141.5}{\text{Specific gravity } 60^\circ\text{F}/60^\circ\text{F}} - 131.5$
 ATF = Accomplished Temperature Fraction (Fig. 19-21)
 C = Isobaric specific heat, $\text{BTU/gram-}^\circ\text{F}$
 D_c = Diameter of cylindrical core, cm
 $e, \text{ exp}$ = 2.71828
 $\text{erfc}(z)$ = Complementary error function = $\frac{2}{\sqrt{\pi}} \int_z^\infty e^{-\alpha^2} d\alpha$
 F, F_g = Viscous and gravity forces, F
 f_i = Fractional flow of fluid i (See Subscripts)
 G = A constant in Equations (11), (12)
 g = Gravitational constant; $g\rho = \frac{980}{1013250} \rho$, atm/cm
 H_i = Rate of heat injection, BTU/minute
 H_{jj} = Enthalpy of fluid jj , BTU/gram (See Subscripts)
 $H(\lambda)$ = Enthalpy of λ quality steam, BTU/gram
 ΔH_v = Heat of vaporization at T_s , BTU/gram
 $\text{HL}_{1,2}$ = Heat losses from injection lines, BTU/gram
 J = A constant in Equations (11), (12)
 K_i = Absolute permeability to phase i , darcies
 k_{ri} = Relative permeability to phase i

$k_2 \rho_2 C_2$	=	Adjacent media's equivalent heat parameter; a product of thermal conductivity, BTU/cm-min-°F; density, grams/cc; and specific heat, BTU/g-°F.
L	=	Length of linear system, cm or inches
M	=	Mobility ratio; defined by Equation (15)
M_i	=	Mass rate of phase i, grams/minute (See Subscripts)
M_t	=	Total mass injection rate, grams/minute
P	=	Pressure, Psia
Q	=	Heat flux into bounding media, BTU/min-cm ²
q_t	=	Total volume flux, cm/sec
ΔR	=	Increment of oil recovery, fraction
S_j	=	Saturation of fluid j, fraction of pore space
S_{ji}	=	Initial saturation of fluid j (See Subscripts)
T	=	Temperature, °F (°R in Equation 12)
T_s	=	Steam temperature, °F
T_o, T_i	=	Original reservoir temperature, °F
$T(t)$	=	Effluent temperature, °F, at time t
ΔT	=	$T_s - T_o$ = Maximum temperature rise, °F
t	=	Time, minutes
t_c	=	Critical time, minutes
\bar{V}_c	=	Dimensionless critical steam front velocity
\bar{V}_s	=	Dimensionless steam front velocity
v_f	=	Velocity of steam front, cm/minute
v_{si}	=	Initial velocity of steam front, cm/minute
\bar{v}_s	=	Specific volume of λ quality steam, cc/gram
WOR	=	Water-oil ratio; volume water/volume oil
X,x	=	Linear distance, cm
x_c	=	Critical distance, cm

α	=	$\frac{4}{\Omega D_c} \sqrt{k_2 \rho_2 c_2} \sqrt{t}$
Δ	=	Signifies a finite difference (e.g., ΔT)
∂	=	Signifies a partial derivative
θ	=	Angle of formation dip, measured from horizontal
λ	=	Steam quality, percent
μ_i	=	Viscosity of fluid i, centipoise
π	=	3.1416
ρ_i	=	Density, grams/cc, of phase i
ϕ	=	Porosity, percent
Ω	=	Specific heat capacity of steamed region, BTU/cc-°F

Subscripts

cw	=	Cold (75°F-80°F) water
d	=	Displacing phase
eff	=	Effective
eq	=	Equivalent
f	=	Steam front
o,or	=	Oil, Residual Oil
s,shs	=	Steam, Superheated Steam
sw	=	Saturated water
t	=	Total
v	=	Vapor phase
w	=	Water (liquid)

TABLE A-1

SUMMARY OF EXPERIMENTAL RESULTS: 27.8°API OIL

S_{wi}	Water Temp.	Cold Water Rate	Rate To Generator	Generator Conditions °F/Psia	Generator-Junction Heat Loss	Junction-Inlet Heat Loss	λ	Oil Recovery
0.278	79°F	9.54 $\frac{cc}{min}$	6.13 $\frac{cc}{min}$	585/196	0.260 $\frac{BTU}{gram}$	0.130 $\frac{BTU}{gram}$	0.0%	76.8%
0.285	79°F	8.06 "	6.84 "	575/192	0.252 "	0.129 "	18.9%	77.6%
0.287	78°F	4.94 "	8.68 "	580/195	0.232 "	0.113 "	45.0%	83.9%
0.272	78°F	4.03 "	11.33 "	570/194	0.228 "	0.125 "	58.0%	88.2%
0.278	79°F	2.50 "	12.90 "	510/195	0.197 "	0.059 "	73.4%	92.9%
0.272	76°F	0.53 "	14.34 "	520/196	0.117 "	0.110 "	92.9%	90.0%
0.278	374°F Waterflood							68.3%
0.284	79°F Waterflood							64.7%

Note: Oil Recovery is the produced fraction of oil initially contained by 338.1 cc pore volume.

TABLE A-2

SUMMARY OF EXPERIMENTAL RESULTS: 24.3°API OIL

S_{wi}	Water Temp.	Cold Water Rate	Rate To Generator	Generator Conditions °F/Psia	Generator-Junction Heat Loss	Junction-Inlet Heat Loss	λ	Oil Recovery
0.258	74°F	9.45 $\frac{cc}{min}$	5.90 $\frac{cc}{min}$	440/195	0.260 $\frac{BTU}{gram}$	0.130 $\frac{BTU}{gram}$	4.8%	70.6%
0.228	76°F	9.30 "	5.75 "	575/196	0.250 "	0.120 "	8.9%	73.0%
0.226	76°F	7.89 "	6.93 "	490/197	0.252 "	0.129 "	17.3%	78.5%
0.274	75°F	6.42 "	8.30 "	470/198	0.232 "	0.113 "	30.8%	83.2%
0.269	74°F	5.27 "	10.80 "	495/198	0.228 "	0.125 "	45.4%	87.0%
0.241	78°F	2.76 "	13.02 "	510/190	0.197 "	0.060 "	71.9%	88.9%
0.244	79°F Waterflood							22.9%
0.239	203°F Waterflood							57.5%
0.228	345°F Waterflood							68.2%

138

Note: Oil Recovery is the produced fraction of oil initially contained by 338.1 cc pore volume.

TABLE A-3

SUMMARY OF EXPERIMENTAL RESULTS: 15.4°API OIL

S_{wi}	Water Temp.	Cold Water Rate	Rate To Generator	Generator Conditions °F/Psia	Generator-Junction Heat Loss	Junction-Inlet Heat Loss	λ	Oil Recovery
0.133	75°F	9.63 $\frac{cc}{min}$	6.59 $\frac{cc}{min}$	580/200	0.263 $\frac{BTU}{gram}$	0.132 $\frac{BTU}{gram}$	1.2%	45.1%
0.140	76°F	9.66 "	6.35 "	577/200	0.258 "	0.130 "	10.2%	63.0%
0.116	77°F	6.95 "	8.88 "	585/202	0.240 "	0.113 "	34.4%	84.5%
0.090	76°F	7.04 "	9.02 "	585/202	0.240 "	0.113 "	34.4%	83.9%
0.094	76°F	3.24 "	12.89 "	565/200	0.196 "	0.059 "	70.9%	85.2%
0.140	76°F	0 "	17.75 "	570/200	0.102 "	0.030 "	99%	82.3%
0.150	75°F Waterflood							4.9%
0.154	209°F Waterflood							23.3%
0.140	350°F Waterflood							41.0%

Note: Oil Recovery is the produced fraction of oil initially contained by 195.7 cc pore volume.

EXAMPLE CALCULATION: $\frac{k_{ro}}{k_{rw}}$

By definition: $f_w = \frac{q_w}{q_o + q_w} = \frac{q_w}{q_t}$

If capillary and gravity forces are ignored,

$$f_w = \left(1 + \frac{k_{ro}}{k_{rw}} \frac{\mu_w}{\mu_o}\right)^{-1} .$$

A cumulative volume, Q , is related to an instantaneous rate, q , by:

$$q = \frac{dQ}{dt} .$$

Thus,

$$f_w = \frac{dQ_w/dt}{dQ_t/dt} = \frac{dQ_w}{dQ_t} = 1 - \frac{dQ_o}{dQ_t}$$

since

$$f_o + f_w = 1 .$$

A mass balance on oil contained by the core at some time, t , is expressed as:

$$A \phi \int_0^L S_o(x) \cdot dx = \phi A L (1 - S_{wi}) - Q_o .$$

The left-hand side may be integrated by parts.

$$A \phi \int_0^L S_o(x) \cdot dx = A \phi \left[x \cdot S_o(x) \right]_0^L - A \phi \int_{S_o(x=0)}^{S_o(x=L)} x \, dS_o$$

Taking the indicated limits yields:

$$A \phi \int_0^L S_o(x) dx = A \phi L \cdot S_o(L) - A \phi (0)(1-S_{wi}) \\ - A \phi \int_{S_o(x=0)}^{S_o(x=L)} x dS_o .$$

Integration of the Buckley - Leverett equation yields, at some time, t ,

$$x(S_w) = \frac{Q}{A \phi} \frac{df_w}{dS_w} . \quad (Q=Q_t)$$

Substitution of this relationship into the last integral yields:

$$-A \phi \int_{S_o(0)}^{S_o(L)} x dS_o = \int_{S_w(0)}^{S_w(L)} Q \frac{df_w}{dS_w} dS_w = \int_{1-S_{or}}^{S_w(L)} Q df_w = -Q f_o \\ = -Q \frac{dQ_o}{dQ} .$$

Substitution into the mass balance yields, after solving for $S_o(L)$,

$$S_o(L) = \frac{1}{A \phi L} \left[A \phi L (1-S_{wi}) - Q_o + Q_t \frac{dQ_o}{dQ_t} \right] .$$

This is Welge's integration of the Buckley-Leverett equation.

The defining equation for f_w and Welge's equation are used in constructing a relative permeability ratio curve. Figure 1-A shows the response of the 27.8° API oil to waterflooding in Boise sandstone at 80°F and 350°F. The 80°F data are used in illustrating the computations.

Experimental Conditions

$$S_{wi} = 28.4\% \quad \mu_o = 21 \text{ cp} \quad \mu_w = 0.86 \text{ cp}$$

$$\text{Pore Volume} = 338.1 \text{ cc (22-inch core)}$$

$$\frac{k_{ro}}{k_{rw}} = \frac{\mu_o}{\mu_w} \frac{1-f_w}{f_w} = 24.4 \frac{\frac{dQ_o}{dQ_t}}{1 - \frac{dQ_o}{dQ_t}}$$

$$S_o(L=54.5 \text{ cm}) = (1-0.284) - \frac{Q_o}{338.1} + \frac{Q_t}{338.1} \frac{dQ_o}{dQ_t}$$

Q_t	Q_o	$\frac{dQ_o}{dQ_t}$	$1 - \frac{dQ_o}{dQ_t}$	$\frac{k_{ro}}{k_{rw}}$	$S_o(L)$	$S_w(L)$
100	81	0.196	0.804	5.9	0.534	0.466
300	114	0.125	0.875	3.5	0.490	0.510
500	132	0.060	0.940	1.6	0.414	0.586
800	144	0.028	0.972	0.7	0.356	0.644
1200	152.5	0.015	0.985	0.38	0.318	0.682
1500	156.4	0.011	0.989	0.27	0.302	0.698

These data are included on Figure 34 in the text.

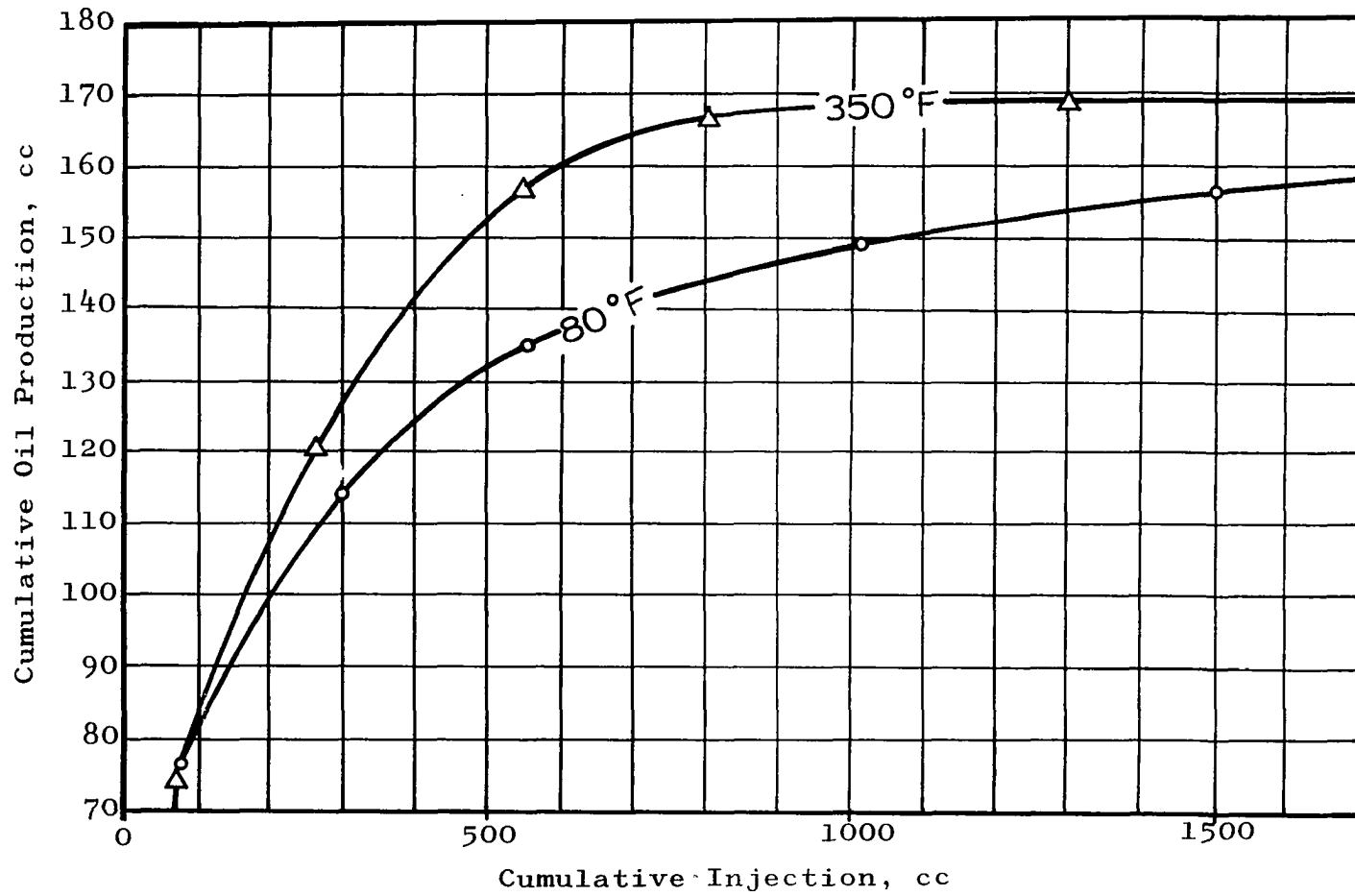


FIGURE 1-A

WATERFLOOD PERFORMANCE, 27.8° API OIL

EXAMPLE CALCULATION: OIL RECOVERY BY STEAM INJECTION

Part I: Water - Oil Displacement

Computations for this phase of total recovery refer to that which is attributed to displacement of oil by liquid water, the water being steam condensate formed by convection losses through a steam front. Attention is directed to the Region B (liquid) side of the saturation - phase discontinuity shown by the following sketch.

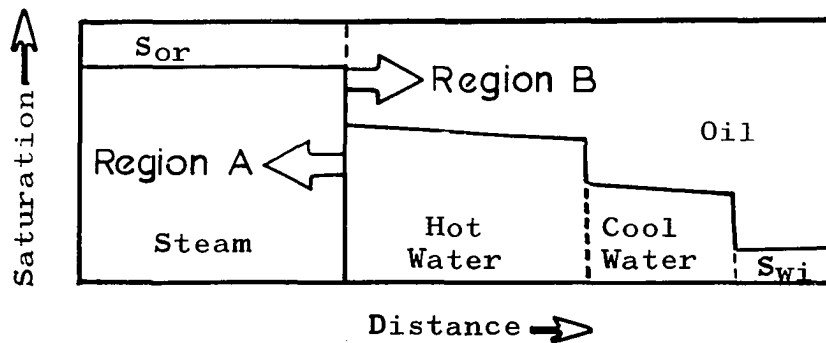


FIGURE 2-A

IDEALIZED SATURATION PROFILE

The fractional flow of steam on the liquid side of the discontinuity is assumed to be zero. The fractional flow relationship for piston-like displacement can be written in terms of mobilities on either side of the displacement discontinuity.

$$\begin{aligned}
 f_A &= \left[1 + \frac{\text{Region B Mobility}}{\text{Region A Mobility}} \right]^{-1} \\
 &= 1 \text{ in region A} \\
 &= 0 \text{ in region B}
 \end{aligned}$$

Assuming that pressure within the oil phase is equal to that within the water phase, the Region B mobility is the sum of water and oil mobilities. Region A mobility is that of steam. Substitution of these quantities into the above relationship yields:

$$f_A = \left(\frac{\frac{k_{ro}}{k_{rw}} \frac{1}{\mu_o} + \frac{1}{\mu_w}}{\frac{k_{ro}}{k_{rw}} \left[\frac{k_{rs}}{\mu_s} \right]_{\text{eff}} + 1} \right)^{-1}$$

after grouping k_{ro} and k_{rw} as a ratio. This is done since values of this ratio are available from measured data. Individual k_{ro} are not readily available from displacement experiments, and they are computed using:

$$k_{ro} = \left[1 - \frac{S_w - S_{wi}}{1 - S_{wi}} \right]^2 \left[1 - \frac{[S_w - S_{wi}]^2}{[1 - S_{wi}]^2} \right],$$

an empirical relationship.

The computational procedure consists of:

- (1) Compute a series of k_{ro} values for various S_w ;
- (2) For a specified steam quality, determine the

steam's effective relative mobility, and compute a series of f_s values corresponding to the S_w 's of Step (1);

- (3) Construct a curve of f_s versus S_w and extrapolate to $f_s = 0$. The corresponding water saturation, $S_w(f_s=0)$, is that saturation which exists on the liquid side of the frontal discontinuity. Recovery due to water displacement and to thermal expansion of connate water is:

$$\Delta R_1(T_s) = \frac{S_w(f_s=0) - S_{wi}(T_s)}{1 - S_{wi}(T_i)} \quad .$$

Displacement recovery is referred to the original temperature according to:

$$\Delta R_1(T_i) = \Delta R_1(T_s) \frac{\rho_o(T_s)}{\rho_o(T_i)} \quad .$$

- (4) Repeat (2) - (3) for different steam qualities.

Computation of k_{ro} (382°F): 27.8°API Oil

$$\begin{aligned} S_{wi}(382^\circ\text{F}) &= S_{wi}(80^\circ\text{F}) \frac{\rho_w(80^\circ\text{F})}{\rho_w(382^\circ\text{F})} \\ &= 0.278 \frac{0.997}{0.874} \\ &= 0.318 \end{aligned}$$

Base k_{ro} calculations on $S_{wi} = 0.318$.

S_w	$S_w^{-0.318}$	$\frac{S_w^{-0.318}}{0.682}$	k_{ro}
0.70	0.382	0.560	0.133
0.75	0.432	0.633	0.081
0.80	0.482	0.707	0.043

$\frac{k_{ro}}{k_{rw}}$ from Figure 34

S_w	$\frac{k_{ro}}{k_{rw}}$
0.70	0.060
0.75	0.027
0.80	0.0022

Computation of f_s : $\lambda = 10\%$

$$\left[\frac{k_{rs}}{\mu_s} \right]_{\text{eff}} = 6.188 \text{ cp}^{-1}$$

$$\mu_o^{-1} = 1/0.12 = 8.33 \text{ cp}^{-1} \quad \mu_w^{-1} = 1/0.14 = 7.14$$

S_w	$8.33 \frac{k_{ro}}{k_{rw}} + 7.14$	$6.188 \frac{k_{ro}}{k_{rw}} \frac{1}{k_{ro}}$	f_s
0.70	7.6398	2.7909	0.268
0.75	7.3649	2.0606	0.219
0.80	7.1583	0.3168	0.042

Equivalent data for 20 percent quality steam (effective relative mobility = 9.108 cp^{-1}) are tabulated as follows.

S_w	f_s
0.70	0.350
0.75	0.292
0.80	0.061

Extrapolation of these data is shown by Figure 3-A.

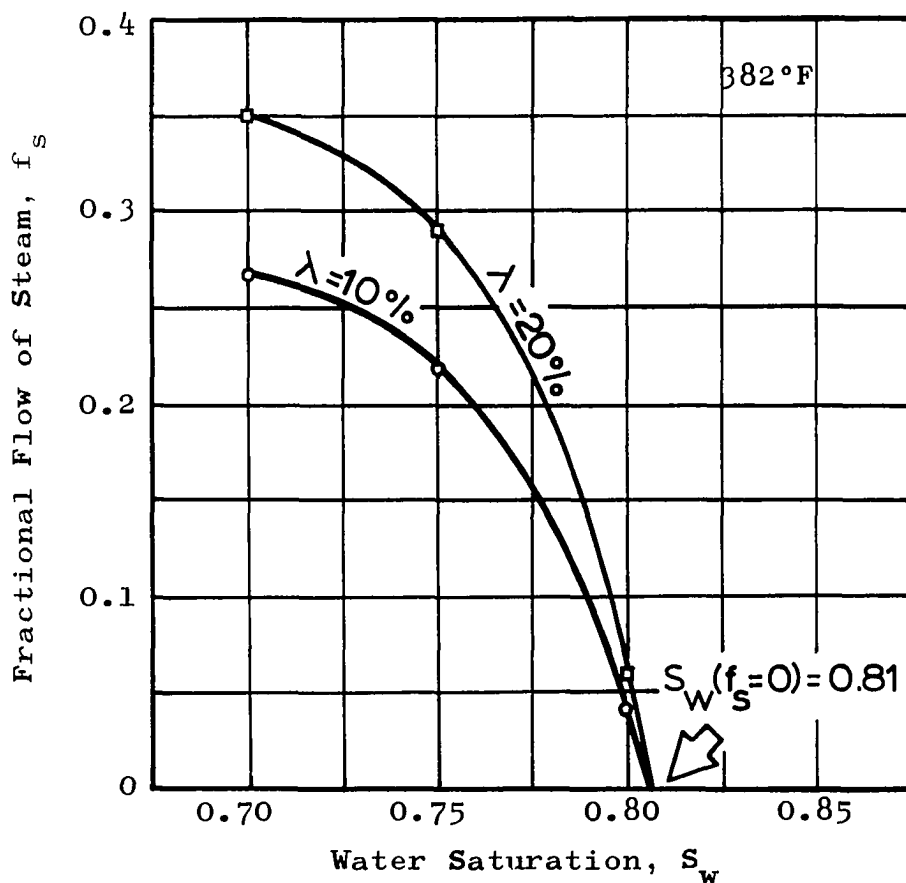


FIGURE 3-A

DETERMINATION OF WATER SATURATION, LIQUID SIDE OF FRONT

The extrapolation of all quality-dependent curves for 382°F steam yields $S_w(f_s = 0) = 0.81$.

$$\begin{aligned} \text{Displacement Recovery} &= (0.810 - 0.318) \frac{0.756}{0.881} \\ &= 0.422 \text{ of } S_{oi} = 1.00 \\ &= 0.585 \text{ of } S_{oi} = 0.722 \end{aligned}$$

Recovery Due to Thermal Expansion

Following displacement by water at reservoir temperature, both the immobile water and the remaining oil respond to increasing temperature by expanding. The maximum degree of expansion is defined by the upper and lower temperature bounds. Connate water is assumed to remain immobile upon expansion; after water expansion, a constant oil saturation is assumed to exist.

$$\begin{aligned} \Delta R_2(T_i) \text{ due to water expansion} &= \frac{S_{wi}(T_s) - S_{wi}(T_i)}{1 - S_{wi}(T_i)} \\ &= \frac{0.318 - 0.278}{0.722} \\ &= 0.055 \end{aligned}$$

Oil expulsion due to its own expansion must be evaluated on the basis of the cool waterflood's residual oil. The experimental 80°F recovery was 64.7 percent of the S_{oi} .

$$\Delta S_o(T_s) = S_o(T_i) \frac{\rho_o(T_i)}{\rho_o(T_s)} - S_o(T_i)$$

$$\Delta R_3(T_i) = \frac{\Delta S_o(T_s)}{S_{oi}(T_i)} \frac{\rho_o(T_s)}{\rho_o(T_i)}$$

$$= (1 - 0.647)(0.722) \left[\frac{0.881}{0.756} - 1 \right] \frac{0.756}{0.881}$$

$$= 0.036 \text{ of } S_{oi} = 1.00$$

$$= 0.050 \text{ of } S_{oi} = 0.722$$

This obviously is a conservative estimate since the ultimate recovery by 80°F (T_i) waterflooding is employed. A rigorous approach would require evaluation of saturation at the junction of hot and cold waterfloods. The quantity of incremental oil recovery is small, and the additional effort demanded by a rigorous analysis is deemed impractical.

Total Recovery: Part I

Total recovery is the summation of incremental values attributed to displacement and to thermal expansion.

$$R(I) = \sum_{i=1}^{i=3} \Delta R_i = 0.585 + 0.055 + 0.050$$

$$= 0.690 \text{ of } S_{oi}$$

Part II: Steam - Oil Displacement

Computations for this portion of the oil recovery model refer to that which arises prior to the onset of convection losses. Contributions by displacement, thermal expansion, and steam distillation are considered separately.

Incremental recovery due to displacement is computed using the fractional flow relationship:

$$f_s = \left[1 + \frac{k_{ro}}{\mu_o} \left[\frac{\mu_s}{k_{rs}} \right]_{\text{eff}} \right]^{-1}$$

$$\text{where } k_{ro} = \left[\frac{S_o}{1 - S_{wi}} \right]^4 .$$

For no distillation, the fractional flow of steam at the steam - oil interface is unity. With distillation, f_s is slightly less than unity since both steam and hydrocarbon vapors and steam can exist at the phase discontinuity.

A fractional flow curve is constructed for a specified steam quality. The following data are used in computing each f_s curve.

$$\begin{aligned} \mu_o &= 0.12 \text{ cp @ } 382^\circ\text{F} & K_{\text{abs}} &= 4.356 \text{ d @ } 382^\circ\text{F} \\ S_{wi} &= 0.318 \text{ @ } 382^\circ\text{F} & \left[\frac{K_s}{\mu_s} \right]_{\text{eff}} &\text{ from Fig.} \end{aligned}$$

Computations are summarized by Figure 4-A. Curves are presented for 10-percent quality increments.

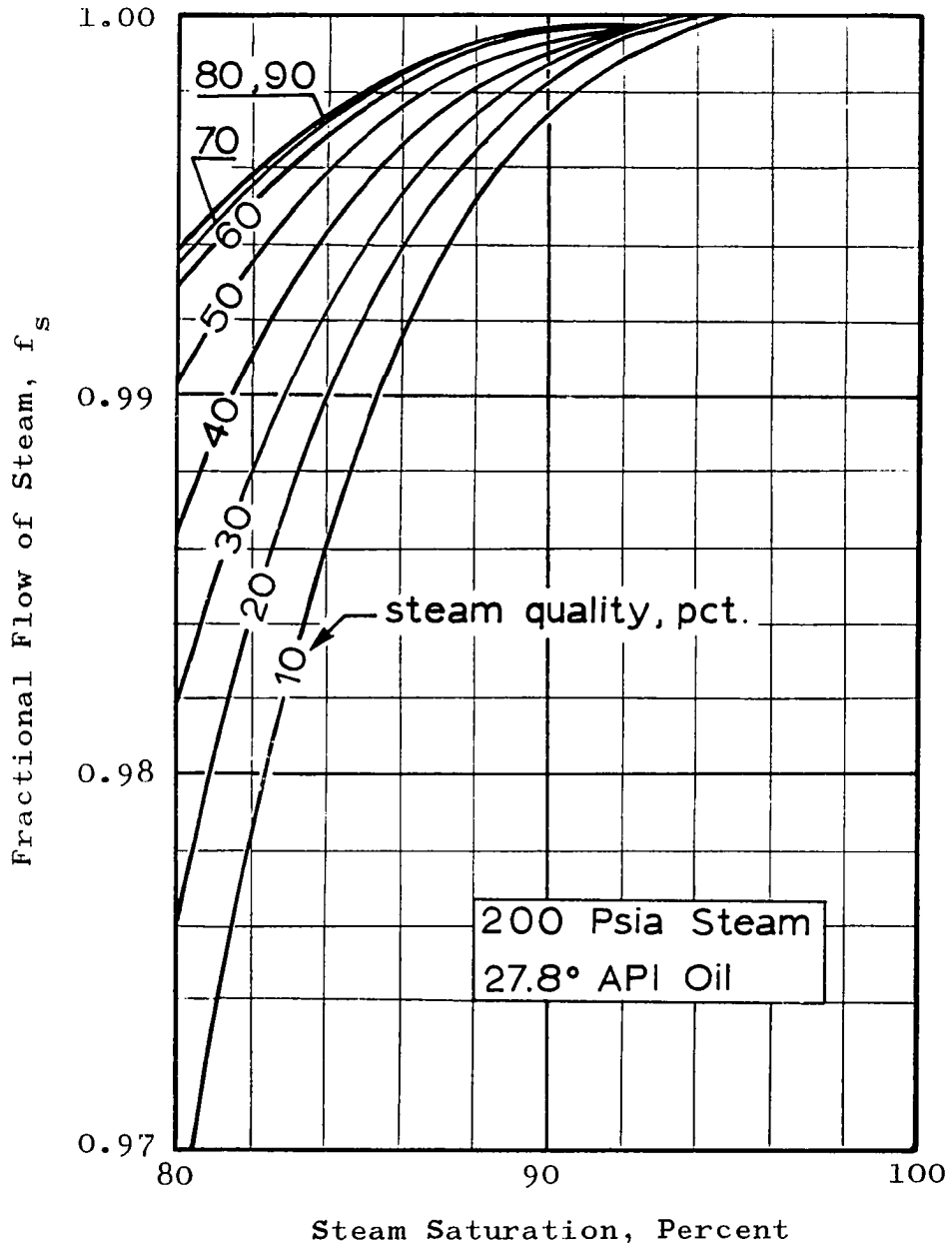


FIGURE 4-A

STEAM - OIL FRACTIONAL FLOW CURVES

Assuming that there is negligible flow of hydrocarbon vapors, the steam saturation at a steam-liquid interface is evaluated at unit f_s . In the present analysis, steam saturation is read at $f_s = 0.9995$ since the curves are difficult to extrapolate beyond this point. The recovery increment due to displacement is

$$\Delta R_4(T_i) = \frac{S_s(f_s=0.9995) - S_{wi}(T_i)}{1 - S_{wi}(T_i)} \quad .$$

Displacement computations are summarized in the following table.

λ	S_s	ΔR_4
10	93.6%	0.911
20	92.7%	0.899
30	92.0%	0.889
40	91.5%	0.882
50	90.8%	0.872
60	90.1%	0.863
70	90.1%	0.863
80	89.6%	0.856
90	89.6%	0.856

Thermal expansion of oil is considered at the front. Having estimated the degree of displacement, thermal expansion computations are executed on the residual oil. The process is identical to that for determining ΔR_3 in Part I.

Thermal expansion recovery is

$$\Delta R_5(T_i) = \frac{0.142 S_{or}}{0.722} \quad . \quad (\text{See } \Delta R_3, \text{ Part I})$$

λ	S_{or}	ΔR_5
10	0.064	0.013
20	0.073	0.014
30	0.080	0.016
40	0.085	0.017
50	0.092	0.018
60	0.099	0.020
70	0.099	0.020
80	0.104	0.020
90	0.104	0.020

Part III: Total Recovery

Total recovery consists of weighted sums of each contributing effect. Weighting is accomplished by using the critical distance curve, Figure 8 . Additional oil recovery due to distillation is simply added to the weighted contributions.

$$R_{total} = \left[1 - \frac{X_c}{L} \right] R(I) + \left[\Delta R_4 + \Delta R_5 + \Delta R_{dist.} \right] \frac{X_c}{L}$$

where $R(I)$ includes distillation.

$$R_{\text{total}} = \left[1 - \frac{X_c}{L} \right] (0.690 + 0.085) + \frac{X_c}{L} (0.085 + \Delta R_4 + \Delta R_5)$$

where 0.085 distillation recovery was experimentally observed.

Total recovery computations are summarized by the following table.

λ	$\frac{X_c}{L}$	R_{total}
10	0.019	0.780
20	0.065	0.790
30	0.142	0.806
40	0.250	0.827
50	0.385	0.852
60	0.547	0.880
70	0.765	0.922
80	0.956	0.956
90	1.000	0.961

DETERMINATION OF HEAT LOSS PARAMETER ($k_2 \rho_2 c_2$)

CORE'S SURROUNDINGS

$$\text{Basis: } X_f = \frac{H_i \Omega}{4(k_2 \rho_2 c_2)_{\text{eff}} \pi \Delta T} \left[e^{\alpha^2} \operatorname{erfc} \alpha + \frac{2\alpha}{\sqrt{\pi}} - 1 \right]$$

$$\text{where } \alpha = \frac{4}{\Omega D_c} \sqrt{(k_2 \rho_2 c_2)_{\text{eff}}} \sqrt{t}$$

Requirement: No change in heat transfer characteristics while propagating a front through the core.

Laboratory Conditions:

Annulus water injection rate: 98 cc/minute

Cold water injection rate: 0.49 cc/min @ 75°F

Water rate to steam generator: 14.62 cc/min @ 75°F

Steam generator conditions: 520°F, 196 psia

Generator-Junction heat loss: 0.108 BTU/gram

Junction-Core Inlet heat loss: 0.097 BTU/gram

Duration of flood, steam in to steam out: 15.6 min

Length flooded: 54.5 cm Core Diameter: 5.25 cm

Enthalpy reference: 75°F, 200 psia

Core Inlet conditions: 382°F steam

Specific volume of cold water: 1.0029 cc/g @ 75°F

$$M_{\text{cw}} = \frac{0.49}{1.0029} = 0.49 \text{ g/min} \quad M_{\text{shs}} = \frac{1.462(10)}{1.0029} = 14.59$$

$$M_t = M_{\text{cw}} + M_{\text{shs}} = 15.08 \text{ g/min}$$

$$H_{cw} = 43.5 - 43.5 = 0 \text{ BTU/lb} = 0 \text{ BTU/g} \quad (75^\circ\text{F enthalpy ref.})$$

$$H_{shs} = 1280.2 - 43.5 = 1236.7 \text{ BTU/lb} = 2.725 \text{ BTU/g}$$

$$H_i = 0.49(0) + 14.59(2.725) = 39.75 \text{ BTU/min}$$

$$H(\lambda) = \frac{39.75}{14.59 + 0.49} = 2.64 \text{ BTU/g} \quad \lambda \cong 100\%$$

$$\begin{aligned} \Omega &= (0.712)(0.00044)(2.52) + (0.288) \frac{2.64}{307} (0.0068) \\ &= 0.000806 \text{ BTU/cc-}^\circ\text{F} \end{aligned}$$

$$\begin{aligned} X_f = 54.5 &= \frac{(39.75)(0.000806)}{(4)(3.14)(307)(k_2 \rho_2 C_2)} \left[e^{\alpha^2} \text{erfc}\alpha + 1.13\alpha - 1 \right] \\ &= \frac{0.830 \times 10^{-5}}{k_2 \rho_2 C_2} \left[e^{\alpha^2} \text{erfc}\alpha + 1.13\alpha - 1 \right] \end{aligned}$$

$$\text{where} = \frac{4 \sqrt{15.6}}{0.000806(5.25)} \sqrt{k_2 \rho_2 C_2} = 3735 \sqrt{k_2 \rho_2 C_2}$$

Solve by trial-and-error computation.

$$\text{Result: } (k_2 \rho_2 C_2)_{\text{eff}} = 13.58 \times 10^{-8} \left[\frac{\text{BTU}}{\text{cm-}^\circ\text{F}} \right]^2 \text{ min}^{-1}$$

Conditions or Restrictions: Core holder and tubing insulated with Urethane. Raise annulus temperature (inlet) to 382°F simultaneously with initiating 382°F flow into core. Core initially saturated with water. Mass injection rates as specified.

COMPUTATION OF CRITICAL DISTANCE

$$\text{Basis: } \frac{X_c}{L} = \frac{H_i \Omega}{4L(k_2 \rho_2 c_2) \pi \Delta T} \left[e^{-\alpha_c^2} \operatorname{erfc} \alpha_c + \frac{2\alpha_c}{\sqrt{\pi}} - 1 \right]$$

$$\text{Where } e^{-\alpha_c^2} \operatorname{erfc} \alpha_c = \frac{H_{sw}}{H(\lambda)} ; \quad \alpha_c = \frac{\sqrt[4]{k_2 \rho_2 c_2}}{\Omega D_c} \sqrt{t_c}$$

Enthalpy Reference: 75°F, 200 psia

Saturation Condition: 382°F

$$H_{sw} = 355.4 - 43.5 = 311.9 \text{ BTU/lb} = 0.687 \text{ BTU/g}$$

$$\Delta H_v = 843 \text{ BTU/lb} = 1.857 \text{ BTU/g}$$

$$H(\lambda) = 0.687 + (\lambda)(1.857), \text{ BTU/g}$$

$$H_i = H(\lambda) \cdot (M_{shs} + M_{cw}) = 15 \cdot H(\lambda), \text{ BTU/min}$$

$$\Omega = 0.000789 + 0.00094 \cdot H(\lambda) \cdot \rho_s(\lambda), \text{ BTU/cc-}^\circ\text{F}$$

$$L = 54.5 \text{ cm} \quad (k_2 \rho_2 c_2)_{\text{eff}} = 13.58 \times 10^{-8}$$

λ	$\rho_s(\lambda)$	$\frac{H_{sw}}{H(\lambda)}$	$\frac{H_{sw}}{H(\lambda)} + \frac{2\alpha_c}{\sqrt{\pi}} - 1$	H_i	Ω	$\frac{X_c}{L}$
0.10	0.0646 $\frac{\text{g}}{\text{cc}}$	0.788	0.045	13.1 $\frac{\text{BTU}}{\text{min}}$	0.000842	0.017
0.20	0.0334 "	0.650	0.140	15.87 "	0.000822	0.064
0.40	0.0169 "	0.480	0.415	21.40 "	0.000812	0.253
0.60	0.0119 "	0.382	0.712	27.00 "	0.000809	0.546
0.80	0.0086 "	0.316	1.050	32.55 "	0.000807	1.0

COMPUTATION OF EXTERNAL HEAT FLUX FROM CORE

A gross heat balance on the core is employed:

Rate of Heat Injected - Rate of Accumulation = Rate Lost.

Symbolically,

$$H_i - v_f A \left[(1-\phi) \rho_r C_r + \phi \rho_s \frac{H(\lambda)}{\Delta T} \right] \Delta T = \pi D_c x_f Q ,$$

where Q is the heat flux from the core into the bounding media.

Experimental Conditions

$$H_i = 32 \text{ BTU/minute} \qquad H(\lambda) = 2.21 \text{ BTU/gram}$$

$$L = 54.5 \text{ cm} \qquad A = 21.65 \text{ cm}^2 \qquad D_c = 5.25 \text{ cm}$$

$$T = 314^\circ\text{F} \qquad \rho_s = 0.0086 \text{ g/cm}^3$$

Flooding time = 30.5 minutes

$$\text{Average frontal velocity} = \frac{54.5}{30.5}$$

$$= 1.785 \text{ cm/min}$$

$$32 - 1.785(21.65) \left[0.712(2.52)(0.00044) + 0.288(0.0086) \frac{2.21}{314} \right] 314$$

$$= 3.14(5.25)(54.5)Q$$

$$Q = \frac{22.23}{898} = 0.0248 \text{ BTU/min-cm}^2$$

This quantity represents an average heat loss flux since an average frontal advance rate is employed which is less than the initial rate and greater than the terminal value.